THE UNIVERSITY OF MANITOBA

POLYATOMIC ANHARMONICITY: A LOCAL-MODE APPROACH TO OVERTONE SPECTRA

by

Rowland John Hayward

A THESIS

SUBMITTED TO THE FACULTY OF GRADUATE STUDIES

IN PARTIAL FULFILMENT OF THE REQUIREMENTS FOR THE DEGREE

OF DOCTOR OF PHILOSOPHY

DEPARTMENT: CHEMISTRY

WINNIPEG, MANITOBA

OCTOBER 1975

POLYATOMIC ANHARMONICITY: A LOCAL-MODE APPROACH TO OVERTONE SPECTRA

by

ROWLAND JOHN HAYWARD

A dissertation submitted to the Faculty of Graduate Studies of the University of Manitoba in partial fulfillment of the requirements of the degree of

DOCTOR OF PHILOSOPHY

To Mom and Dad with my thanks.

Mom. I now more fully realize the selfless time, care and love which I was given at home. It would not be possible to have this science on this paper in 1975 if it weren't for that support.

Dad. Doug and I never convinced you that the world was flat in all our years at school. And yet, you still encouraged us to go out and learn to play at our impractical games. I suppose I shall never understand all of what it means to be a parent.

Doug. Notwithstanding peanut butter sandwiches, I learned in work and play from you in many ways. Merci mon frère.

Dr. Henry. I'm not sure how you stood it. I enjoyed working for you and wish you better luck in choosing your prospective students in the future. Your influence on my thinking will be clear to any readers who know you well. Your patience and kindness will not soon be forgotten.

Jim. Well James, the two years in 449 Parkerville with me must have been painful at times for you. I had great fun working and learning from and with you.

Marilyn. Well professor, your influence on my science was perhaps greater than you imagine. I find the biosphere holds great wonder for the physical scientist and my discovery of this was through you and your approach to science.

Staff in Chemistry. You were very patient with me. Thank you for the time and insights you shared with me.

Looking back, I was not a very good scientist, but I did have great fun finding out.

ACKNOWLEDGMENTS

Dr. Henry and Dr. Siebrand really had the ideas. Each reading of their 1968 paper reveals more to me.

Mr. R. B. Hayward made possible the photographs of the overtone spectra included here. Thanks Dad.

Mr. J. D. Morrison spent many long hours discussing various aspects of this work and other science with me. Undoubtedly his insights have found their way onto the pages of this report.

Mrs.P.Henderson spent many long hours typing this report. The only errors that I found were mine. Please accept my most sincere thanks for a job most should not wish to have tackled.

The people of Canada, through NRC, funded my studies. I am very grateful to each of you. Thankyou.

ABSTRACT

The vibrationally excited states of polyatomic molecules containing XH_n moeities have been examined. Anharmonic coupling among the normal modes of vibration has been investigated, quantitatively, by assuming the XH oscillators in the molecule vibrate anharmonically, but essentially independently. The position of the overtone band maxima for benzene, ammonia and methane were predicted using this assumption when full account was taken of the technique of superimposing oscillator amplitudes. Off-diagonal anharmonic normal-mode coupling constants, X_{KL}, were found to be much larger than heretofore predicted in recent force constant calculations. The coupling effects were so large that it seems unreasonable to think of overtone bands as arising from transitions from the ground state to a set of symmetry allowed, anharmonic, normal-oscillator states. By assuming that local-oscillator excitation is a more probable type of transition, an explanation of band maxima and band width in the experimental overtone spectra is possible. This assumption is tested for ammonia and dichloromethane. The v_{CH}=5 and 6 transitions were observed for dichloromethane at 7223 and 6165 $\mathring{A}$ respectively. To generalize the theory to include molecules with non-equivalent CH groups the overtone spectra of toluene and the xylenes were recorded and aspects of the structure of their CH overtone bands discussed and correlated to their primary

molecular structures. The gas phase spectra of methane and ethane, recorded using apparatus described in the appendix lend further support to the proposal that overtone spectra for these types of molecules are simpler than expected on a normal-mode basis.

A problem with the formulation of the RRKM unimolecular reaction rate expression is identified. The effect of anharmonicity on the RRKM calculations is investigated in relation to the general local-mode theory.

In the appendix, a stainless steel, high pressure gas line, linking a gas cylinder with a gas cell is described and a convenient mode of operation given so that the infrared spectra of gases at high pressure may be obtained.

TABLE OF CONTENTS

LIST OF FIGURES

LIST OF FIGURES (continued)

LIST OF TABLES

CHAPTER 1

INTRODUCTION

Analysis of infrared and Raman spectra has led to the determination of the structure of many molecules (1). The eigenstates of the molecular vibrational Hamiltonian, the normal modes, depending on their symmetry will, or will not absorb or scatter a photon according to well established selection rules (2). Most of the experimental data in the fundamental regions of the infrared spectra can be understood, rather completely, by assuming that a polyatomic molecule consists of a set of 3N-6(5) coupled harmonic oscillators orientated, one with respect to the other, according to the ground state equilibrium vibronic geometry. The resulting stationary states, the normal modes, then become a convenient basis set or point of reference for the analysis of any physical phenomena involving the vibrational manifold of states.

It has always been recognized, however, that all vibrations of a molecule can not be simultaneously harmonic under all conditions for in this case there could never be a thermal dissociation of a bond. The molecular potential 'within which the nuclei move' is not a quadratic form and

its deviation from this mathematical structure is referred to as mechanical anharmonicity. The primary effects of anharmonicity result from the destruction of the Hermite polynomial character of the basis functions. The physical results of the modification to the vibrational wave functions can be summarized;

1) Normal modes are no longer the stationary states of the vibrational Hamiltonian.

2) Previously forbidden transitions in infrared and Raman spectra become allowed to some extent.

3) Chemical reactions involving bond breaking (aside from predissociative type reactions) become possible. Anharmonicity, therefore, is an extremely important concept since much chemistry cannot be adequately described on a molecular basis without it.

The work here is divided into two sections. The first section is comprised of a study of polyatomic anharmonicity, probed theoretically and spectroscopically. The ideas, specifically the concept of local modes, are used in a slightly different way to generate a different first order description of overtone spectra. The basic ideas are those of Henry and Siebrand (3). The latter part of this work represents a departure from traditional theory of overtone spectra (2) in that the representations of the excited state energies are generated almost without the use of the concept of normal modes at all. This involves a certain degree of

parameterization but the assumptions required seemed at all times physically meaningful.

The final chapter consists of a short survey of RRKM unimolecular reaction theory with an emphasis on a problem with the analytical setup of the theory. The effect of anharmonicity on aspects of the theory is discussed. This section represents an attempt to find out where and how information about vibrationally excited states might be used to extract chemically useful information.

A. NORMAL MODES AS A BASIS

In this introductory chapter some aspects of experimental overtone spectra are discussed in order to point out in a concrete fashion what is to be investigated and why. Because of the relatively high intensity of XH overtone transitions relative to overtone transitions of lower frequency oscillators, and because of the importance of XH oscillators in the theory of radiationless transitions (4), it is, for the most part, the excited states of these oscillators that are studied here. Because of the low atomic weight of H relative to carbon or nitrogen the results of this study do not necessarily represent those of a typical oscillator in a polyatomic molecule and extrapolation of the results here to other types of molecules, not containing these XH_n moeities, would be dangerous. With this qualification in mind, what general features of overtone spectra might one expect using anharmonic normal modes as one's point of reference?

The combination bands in substituted benzene rings in the regions between 1600 and 2000 cm^{-1} have long been used in qualitative analysis as an indicator of the substitution pattern or the symmetry of the molecule (5). This is illustrative of one of the criteria for the assignment of overtone and combination bands in polyatomic molecules, namely that the symmetries of the excited states must be

appropriate for absorption. In the general sense of this statement this is of course true but to assume symmetries based on ground state calculations for the excited states of the real molecule may not be realistic (see the discussion of couplings in Chapter 2). In fact all symmetry allowed transitions have been expected to appear in the overtone spectrum with intensities varying from transition to transition because of the effects of mechanical and electrical anharmonicity as well as other higher order interactions. As for benzene derivatives this concept has lead to the assignment of overtone bands in many molecules. The classic example has been the first overtone of the 667 cm^{-1} transition in CO_2 which 'steals intensity' from the fundamental at 1300 cm^{-1} which has the same symmetry. The higher order perturbation, 'Fermi Resonance' gives the overtone anomalously high intensity relative to the fundamental (6).

The point here is that the normal-mode reference system seems to be a very adequate first order basis on which to understand the complexities of these overtone spectra. For XH_n overtones, for example, in methane the $\Delta v_{CH}=3$ overtone structure has been assigned based on the assumption that it is composed of three infrared allowed anharmonic normal-mode CH stretch components (7, 8). It is important to point out here that overtones and combinations of nearly degenerate anharmonic normal modes of vibration should tend to ever increasingly spread out in energy at higher and higher energies

as will be shown in detail in chapter two. Thus one might expect , for the higher and higher overtones , a complicated series of bands or a very broad single band (if the components were not resolvable). This is indeed observed (1) for molecules in the lower overtone regions.

There are two problems however. How can one calculate the complex couplings between modes in polyatomic molecules? Secondly, given that the anharmonic couplings might be quite large, does this affect the degree to which the overtone spectra can be understood using normal modes as a first order basis?

The second of these problems has not been discussed to any degree in the literature on overtone spectra except perhaps implicitly. Normal modes are assumed the point of reference even for higher overtones where anharmonic couplings can be very large indeed. The first of the problems has been worked on from two angles, and is discussed at length in chapter two.

The logic of chapter two therefore will be as follows. The computation of normal-mode anharmonic coupling constants will be investigated. The results of these calculations, in conjunction with some experimental data will then be used to derive a rather different first order description of XH_n overtone spectra which has many simplifying characteristics, both from a conceptual and computational point of view.

CHAPTER 2

POLYATOMIC ANHARMONICITY

The role of vibrational degrees of freedom in determining thermodynamic, spectroscopic and chemical properties of polyatomic molecules has been recognized for some time. In fact, the harmonic oscillator is one of the most fundamental models in physics and chemical physics for many types of physical processes. The classical solution to the equations of motion for a set of coupled harmonic oscillators, with its eigenfunctions, the normal modes of vibration, forms the basis for how most chemists think about the molecules they synthesize and probe by the physical tools available to them.

If you assume a potential between two nuclei of which the second derivative with respect to internuclear separation is constant and similarly couple these nuclei to others in the polyatomic molecule, the stationary states of such a system are an orthonormal set of functions which themselves are uncoupled and each of which correspond to the system moving in simple harmonic motion with each nucleus vibrating with the same frequency (1). Furthermore because the vibrational Hamiltonian and the operator corresponding

to any symmetry operation of the point group of the equilibrium configuration of the molecule commute, the eigenfunctions of normal modes are symmetry adapted.

These two concepts of symmetry and harmonicity will take one a long way in assigning fundamental frequencies in infrared and Raman spectra but are not of unlimited usefulness in understanding the physical processes which involve molecular vibrations. For example as mentioned before the very fact that oscillators will dissociate implies harmonic potentials are but a first approximation. Deviation from this harmonic approximation is generally referred to as anharmonicity. It is to this deviation that the dissociation phenomena and overtone intensity in absorption spectra owe their origins in our current model of the polyatomic molecule.

How does one include the effects of anharmonicity in the description of a vibrating molecule? What effect will anharmonic couplings have on the eigenfunctions of the vibrational Hamiltonian? Or more simply, how do we understand the motion of the nuclei in an other than harmonic force field?

The concept of anharmonicity can be introduced on a more rigorous but still an intuitive basis as follows. This basis will illustrate the origins of the approach to anharmonicity in polyatomics taken in this work.

Expressed in terms of normal coordinates the harmonic oscillator potential energy matrix is diagonal. Internal coordinates do not form an orthogonal set but in practice it is often assumed that the normal coordinate force constants F_{ij} may be obtained by a simple unitary transformation S, from local coordinates assumed orthogonal to normal coordinates (2);

$$S\ f\ S^{-1} = F \qquad (2.1)$$

where F = matrix of normal coordinate force constants

f = matrix of local or internal coordinate force constants

S = orthogonal transformation from internal coordinates to normal coordinates

The S matrix is obtained from symmetry considerations, neglecting internal coordinate overlap, if the molecule has symmetry. A very close analogy may be found in the Huckel treatment of p_z orbitals in pi systems where symmetry can simplify the calculation of the stationary state of the approximate Hamiltonian (9). Many other approximations are used to try to simplify the form of the normal coordinates in qualitative work (for example the separation of high frequency modes of the same symmetry). Once the F matrix has been found the stationary states of the approximate Hamiltonian are found by matrix methods as described in the classic

book by Wilson, Decius and Cross (2). For the purposes of this discussion however attention is focussed on the potential surface alone.

For anharmonic oscillators however the transformation $Sf'S^{-1}$ no longer diagonalizes the force constant matrix because of the appearance of new terms in the vibrational Hamiltonian. For harmonic oscillators

$$F_{ii}(Q_i) = - \left.\frac{\partial V}{\partial Q_i}\right| \quad Q_j, Q_k \ \ldots \text{ constant} \tag{2.2}$$

and the potential energy corresponding to this term is

$$U_i(Q_i) = U_i \Big|_{Q = Q_i} \tag{2.3}$$

where Q_i is a normal coordinate whose contribution to the total energy of the system is exactly separable from those of other degrees of freedom. Thus

$$U_{total} = U = \sum_{i=1}^{3N-6(5)} U_i = \sum_i U_i \Big| Q = Q_i \tag{2.4}$$

Also for the harmonic oscillator

$$- \frac{\partial F_{ii}(Q_i)}{\partial Q_i} = \frac{\partial}{\partial Q_i}\left(\frac{\partial V(Q_i)}{\partial Q_i}\right) = \frac{\partial^2 V(Q_i)}{\partial Q_i^2} = k_{ii} \tag{2.5}$$

is constant and higher order terms in the potential energy matrix for example, $\left\langle \left| \frac{\partial^3 V}{\partial Q_i^3} \right| Q_i Q_i Q_i \right\rangle_{Q_j \text{constant}}$ are zero. Similarly the separability of contributions requires even the quadratic off diagonal potentials to vanish;

$$\frac{\partial F(Q_i)}{\partial Q_j} = \frac{-\partial}{\partial Q_j} \frac{\partial V(Q_i)}{\partial Q_i} = 0 \quad \text{since } (Q_i) \text{ in no way}$$

depends on Q_j.

For the anharmonic oscillator however, where the Q_i are no longer considered as infinitesimally small and where cubic and other higher order terms in the potential energy expression are no longer zero, the potential energy operator U can be expanded in a multicoordinate Taylor series expansion

$$U = \sum_i U_i(Q_i) + \sum_i \frac{\partial U}{\partial Q_i}\Big|_{Q_i \ldots} Q_i$$

$$+ \frac{1}{2!} \sum_i \sum_j \frac{\partial^2 U}{\partial Q_i \partial Q_j}\Big|_{\substack{Q_i Q_j \\ Q_i = Q_j = 0}} \tag{2.6}$$

$$+ \frac{1}{3!} \sum_i \sum_j \sum_k \frac{\partial^3 U}{\partial Q_i \partial Q_j \partial Q_k}\Big|_{\substack{Q_i Q_j Q_k \\ Q_i Q_j Q_k = 0}}$$

These terms , evaluated at Q_i, $Q_j = 0$,are all constants (non zero or otherwise) and thus some of the corresponding matrix elements which contribute to the potential energy would look like, $B_{ijkl} \langle \chi_i | Q_i Q_j Q_k Q_l | \chi_i \rangle$ and to perturbation terms like, $\sum_{\Theta_i} \langle \chi_i | \alpha_{ijk} Q_i Q_j Q_k | \Theta_i \rangle \langle \Theta_i | H^1 | \chi_i \rangle$ / $E_\Theta - E\chi_i$

where $B_{ijkl} = \frac{\partial^4 V}{\partial Q_i \partial Q_j \partial Q_k \partial Q_l}\Big|_{Q_i = Q_j = Q_k = Q_l = 0}$

χ_i, Θ_i are normal mode product wave functions

$$\alpha_{ijk} = \frac{\partial^3 V}{\partial Q_i \partial Q_j \partial Q_k}\Big|_{Q_i = Q_j = Q_k = 0}$$

In particular the last two terms in (2.6) show that the potential energy, or the force 'constant' matrix will no longer be diagonal in a normal coordinate basis since the energy is no longer a sum of terms, each of which depends on the coordinates of only one normal oscillator. This important fact gives rise to the same mathematical problems as including the electron repulsion terms $\frac{1}{r_{ij}}$ in the electronic Hamiltonian. (Note that the non-diagonal character of the normal mode based matrix does not imply that there is no coordinate system which will diagonalize the matrix, although the principal axis system might appear to change as energy of excitation increases because of the simplifications made while trying to visualize the diagonalizing coordinates in terms of molecular structure.)

There are basically two approaches to the problem of eigenvalues for anharmonic states which are tractable from a practical point of view.

1) Include the $a_{ijk}Q_iQ_jQ_k$, $b_{ijkl}\ Q_iQ_jQ_kQ_l$, etc., terms in the vibrational potential and carry out a perturbation calculation to find the eigenstates of an approximate Hamiltonian. The eigenvalues are then used to generate energy differences which correspond to the observables.

2) Take a numerically orientated approach by fitting the experimental data to as low an order polynomial in v_i, v_j, the vibrational quantum numbers for an unknown set

of coordinates, as is possible, and search for a set of coordinates which best satisfy the conditions or parameters observed in experiment. (This is the same procedure in principle as the Wilson FG matrix method which generates force constants and 'normal' modes from frequency data except here the form of the modes can be more general.)

An obvious disadvantage to this second approach is that if the set of coordinates is not simple one may never find an unambiguous set numerically. The principal axis system could appear to change with state energy in a more complicated way than the simple Hermite polynomials so that a polynomial fitting may be impossible. Also this approach is certainly not part of a coherent development of the theory from first principles. However, for such a complicated question this is perhaps to be expected. The hope in this second approach is that the coordinate of best fit will have a physical interpretation which can then be applied directly in calculations for another relatively unrelated molecule.

The first approach, which has appeal in its organization and deductive structure has the difficulty that the expected size of the perturbation (on physical grounds) is so large that even second order perturbation corrections are insufficient. The perturbation modified wavefunctions would be very complex to work out and it would be difficult to see if the new diagonalized coordinate system has a simple

physical interpretation. Also there is not even any guarantee that the perturbation series will converge at all.

A common variation on the first approach, necessitated by the obtainability of data, gives a clue as to the type of potential expression that might be looked for in the second. Instead of trying to obtain the potential surfaces and thus the a_{ijk}, b_{ijkl}, etc. directly from experiment, frequency data is fitted to an energy expression which lumps cubic and quartic terms in the energy matrix together and neglects other higher order terms. Although very much like the second approach this mode of dealing with the problem has the advantage that all the results have an interpretation in terms of the perturbation expansion of the normal-mode basis set.

The energy is now written (instead of as in (6)) as

$$E = E_o + \sum_K v_K \hbar \omega_K^o + \sum_{K \geq L} \sum v_K v_L X_{KL}^o \qquad (2.7)$$

Here the X_{KL}^o can be written in terms of a_{ijk} and b_{ijkl} etc., but there are fewer parameters (and also less detailed information about the potential surfaces) so that with the aid of isotope data these constants can sometimes be obtained spectroscopically. Generally there still is a problem because the X_{KL}^o are quite large and a self consistant set may not be a unique set. The amount of spectroscopic data is generally insufficient except for very small molecules.

This illustrates why it is important to try to relate the constants to structure since there is no other obvious way to establish whether or not a given set of X^o_{KL} are reasonable. (It may seem unreasonable for a term $v_K v_L X^o_{KL}$ to satisfactorily account for cubic terms a_{ijk} in the potential energy expression. However second order perturbation theory (since all cubic first order terms are zero by symmetry) gives the quantum numbers coming out in pairs in the energy expression. For example a typical energy term looks like (2);

$$a_{klm}{}^2 \quad (v_K+1)\ (v_M+1)\ (v_L+1) - v_K v_L v_M \ = \tag{2.8}$$

$$a_{klm}{}^2 \quad (v_K+\tfrac{1}{2})(v_L+\tfrac{1}{2}) + (v_L+\tfrac{1}{2})(v_M+\tfrac{1}{2}) + (v_M+\tfrac{1}{2})(v_K+\tfrac{1}{2}) + \tfrac{1}{4}$$

It is these groupings into pairs which makes the polynomial expansion;

$$E = \sum_i v_i E^o_i + \sum_i v_i^2 X_{ii} + \sum_{i>j} \sum v_i v_j X_{ij} \tag{2.9}$$

theoretically exact to second order so that terms such as $v_i v_j v_k Y_{ijk}$ do not appear in this approximation.)

Approach 2 abandons the perturbation theory relations between the X_{ij} and the a_{ijk}, b_{ijkl} etc., and concentrates on the mathematical form of (2.9). More specifically, a simplified form of (2.9) is fit to experimental data and a set of parameters E^o_i, X_{ij} generated. These parameters are then used to generate more overtone frequencies which act

as checks on the self consistancy of the set of parameters. The work described here tries to generate a set of X_{ij} which are essentially transferable from molecule to molecule, given a set of simplifying assumptions. Normal mode coupling constants are not even approximately transferable . Also , this information gives rise to a new understanding of vibrationally excited states. An account of the route to the theory as it stands presently is given below.

A. XH OSCILLATORS -LOCAL MODES AND INFRARED SPECTRA

Attention in this work is focussed on XH oscillators in polyatomic molecules. Their role as acceptor modes in the theory of radiationless transitions is closely linked up with the Franck Condon overlap factor which is maximized for anharmonic modes of large frequency (lowest possible change in vibrational quantum number)(10). Thus the understanding of this dynamical process may be enhanced if the anharmonic problem for even XH oscillators is better understood. Their frequency makes separability of their contribution to the potential energy a good approximation since modes of widely different frequency do not mix appreciably,

i.e., $$\sum_i \frac{\langle \chi_i | V^1 | \theta_j \rangle \; | \theta_j \rangle}{\Delta E | \theta_j \rangle - | \chi_i \rangle}$$

where $|\theta_j\rangle$ are normal modes of vibration,

$|\chi_i\rangle$

as the appearance of the delta E in the denominator of the first order correction to a normal mode wave function illustrates. This separability and high frequency also makes the XH oscillator overtone and combination progression in an infrared or Raman spectrum particularly easy to identify and thus study in a relative degree of isolation. The simplicity of the theory of local modes is very much linked up with the

fact that H is such a light atom making the separability assumptions which are outlined below very good assumptions. For heavier atoms Y the XY vibrations, or rather modes containing these vibrations, are not separable but even still coupling information may be lost in the overtone spectra because of lack of resolution under conditions necessary to observe the spectra. A demonstration of the insensitivity of the observables to coupling information will be shown in some detail in the work below. Thus the theory here lacks generality, but this does not detract seriously from its usefulness.

The usefulness of considering eigenvalues of a particular vibrational Hamiltonian from a local mode point of view lies in these intermodal couplings. Consider a one dimensional system of two identical, coupled, anharmonic oscillators, s_1, s_2. For infinitesimal amplitudes of vibration this coupling will give rise to two stationary states of the vibrational Hamiltonian, the normal modes of vibration, Q_1, and Q_2 where

$$\begin{aligned} Q_1 &= N(s_1 + S_2) \\ Q_2 &= N(s_1 - s_2) \end{aligned} \tag{2.10}$$

and N is a normalization constant. For very large vibrational amplitudes, however, local mode coupling, on physical grounds must play a smaller role in determining the eigenstates of the molecular Hamiltonian relative to diagonal couplings since the large amplitude vibration corresponding

to dissociation leads to a physical separation of what were two coupled oscillators. This will become more explicit as the expression for the energy in the system is written down first in terms of normal coordinates and then in terms of local coordinates to the order of approximation described above. In terms of normal coordinates as in (2.9)

$$E = E_o + \sum_K v_K \hbar\omega_K + \sum_{K>L} v_K v_L X_{KL} + \cdots \qquad (2.7)$$

In terms of local modes, (the basis of the normal mode description);

$$E' = E_o + \sum_i v_i \hbar\omega_i + \sum_{i>j} \sum c_{ij}\ \omega_{ij} + \sum_{i>j} \sum v_i v_j\ X_{ij} + \cdots \qquad (2.9)$$

The energy of the system is independent of the basis set used to describe it, so that, $E = E'$ and (2.7) and (2.9) may be equated. The c_{ij} are harmonic coupling terms, not equal to zero in the case of local modes since the potential energy even in the harmonic approximation is not diagonalized. The E_o is the zero point energy and the X_{KL} and X_{ij} are the normal mode and local mode anharmonic couplings respectively. Since these couplings depend on the frequency difference between these local modes, and here, these local oscillators are identical, the ω_{ij} should be small. Also the c_{ij} are of the order $(v_i v_j)^{\frac{1}{2}}$ so for all practical purposes this whole harmonic coupling term can be neglected. This approximation is retained in future arguments (3).

Consider the specific case of benzene with its six equivalent CH oscillators. For reasons mentioned earlier the modes are assumed separable from the normal modes of vibration; some 3N-12=24 of them. Symmetry then requires all the X_{ii} and ω_i to be equivalent and also there are symmetry restrictions on the X_{ij}. Thus the number of unknowns in the local mode representation is considerably less than that in the normal mode representation. In principle, the X_{ij} being associated with the interaction between 'chemical bonds', should be easier to estimate than the more difficult X_{KL} couplings. The equivalence relationship,

$$\sum_K v_K \hbar\omega_K + \sum_{K>L} \sum v_K v_L X_{KL} = \sum_i v_i \hbar\omega_i + \sum_i \sum_j c_{ij}\omega_{ij} + \sum_{i>j} \sum v_i v_j X_{ij} \qquad (2.11)$$

will allow the X_{KL} to be expressed in terms of the X_{ij} to the approximation mentioned above. The application of (2.11) is considered in some detail since the method will prove quite general in application from molecule to molecule.

In using (2.11) there are two cases which can arise in general.

1. Each excited normal mode may have the same number of quanta of excitation energy in it and similarly for the corresponding local mode excitation. That is, all the v_K are either equal or zero and all v_i are either equal or zero. Then (2.11) breaks down to two equations; one linear in v and one quadratic in v,

$$N_K v_K = N_i v_i \tag{2.12}$$

$$\sum_{K>L} \sum v_K v_L X_{KL} = \sum_{i>j} \sum v_i v_j X_{ij} \tag{2.13}$$

where the N_K, and N_i equal the number of normal modes and local modes excited. Substituting (2.12) into (2.13) one obtains

$$\sum_{K>L} \sum \left(\frac{N_i}{N_K}\right)^2 X_{KL} - \sum_{i>j} \sum X_{ij} = 0 \tag{2.14}$$

The values for N_i and N_K are easily obtained by writing down the normal coordinates in terms of a linear combination of local coordinates. For example, in benzene the totally symmetric normal CH vibrational wavefunction may be written,

$$Q_{A_{1g}} = 1/(6)^{\frac{1}{2}} \quad (s_1+s_2+s_3+s_4+s_5+s_6) \tag{2.15}$$

where the s_i represent internal coordinates corresponding to CH stretching bond displacements. Here $N_K/N_i = 1/6$. Since all X_{ii} are equal and symmetry requires all corresponding X_{ij} to be equal and thus (2.14) gives,

$$\sum_{K>L} \sum (6)^2 X_{KL} - \sum_{i>j} \sum X_{ij} = 0$$

$$36X_{AA} = 6X_{11} + 6X_{12} + 6X_{13} + 3X_{14} \tag{2.16}$$

The other CH stretching coordinates in complex form for benzene are given by,

$$Q_L = 6^{-\frac{1}{2}} \sum_{j=i}^{6} \exp\ (2\pi i L(j-1)/6) S_j \qquad (2.17)$$

where L = 1, 2, ...5

In a similar fashion, anharmonicity relations for non degenerate vibrations can be written with little difficulty. Degenerate vibrations and combination modes present a problem, however and must be treated more carefully.

Vibrational anharmonicity constants for degenerate vibrations are generated in an averaging process which treats the left hand side of (2.11) as if both members of the degenerate pair were equally excited. Splitting of degeneracy is neglected and the average values are used because experiment does not warrant a more detailed treatment which includes the effects of Fermi resonance for example.

2. In averaging procedures such as the above the superposition of normal modes can lead to unequal local mode excitation as in the case of the methane CH stretch modes. There an averaging involving the triply degenerate mode Q_T, Q_T',Q_T'', yields,

$$Q_T + Q_T' + Q_T'' = \tfrac{1}{2}(3r_1 - r_2 - r_3 - r_4) \qquad (2.18)$$

where the r_i represent internal stretching coordinates. Here although $\nu_T = \nu_T' = \nu_T''$ (2.19)

it is not the case that $\nu_1 = \nu_2 = \nu_3 = \nu_4$ (2.20)

so that, $N_i v_i = N_K v_K$ is not applicable. A solution to this problem lies in the relationship between the classical and quantum mechanical harmonic oscillator. The quantum restrictions on the oscillator's motion do not affect, except for a very small nonclassical penetration into the potential barrier, the classical limits or amplitudes of motion. That is, the potential energy at the turning points of the motion is proportional to the square of the amplitude of vibration. Specifically, to excite a local mechanical harmonic oscillator with an amplitude of three times that of another with an equivalent harmonic force constant, then nine times the energy or nine quanta of excitation would have to be put into the first oscillator relative to the second. That is the semi-classical Hooke's Law identity,

$$(\tfrac{1}{2})\ k(r_i - r_e)^2 = (v + \tfrac{1}{2})h\nu_i \qquad (2.21)$$

would suggest a relationship $(r - r_e) \propto (v + \tfrac{1}{2})^{\frac{1}{2}}$. The conservation of energy restriction as in (2.21) is controlled by the normalization of the wave functions such that if

$$\sum_K a_K Q_K = \sum_j b_j s_j \qquad (2.22)$$

then since Q_i and s_j are assumed to form orthonormal sets in this approximation, it follows that

$$\sum_K |a_K|^2 = \sum_j |b_j|^2 \ . \qquad (2.23)$$

This is easily shown by multiplying (2.22) by $\sum_l a_l^* Q_l^*$ and integrating, then the complex conjugate of (2.22) by $\sum_m b_m s_m$ and integrating and then comparing the results.

$$\left(\sum_l a_l^* Q_l^*\right)\left(\sum_K a_K Q_K\right) = \left(\sum_l a_l^* Q_l^*\right)\left(\sum_j b_j s_j\right)$$

$$\sum_i |a_K|^2 = \sum_l \sum_j a_l^* b_j \langle Q_l | s_j \rangle \qquad (2.24)$$

similarly $\sum_j |b_j|^2 = \sum_m \sum_i b_m a_l^* \langle Q_l | s_m \rangle$

The Q and s are real, Hermite, polynomials so that the overlap integrals are real and therefore (2.23) holds. But for local and normal oscillators of almost the same frequency (2.11) still gives that

$$\sum_K v_K = \sum_j v_j \qquad (2.25)$$

and comparison of (2.23) and (2.25) further suggest an identification,

$$v_K = |a_K|^2 \qquad (2.26)$$

Using this with (2.15)

$$Q_{A_{1g}} = (1/6)^{\frac{1}{2}} (s_1+s_2+s_3+s_4+s_5+s_6) \qquad (2.15)$$

the relationship connecting normal mode anharmonicity constants to local mode anharmonicity constants (2.16), can be

reproduced as well as all the other equal excitation mode combinations. But using (2.26) in (2.11) makes the qualification of equal excitation as in (2.13) unnecessary and,

$$\sum_K v_K \hbar\omega_K + \sum_{K>L} \sum v_K v_L X_{KL} = \sum_i v_i \hbar\omega_i + \sum_i \sum_j c_{ij}\omega_{ij} + \sum_{i>j} \sum v_i v_j X_{ij} \tag{2.11}$$

can be used directly.

Thus the anharmonicity relationship generated by (2.18) is just

$$X_{TT} = (14X_{11} + 5X_{12})/16 \tag{2.27}$$

with only an average X_{TT} defined and where $X_{12} = X_{13} = X_{14} \cdots = X_{34}$ by symmetry. This generalization of the relation generating procedure allows any excitation (subject to the qualifications below) to be used as a generator.

The equivalence relations for benzene, therefore reduce to,

$$\begin{aligned} X_{AA} &= (2X_{11} + 2X_{12} + 2X_{13} + X_{14})/12 \\ X_{AB} &= (6X_{11} + 6X_{13} - 2X_{12} - X_{14})/6 \\ X_{CC} &= (2X_{11} + X_{12} + X_{13} + X_{14})/6 \\ X_{CD} &= (6X_{11} + 3X_{13} - X_{12} - X_{14})/4 \\ X_{AC} &= (10X_{11} - 2X_{13})/3 \end{aligned} \tag{2.28}$$

subject to the following assumptions,

$$X_{AA} = X_{BB} \qquad X_{CC} = X_{CC'}$$

$$X_{CC} = X_{C'C'} = X_{DD} = X_{D'D'} \qquad X_{CD} = X_{CD'}$$

$$X_{CC'} = X_{DD'} \qquad X_{AC} = X_{AD} \qquad (2.29)$$

$$X_{CD} = X_{C'D'}$$

$$X_{CD'} = X_{C'D}$$

$$X_{AC} = X_{AC'} = X_{BD} = X_{BD'}$$

$$X_{AD} = X_{AD'} = X_{BC} = X_{BC'}$$

based upon the number of local mode excitations generated by a linear superposition of these normal modes and where A,B are singly degenerate and C,D doubly degenerate normal modes of vibration. (A more complete discussion of benzene modes can be seen in (3).)

OVERTONE INTENSITY

To put relations (2.28) into use in interpreting I.R. overtone spectra, X_{ij} must be assigned and also some sort of intensity scheme for the formally forbidden transitions must be worked out. Both these problems are really ones of an ongoing nature and this study represents only initial attempts to understand them.

Because the X_{ij} are so closely linked with chemical bonds in this model and especially since XH oscillators are physically suited to the various separability assumptions, an identification is made with the diatomic Morse oscillator. For two diatomics, the dissociation energy, fundamental frequency and anharmonicity are related (1);

$$X_{ii} = \left(\frac{\omega_i}{\omega_{CH}}\right)^2 \cdot \left(\frac{D_{CH}}{D_i}\right) \cdot X_{CH} \qquad (2.30)$$

All the quantities on the right hand side of (2.30) have been measured (for benzene) and therefore X_{11} the local mode diagonal anharmonicity constant is determined. (Originally this was treated as a parameter and altered to give the best fit to experimental results.) As is shown later the off-diagonal local mode coupling constants X_{12}, X_{13}, X_{14} do not affect the band maxima significantly and the physical separation of the CH oscillators suggest the initial approximation that

$$X_{12} = X_{13} = X_{14} = 0 \qquad (2.31)$$

The theoretical implications of such an assumption in an absolute sense are unbearable in the light of experimental evidence concerning thermal chemical reactions, but if the overtone spectra are insensitive to substantial changes in the X_{ij} then (2.31) is a reasonable starting point. Therefore all the normal mode anharmonicity constants X_{AA}, X_{BB}, X_{CC}, X_{AC}, etc., can be numerically evaluated

given (2.31) and (2.30). As will be discussed more critically later, this determination of all the X_{KL} from a force constant calculation is almost always in considerable error (i.e., X_{KL}, $K \neq L$ is usually underestimated).

The question of overtone intensity is more difficult to deal with. There are two interdependent factors to consider ; the symmetry of the excited vibration and the transition moment integral (which is zero for harmonic oscillator multiple excitations, because of the properties of the Hermite polynomials). Effectively mechanical anharmonicity removes the Hermite polynomial character from the excited state vibrational wavefunctions and thereby introduces allowed character to 'forbidden transitions'. (Electrical anharmonicity is not considered here since the intensity from this source is very sensitive to details of the excited state function.)

The symmetry of an overtone (combination) state function is obtained assuming components of the excited state are separable (can be written as a product of single coordinate functions) which is clearly not the case (strictly) if off diagonal X_{KL} are non zero. The method is straightforward and is described in the classic book by Wilson, Decius and Cross (2). The only point needing some intuitive clarification is in the consideration of the symmetry of overtones of degenerate vibrations. Here the

symmetry species of a mode containing more than one quantum of excitation is not found by decomposing the direct product representation of the overtone species with itself (n times). Since this is how one is used to dealing with the symmetry of product functions (decomposing the direct product representation) this may seem puzzling. If one works from first principles, considering the effect of a symmetry operation R on the appropriate functions, there is of course no problem. An intuitive feeling for why a 'symmetrized' direct product must be used can be gleaned as follows.

An n fold degenerate state will normally require an n by n matrix to describe the effect of a symmetry operator R on any of its members (11).

$$R(f\ (Q_1,\ Q_2)\ ) = f(R^{-1}(Q_1),\ R^{-1}(Q_2)\ ) \qquad (2.32)$$

For any product function of an n fold and an m fold degenerate vibrational function (combination band) an n*m by n*m matrix is needed to completely describe the effect of a symmetry operation on the product function. However the effect of a symmetry operator on the function corresponding to multiple excitations of a single oscillator (degenerate or nondegenerate) involves a higher order Hermite polynomial in some coordinate rather than a product of polynomials involving different coordinates. Fewer basis functions and thus a smaller dimensional matrix is needed to describe the trans-

formation. Consider as an example the arbitrary set of triply degenerate normal modes

$$\underline{S}_1 - (s_1, s_2, s_3) \qquad \underline{S}_2 - (r_1, r_2, r_3)$$

where the s_i, and r_i represent members of the degenerate set. To describe the effect of a symmetry operation on a product function involving a member from each of these sets a nine by nine matrix with basis functions s_1r_1, s_1r_2, s_1r_3, s_2r_1, etc., is needed but for the product function involving a member of a set with itself or another member from that set only a six by six matrix with basis functions s_1s_1, s_2s_2, s_3s_3, s_1s_2, s_1s_3, s_2s_3 is needed. This illustrates why the direct product representation contains redundant information and why a symmetrized direct product might be expected, when an overtone of a degenerate species is being decomposed into its irreducible representations. There is no problem for non degenerate vibrations since matrices describing their transformation are all one by one matrices. (The argument above is actually a little misleading since it would lead one to expect that the symmetrized direct product when reduced is always contained in the direct product representation. This problem is removed by noting that when finding the direct product representation one is trying to find the effect of symmetry on a function

$$H_1 (Q) * H_1 (Q) * \cdots \text{ (n times)}$$

where H is the Hermite polynomial corresponding to mode Q with one quantum of excitation. However when one finds the symmetrized direct product, one is trying to find the effect of symmetry on the function

$$H_n(Q)$$

corresponding to the Hermite polynomial of a mode with v=n. These are very different functions and would not be expected to transform identically nor would the reduction of one be expected a priori to be a subset of the reduction of the other.) With this qualification the need for the symmetrized direct product may be more clear.

Since the state of origin, the ground state, is totally symmetric then the symmetry adapted direct product representation must contain an irreducible representation transforming as one of the three cartesian displacement vectors in order that a transition (overtone) be at least symmetry allowed. Recall that even this allowedness is only within the context of the separability approximation above.

The second factor is the relative intensity of one symmetry allowed transition as weighted against another; both involving the same number of quanta of excitation. This problem in principle involves a complete knowledge of the excited state wave functions. Clearly this information is simply not available and almost nothing is known of

polyatomic vibrationally excited functions, the ongoing object of this work. An intuitive intensity factor scheme was developed by Henry and Siebrand in their 1968 paper (3) based on an analogy with the Morse diatomic intensity expression derived by Scholz , in 1932 (12). Scholz's equation predicted that the ratio of the intensity of the vth overtone to the fundamental of a Morse oscillator is proportional to X_{ii}^{v-1}. The polyatomic intensity ratio should reduce to the diatomic expression if only single oscillator excitation is involved and must fall to zero if two or more excited oscillators are uncoupled ($X_{KL} = 0$). This last restriction is not really applicable since it is these couplings in the normal mode basis which are so large that the normal mode description breaks down. However the physical basis of the restriction along with the gradually emerging importance of local modes in the interpretation of overtone spectra will lead to interesting insights into intensity selection rules. Off-diagonal mode couplings give rise to many problems and are much more difficult to deal with than diagonal couplings, but their importance to the physical processes involved in a photophysical process can not be overlooked.

Therefore Henry and Siebrand constructed a binary weighting factor as follows. "For the components of a given overtone all binary combinations of the anharmonic coupling

constants are formed subject to the restriction that the two components have at least one vibration in common. For the overtones corresponding to quantum number v, each anharmonicity is raised to the power (v-1)/2 so that each term will be of degree (v-1)." They illustrate the procedure with the example for benzene where mode A has two quanta, mode B one and one in mode D. The weighting factor J is then;

binary combinations AA AB, AA AD, AA AB, AA AD,
AB AD, AB AB, AB BD, AB BD, AB AD,
AD AD, AD AD, AD BD

(most easily written by assigning each quanta of excitation a number and forming the binary combinations of these with at least one common integer: 12 13, 12 14, 12 23, 12 24, 13 14, 13 23, 14 24, 14 34, 13 34, 23 34, 23 24, 24 34.) Since $X_{AD} = X_{BD}$

$$J = 2(X_{AA}X_{AB})^{3/2} + 2(X_{AA}X_{AD})^{3/2} + 4(X_{AB}X_{AD})^{3/2} + (X_{AB}X_{AB})^{3/2} + 3(X_{AD}X_{AD})^{3/2} . \quad (2.33)$$

Using the J's as ordinates for a component of frequency computed from (2.9), an absorbance curve, the logarithm of the Lorentzian Cauchy product curve was generated (13);

$$I = I_0 \exp(-x_1/(1 + x_3^2(\nu - x_2)^2)) \quad (2.34)$$

where x_1 is J for that component, the relative peak height, x_2 is the frequency of the band center as computed from (2.9)

and x_3 is related to the halfwidth by; halfwidth = $2/x_3$, that is, at a given ν for each component in a band the expression in brackets in (2.34) was evaluated and the resultant numbers summed to give a number proportional to the absorbance at frequency ν. The bandwidth was treated as a parameter which was adjusted so that resolution of individual components in a band was lost as was observed experimentally.*

Combining (2.34), (2.33), (2.31), (2.29), (2.28), and (2.9) with the symmetry restrictions mentioned and using two parameterized values of X_{11}, Henry and Siebrand generated a series of band maxima for the $\Delta v = 1$ to $\Delta v = 6$ overtone bands in benzene. Their numerical results are included in table (2.1) with the calculations subsequently described herein.

Footnote The term, bandfit, used in this report, is a term which refers to the procedures and computer program which construct Gaussian or other named functions around maxima in line spectra.

* A computer program for the bandfit written by Pitha and Jones (13) was modified to include the total calculation of energies and anharmonicities as well as the actual fitting procedure. The changes were straightforward and are not described further here.

B. PROBLEM OF PHASE COINCIDENCE

The 'best' set of normal mode anharmonicity constants generated in (3) were with a value of X_{11}= -55.2 cm^{-1},

$$X_{AA} = -9.2\ cm^{-1} \qquad X_{CC} = -18.4$$
$$X_{CD} = -82.8 \qquad X_{AC} = -184.0 \qquad (2.35)$$
$$X_{AB} = -55.2$$

The paramount importance of the off-diagonal couplings in the normal mode representation, as expected, was the most clear indication of the importance of reconsidering the nature of overtone spectra. The band maxima (table (2.1)) agreed remarkably well with experiment considering the crudeness of the model.

Although a similar treatment was found to be successful for the OH vibrations of H_2O (14), attempts to generalize the procedure in order to obtain anharmonicity constants for the XH vibrations of other polyatomic molecules met with some difficulties. These difficulties arose from the necessity of having to make specific phase designations for the normal modes in obtaining transformation equations from normal to local-mode anharmonicity constants.

To demonstrate the difficulty involved, consider a simple model consisting of N equivalent local modes, labeled

1 through N, which are assumed to be completely decoupled from the rest of the molecule. Assuming further that the molecule has only twofold symmetry elements, we obtain from these local modes n nondegenerate normal modes A,B,C,$\cdots$, by a linear transformation. For N larger than two there is a slight inconsistancy between the equivalence of the N local modes and the absence of a more than twofold symmetry axis. However for our purpose it is sufficient if the equivalence holds approximately so that $\omega_1 = \omega_2 = \cdots$, and $X_{11} = X_{22} = \cdots$ are reasonably accurate approximations. The approximation is also made, which was found satisfactory in the case of benzene, that $\omega_A = \omega_B = \cdots$ so that $\omega_{12} = \omega_{13} = \cdot = 0$ and that off-diagonal local-mode anharmonicity constants $X_{ij} = 0$ ($i \neq j$). In order to proceed a set of transformation coefficients is specified. For simplicity select those cases where all coefficients are $N^{-\frac{1}{2}}$ (overlaps assumed zero in the local mode basis). The naphthalene molecule is an example. In that case it can be seen that every linear combination of two normal modes with the same amplitudes yields N/2 local modes, so that $X_{AB} = X_{AC} = \cdots$ for all normal modes (follows directly from the nature of the D_{2h} character table). More generally each superposition of p normal modes yields N/p local modes if N/p is an integer.

Now applying the methods developed earlier (equations (2.12) and (2.13)), equate the vibrational energy expressions in the two representations. Thus from equal

excitation of p normal modes

$$pv_A\omega_A + pv_A^2X_{AA} + \tfrac{1}{2}p(p-1)v_A^2X_{AB} = (N/p)v_1\omega_1 + (N/p)v_1^2X_{11} \tag{2.36}$$

(p(p-1)/2 is the number of possible binary combinations of normal modes eqn. (2.14))

Under the approximations made above this equation is an identity so terms linear in v can be equated and similarly terms quadratic in v;

$$pv_A = (N/p)v_1 \tag{2.37a}$$

$$pv_A^2X_{AA} + \tfrac{1}{2}p(p-1)X_{AB}v_A^2 = (N/p)v_1^2X_{11} \tag{2.37b}$$

and substituting (2.37a) into (2.37b);

$$pX_{AA} + \tfrac{1}{2}p(p-1)X_{AB} = p^3X_{11}/N \tag{2.38}$$

which gives

$$X_{AA} = X_{11}/N \tag{2.39}$$

for p = 1. Using this result in (2.38) it follows that;

$$X_{AB} = (2(p+1)/N)X_{11} \tag{2.40}$$

where any value of p such that N/p is an integer is allowable. However this result is physically unreasonable unless N = 2 since for $N > 2$, X_{AB} would depend on p the number of modes superimposed in the generating procedure. In other words,

this argument does not lead to a unique value of X_{AB} but leads to a number of values depending on the number of normal modes used to construct the local modes. The precise form of (2.40) depends on the details of the model but the conclusion that X_{AB} depends on p is much more general. The reason why the model worked quite well for H_2O and benzene is due to the fact that for these molecules effectively N=2. For water this is immediately obvious. For benzene there are two nondegenerate and two doubly degenerate modes which mix pairwise. In general because of the quadratic nature of equations (2.7) and (2.9) one would expect the model to work if the normal modes could be grouped into pairs characterized by a specific X_{AB}.

Look more closely at the method used to derive the relationships between the normal mode and local mode anharmonicity constants. The energy equivalence expression which leads to the relations $X_{KL} = f(X_{ij})$, (2.11), was used with the assumption that the superposition of N normal modes with specific phase designations leads to a certain linear combination of local modes. In reality the assignment of specific phase relationships among the normal modes is physically unreasonable. A superposition of normal modes with random phase relationships should be considered, in a matter similar to incoherent wave construction in optics (16). (The synergistic effects of wave amptitude superpositions are

critical to the understanding of experiment in a wide variety of physical experiments; especially those of quantum physics.) If, for example, we designate the local CH stretching motion in benzene at carbon atom i by S_i, then when normal modes A + B are excited the resultant motion in terms of local modes is probably not $(2/3)^{\frac{1}{2}}$ $(s_1+s_3+s_5)$. Instead the coefficients of s_1, s_3, s_5 are probably less than $(2/3)^{\frac{1}{2}}$ and the coefficients of s_2, s_4, s_6 not exactly equal to zero. However as for randomly phased light waves of a similar frequency, when only two normal modes are superimposed, with due regard for random phase differences, the approximation for constructive interference (similarly for destructive interference) is considerably better than when four normal modes are superimposed.

Consider the superposition of N harmonic oscillators of only slightly different frequencies. For complete coherence;

$$A(t) = \sum_{i=1}^{N} A_i \sin(\omega_i t + k_i) = NA_i \qquad (2.41)$$

where A_i is the amplitude of the wave and N is the number of modes superimposed. This requires that at some time t_x

$$\omega_i t_x + k_i = n_i \pi/2 \qquad n_i \text{ an integer} \qquad (2.42)$$

or that simultaneously

$$(\tfrac{1}{2}n_1\pi - k_1)/\omega_1 = (\tfrac{1}{2}n_2\pi - k_2)/\omega_2 = \cdots = (\tfrac{1}{2}n_i\pi - k_i)/\omega_i \qquad (2.43)$$

where all n_i are integers. If N=2 then (2.43) reduces to;

$$n_1\pi/2\omega_1 = n_2\pi/2\omega_2 - k_2/\omega_2 \qquad (2.44)$$

where k_2 characterizes the phase difference between the two modes or just;

$$n_2 = (\omega_2/\omega_1)n_1 + (2k_2/\pi) \qquad (2.45)$$

there are many choices of k_2 for which n_1 and n_2 are simultaneously integers. However for $N > 2$ the probability of simultaneous overlap decreases rapidly for increasing N. In other words, for higher N fewer combinations of these phase constants k_i will satisfy (2.43).

Thus as the number of normal modes which are superimposed increases, the 'incoherent' wave nature of the motions becomes more important and specific phase assignments a poorer and poorer approximation. Conversely the fewer the number of normal modes that are employed in any superposition argument, the better the approximation when a specific phase designation is made in setting up the energy expression, and the more meaningful the set of constants derived from such a model.

C. APPLICATION TO BENZENE

The above considerations imply that in the work described earlier, the expressions for X_{AA} and X_{BB} are exact (no superpositions needed), those for X_{CC}, X_{DD}, X_{AB}, X_{CD} are fairly good approximations, but that the expression for X_{AC} derived from the superposition of four normal modes with specific phase designations, is probably not valid.

Here this anharmonicity constant is treated as a variable parameter while simultaneously fixing X_{11} via relationship (2.30) thus maintaining the same number of input parameters (recall that in(3)X_{11} was varied to achieve the fit with experiment). Using the benzene data listed in (3) (an iterative calculation of ω_e from ω_o, and a chosen X_{AC}), the CH data listed by Herzberg (17) and D_1= 104kcal/mole (18), one obtains X_{11}= -57.5 cm^{-1}, rather than the value X_{11}= -55 cm^{-1} obtained by parameterization in(3) -57.5 cm^{-1} is also the value obtained empirically by Ellis (19). An earlier study by Barnes and Fulweiler (20), who fitted overtone data to the relation,

$$\omega_m = m\omega_o(1-mX) \qquad (2.46)$$

where ω_m is the wavenumber of the radiation absorbed by the oscillator and ω_o and X are constants, gives a value of about -56 cm^{-1}.

Using the above value of X_{11} and the values of X_{AA}, X_{CC}, X_{AB}, and X_{CD}, generated by the transformation equations, X_{AC} was varied to obtain a satisfactory description of the results with a single value of X_{AC}. Also the results from (3)were extended to the v=7 and v=8 bands. The same technique as used in (3) (described earlier herein) was used to construct the spectra. The halfwidths of the component Lorentzian curves for v=7 and v=8 were taken the same as for v=6 (in (3)), i.e., 350 cm^{-1} since no overall structure was observed with these halfwidths.

In figure (2.1) a plot of the ratio of the experimental and calculated energies for the overtones v=3, 4, 5, 6, 7, 8 is illustrated. The linearity suggested in this figure is a real result and not a simplification for the sake of graphing. Except for v=3, 4 the convergence to the experimental frequencies for the value of X_{AC} for other calculated overtones is very good. As pointed out in (3) agreement with experiment is not expected for low v because of higher resolution where the effects of Fermi resonance, etc., would probably be observable and not cancel out as they might be expected to for the many components of a higher overtone band. The behavior of the curves over the range of v studied in figure (2.1) would suggest better convergence at the higher overtones which is in agreement with the above observation. Thus the optimum value of X_{AC} was

found to be $-183.5cm^{-1}$ and the results obtained with this value are shown in table (2.1) along with the previously calculated results from (3) and the new results for v=7 and v=8 using both sets of anharmonicity constants. It should be noted that the value of X_{AC} is not very precise since the results are insensitive to slight variations of X_{AC} as can be seen by the scaling of figure (2.1). The agreement with the experimental values of Ellis (table (2.1)) is excellent and would appear to be well within the expected experimental error for these broad liquid phase peaks. Thus it appears that a single value of X_{AC} is capable of giving a satisfactory explanation of the band centers of the overtone spectrum of benzene.

Figure (2.1) Sensitivity of the calculated CH-stretching overtone frequencies to variations in the normal-mode anharmonicity constant X_{AC}

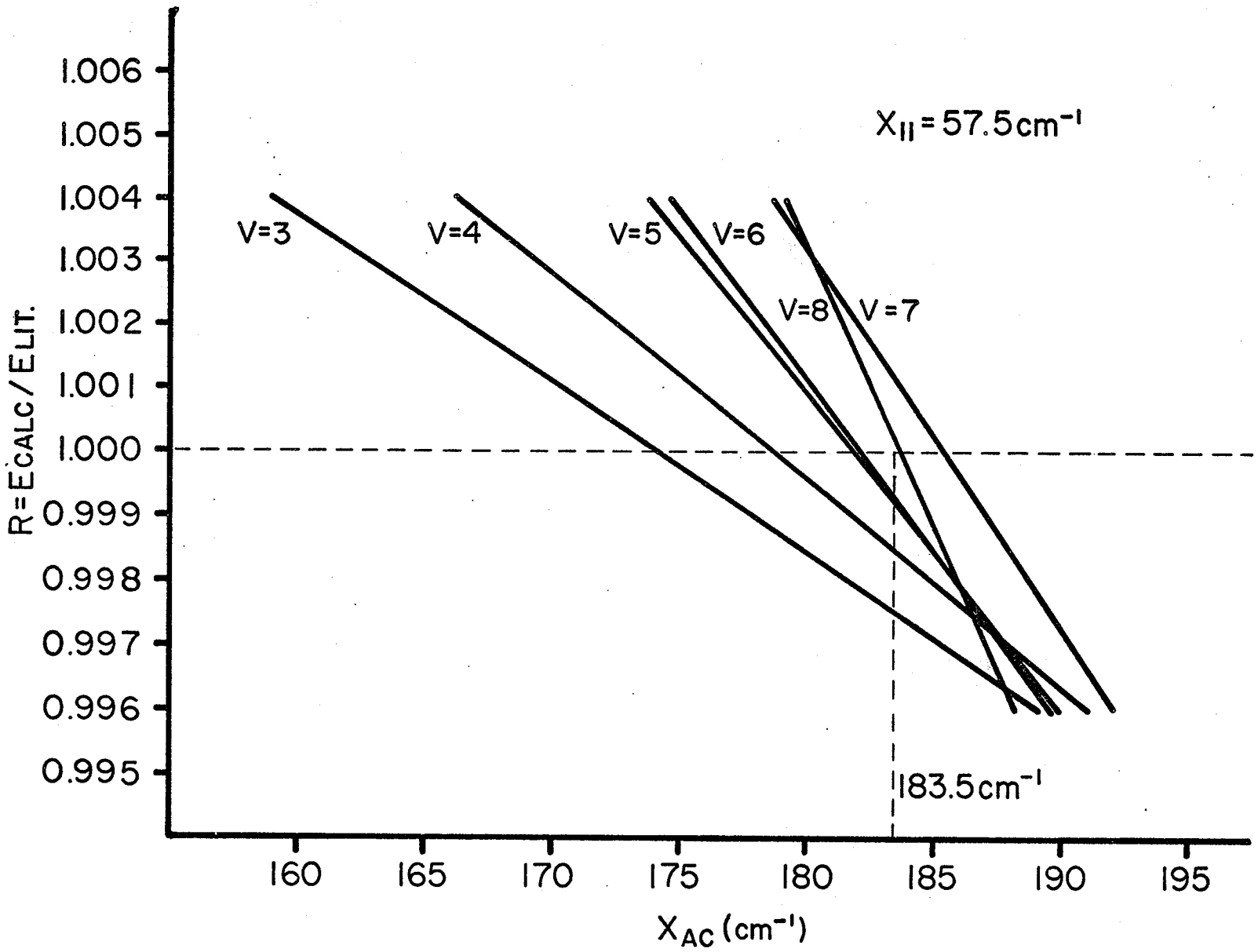
1.006
1.005
1.004
1.003
1.002
1.001
1.000
0.999
0.998
0.997
0.996
0.995
R=ECALC/ELIT.
X11=57.5cm-1
V=3
V=4
V=5
V=6
V=8
V=7
183.5cm-1
160
165
170
175
180
185
190
195
XAC (cm-1)

Table (2.1)

Observed and Calculated CH-Overtone Frequencies in Benzene (cm^{-1}).

v	ν_{obs} [a]	ν_{calc} [b]	ν_{calc} [d]	Components [e]
1	3 060	3 053	3 053	1
2	5 950	5 939	5 940	3
3	8 760	8 740	8 737	8 (9)
4	11 430	11 430 [c]	11 411	14 (20)
5	14 015	14 002 [c]	14 003	25 (42)
6	16 470	16 468	16 458	37 (75)
7	18 800	18 842	18 807	41 (104)
8	21 000	21 015	21 025	55 (167)

[a] Taken from Ref. (19).

[b] Obtained with $X_{11} = -55.2\ cm^{-1}$.

[c] Small differences here from (3) are due to a corrected error in statistical weighting.

[d] Values for $X_{AC} = -183.5\ cm^{-1}$.

[e] Values in parenthesis include statistical weighting.

The new values of the anharmonicity constants generated by the treatment (to be compared with the values from (3) given earlier in equation (2.35)) are,

$$
\begin{aligned}
X_{11} &= -57.5\ \text{cm}^{-1} \\
X_{AA} &= -9.6 \qquad & X_{CC} &= -19.2 \\
X_{CD} &= -86.3 \qquad & X_{AC} &= -183.5 \\
X_{AB} &= -57.5
\end{aligned}
\tag{2.47}
$$

These constants are changed only slightly from the previous set. X_{AA} is in a little better agreement with the experimental value of 12.6 cm^{-1} obtained by Burland and Robinson (see (3)) from an analysis of the CH vibrations in the low temperature mixed crystal phosphorescense of benzene. (This number is not directly comparable because of the dependence of anharmonicity on the medium but should serve as a guide.)

D. GENERALIZATION OF METHOD

A generalization of the approach used in (3) to calculate anharmonicity constants for molecules consisting of sets of nearly identical oscillators whose vibrational motion is approximately independent of the rest of the molecule would be a good start to testing the understanding about the way large molecules move in excited vibrational states. The problem of phase coincidence has been removed and thus other aspects of the theory can be tested. In particular smaller molecules would seem the logical choice to test the effects of the assumption that off-diagonal local mode couplings can be ignored. A first attempt at understanding the structure, if any, of the overtone bands is included in the tests on the smaller molecules although this question is carried further later and is still an on-going problem. The gradual evolution of a different way of thinking of these overtone spectra also has its roots in observations made in the attempt to generalize the methods of (3).

The most important assumption that allowed the CH overtone spectrum of benzene to be described in terms of a single anharmonicity constant X_{11}, was that the off-diagonal local-mode anharmonic coupling constants X_{ij} were negligible. This approximation was justified in terms of vanishing long range coupling for large molecules. A second and concept-

ually more important justification, within the general context of the method, was that by comparison with the dissociation energies of normal modes (involving several oscillators), the much smaller dissociation energies of local modes (single oscillator dissociation) implied a much more diagonal form of the potential energy matrix. In other words, for normal modes the major contributions to the anharmonicity are contained in the off-diagonal anharmonicity constants coupling the normal modes, whereas for local modes the major contributions lie in the diagonal anharmonicity constants. For small molecules, especially for a number of vibrations involving a common atom, contributions from these off-diagonal local-mode anharmonicity constants might be expected, if only for their physical proximity, to play a more important role.

Aside from their obvious structural suitability, ammonia and methane were chosen because of the relatively large amount of experimental data on their overtone spectra so that some comparison of theory and experiment is possible.

E. AMMONIA: A FIRST LOOK

There are two normal-mode stretching vibrations for ammonia of A and E symmetry, (one singly degenerate and one doubly degenerate), respectively (1). The local NH-stretching coordinates are equated to the standard internal coordinates r_j along the NH bonds. In terms of these coordinates the normal modes are written as

$$\begin{aligned} Q_A &= 3^{-\frac{1}{2}} (r_1 + r_2 + r_3) \\ Q_E' &= 3^{-\frac{1}{2}} (r_1 + \varepsilon r_2 + \varepsilon^* r_3) \\ Q_{E'}' &= 3^{-\frac{1}{2}} (r_1 + \varepsilon^* r_2 + \varepsilon r_3) \end{aligned} \qquad (2.48)$$

where $\varepsilon = \exp(2\pi i/3)$. Real functions may be obtained by taking suitable linear combinations, and give;

$$\begin{aligned} Q_E &= 6^{-\frac{1}{2}} (2r_1 - r_2 - r_3) \\ Q_{E'} &= 2^{-\frac{1}{2}} (r_2 - r_3) \end{aligned} \qquad (2.49)$$

Again the NH-stretching modes are thus considered as pure modes and their mixing with bending modes of the same symmetry is neglected. This constraint on the motion will yield slightly higher frequencies in principle but within the approximations of our model, the effect should not be important. Also there are two equilibrium configurations of ammonia but in the light of the first approximation the inter-

conversion to the other configuration will not affect the energy levels.

Again by writing down expressions for the vibrational energy in a normal-mode basis and a local-mode basis, and equating terms linear in v and quadratic in v, relations between normal-mode anharmonicity constants and local-mode anharmonicity constants are generated. For example, excitation of Q_A yields,

$$X_{AA} = (X_{11} + X_{12})/3 \qquad (2.50)$$

where $X_{11}=X_{22}=X_{33}$ and $X_{12}=X_{13}=X_{23}$ from a consideration of the high symmetry. Also for Q_E and $Q_{E'}$, an average value of the diagonal normal mode anharmonicity is taken neglecting the splitting of degenerate overtones as described earlier. Since Fermi resonance is also neglected this is in keeping with the general level of approximation. Thus the superposition of Q_E with $Q_{E'}$ gives,

$$X_{EE} = X_{EE'} = X_{E'E'} = (2X_{11} + X_{12})/3 \qquad (2.51)$$

Finally considering the superposition of Q_A with Q_E and $Q_{E'}$ gives,

$$X_{AE} = (10X_{11} - 2X_{12})/3 \qquad (2.52)$$

For benzene, X_{11} was determined on the basis of equation (2.30), the Morse relationship, and a similar treatment is used for ammonia with a few qualifications. Because

equation (2.30) is based on Morse oscillators, the frequencies are the harmonic frequencies and differ from the observed frequencies by the appropriate diagonal anharmonicity, $\omega_1^0 = \omega_1 + X_{11}$. (This is not strictly true since the anharmonic contribution to the respective zero point energies will not be identical in the two representations in the approximation of (2.7).) Similarly the dissociation energies are measured from the bottom of the Morse potential well and thus differ from the chemically observed dissociation energies, e.g., $D_1^0 = D_0^0 + \frac{1}{2}\omega_1^0 + \frac{1}{2}X_{11}$. Thus the procedure involves starting with the observed ω's and dissociation energies, and a value for X_{NH}, guessing a reasonable value X_{11} to obtain ω_1^0 and D_1^0, and proceeding iteratively to obtain a final value for X_{11}.

In ammonia the procedure is complicated in that a value for X_{NH} is not available experimentally. However this value can be estimated by inference from a plot of X versus ω for a large number of other diatomic molecules (17) as is illustrated in figure (2.2). Thus a value of -75 cm^{-1} for X_{NH} is taken from such a plot and using the observed fundamental frequencies and dissociation energies a value $X_{11} = -70$ cm^{-1} is obtained.

As an initial approximation, a vanishing coupling between local modes is assumed, $X_{12} = 0$. This gives the

following values for the normal-mode anharmonicity constants,

$$X_{AA} = -23 \text{ cm}^{-1},\ X_{EE} = -47 \text{ cm}^{-1},\ X_{AE} = -233 \text{ cm}^{-1} \quad (2.53)$$

From these constants and the values for the fundamental frequencies given by Herzberg, $\omega_A = 3336 \text{ cm}^{-1}$, $\omega_E = 3414 \text{ cm}^{-1}$, the energies of all the overtone components from v=1 to v=6 are calculated. The symmetry selection rule described earlier is applied, with the number of times a symmetry allowed component appears in the reduction of the reducible species used as a weighting factor or statistical factor in the weighting scheme, (J), as was done for benzene. A second factor in the intensity of any overtone component is taken to be the anharmonic contribution to the energy in relation to the anharmonic contributions of other components of the same overtone band. These factors are combined and a weighted average transition energy for each overtone up to v=6 calculated. More elaborate intensity schemes for example the one described for benzene were deemed inappropriate in that the observed bands seemed to possess considerable structure and probably contained significant contributions, as far as intensities are concerned, from Fermi resonance which is neglected here. Secondly, the frequency spread in the calculated components was invariably greater than the observed frequency spread in the overtone band. (This is a significant observation when trying to follow the development of the theory as presented below. These two points will be dis-

Figure (2.2) Diatomic anharmonicity constants for a series of diatomic molecules from which the anharmonicity constant for the NH molecule can be inferred, from its observed fundamental frequency.

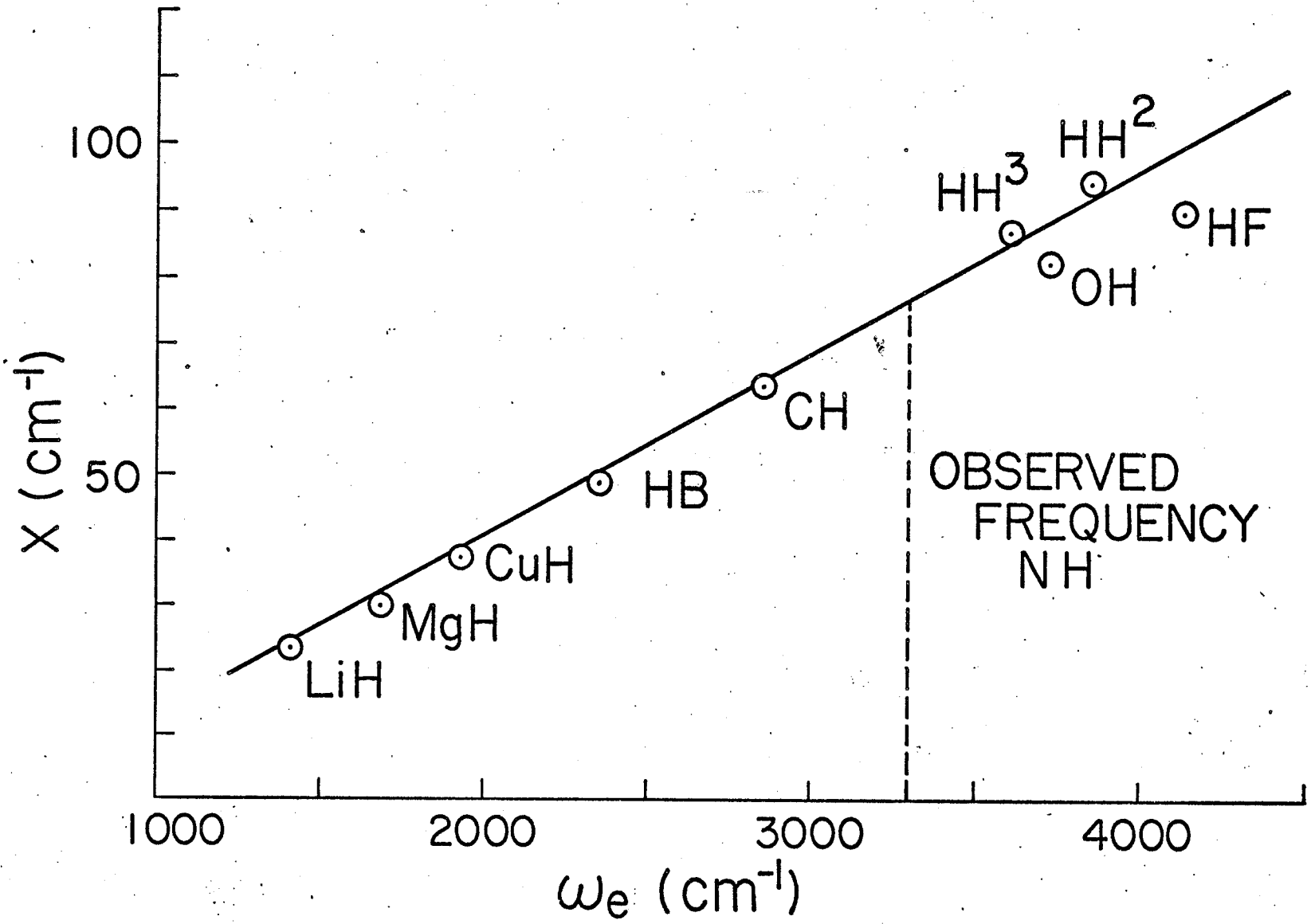
100
50
X (cm⁻¹)
1000
2000
3000
4000
ωe (cm⁻¹)
LiH
MgH
CuH
HB
CH
HH³
HH²
HF
OH
OBSERVED
FREQUENCY
NH

cussed in greater detail in subsequent sections of this chapter.)

The results and a summary of the elements of the calculation using this rather simple weighting scheme are given in table (2.2). The agreement is quite good except for v=3 where an average value has little meaning anyway because of the separation of peaks which is also observed experimentally.

It is of interest to compare the calculated anharmonicity constants with the values given by Bron and Wolfsberg (21). They obtain,

$$X_{AA} = -32.5^{-1},\ X_{EE} = -30.8\ cm^{-1},\ X_{AE} = -79.2\ cm^{-1} \tag{2.54}$$

from force constant calculations of the type described in the introduction to this chapter where the anharmonicity constants are derived from the perturbation theory expansions of the potential energy, which included cubic and quartic terms in the potential energy expression. Although Morino et al (22) obtain slightly higher values for X_{AA} and X_{EE} and a value close to double $-79.2\ cm^{-1}$ for X_{AE} neither set of constants give realistic band energies. These calculations consistantly underestimate the effects of normal mode coupling as can be seen in the first column of table (2.3) where the average energies of the overtone bands are calculated in a similar manner to before except that the anharmonicity

Table (2.2)

Calculated and Observed NH-Overtone Frequencies in Ammonia (cm^{-1})

Component		Symmetry	Calculated Frequency	Weighted Average	Observed Frequency (1)
A	E				
2	0	A_1	6 626		6 595
0	2	A_1+E	6 734	6 615	6 624
1	1	E	6 517		
3	0	A_1	9 870		
0	3	$E+A_1+A_2$	9 960	9 699	9 760
2	1	E	9 574		10 099
1	2	$E+A_1$	9 604		
4	0	A_1	13 068		
0	4	$2E+A_1$	13 092		
3	1	E	12 585	12 683	12 614
2	2	$E+A_1$	12 428		
1	3	$E+A_1+A_2$	12 597		
5	0	A_1	16 220		
0	5	$2E+A_1+A_2$	16 130		
4	1	E	15 550		
3	2	$E+A_1$	15 206	15 546	15 440
2	3	$E+A_1+A_2$	15 188		
1	4	$2E+A_1$	15 496		
6	0	A_1	19 326		
0	6	$2E+2A_1+A_2$	19 074		
5	1	E	18 469		
4	2	$E+A_1$	17 938		
3	3	$E+A_1+A_2$	17 733	18 222	18 150
2	4	$2E+A_1$	17 854		
1	5	$2E+A_1+A_2$	18 301		

Table (2.3)

Comparison of Calculated NH-Overtone Frequencies in Ammonia (cm^{-1})

Over-tone	ω^{a}_{calc}	ω^{c}_{calc}	ω^{d}_{calc}	ω^{e}_{calc}
2	6 681(71)[b]	6 626	6 615	6 625
3	9 919(159)	9 752	9 699	9 709
4	13 088(474)	12 754(+140)	12 683(+69)	12 682(+68)
5	16 602(762)	15 632(+192)	15 546(+106)	15 524(+84)
6	19 220(1070)	18 385(+235)	18 222(+72)	18 187(+37)

[a] Obtained with X_{KL} from (21) using unweighted average.

[b] Difference from the observed frequencies given in brackets.

[c] Obtained with $X_{12} = 0$ using unweighted average.

[d] Obtained with $X_{12} = 0$ using statistical weighted average.

[e] Obtained with $X_{12} = -28\ cm^{-1}$ using statistical weighted average.

constants of Bron and Wolfsberg are used. The increasing overestimation of the overtone energy with increasing v is clearly related to the low off-diagonal normal-mode coupling constant.

Force constant calculations appear to be quite consistant in finding the diagonal normal-mode anharmonicity constants for nondegenerate vibrations. An estimate of X_{12} can be obtained from equation (2.50), a value of X_{11}as calculated and Bron and Wolfsberg's value for X_{AA}. Thus equation (2.50) yields $X_{12} = -28\ cm^{-1}$ for $X_{AA} = -32.5\ cm^{-1}$ and $X_{11} = -70\ cm^{-1}$. Using equations (2.51) and (2.52) the following new values for the normal-mode anharmonicity constants are obtained,

$$X_{AA} = -33\ cm^{-1},\ X_{EE} = -56\ cm^{-1},\ X_{AE} = -215\ cm^{-1} \tag{2.55}$$

Comparison with the values in equation (2.53) shows that the effect of including the off-diagonal local-mode anharmonicity (local-mode coupling) is to partially transfer the anharmonic contribution to the energy from the off-diagnonal to the diagonal potential energy matrix elements. However, the fact that normal-mode coupling retains its paramount importance despite local-mode coupling is still abundantly clear.

With these values for the anharmonicity constants, the overtone band energies were calculated again and the weighted averages are given in column four of table (2.3).

The principal effect of inclusion of local-mode coupling is to slightly decrease the spacing of the calculated overtone components and to produce a small decrease in their energies. These results, as do the weighted average results for $X_{12}= 0$, provide satisfactory agreement with experiment within the errors caused by both experimental causes and the averaging procedures inherent in the calculations. Calculations with other values of X_{12} confirm that in general the results are insensitive to X_{12} although they suggest that X_{12} is less than zero. A similar result was obtained in the benzene calculations. This question of sensitivity of the observable to a part of the theory of such major physical importance to dynamical photophysical processes (see later chapters) will be discussed in more detail but certainly it represents a disappointment. However, with the coming of better laser techniques the possibility of increased resolution, by studying the gas phase overtone spectra at lower and lower pressures, remains a possibility. The couplings more easily observed are those between modes of different physical character; e.g., between bending and stretching modes. Certainly the spectral shifts predicted with various X_{ij} are not so small that their effects would not be observable in principle. On the contrary, the shifts are even noticable with all structure removed from the spectra (liquid phase) so that in the gas phase with increased resolution expected, the opportunity to study this aspect of the theory remains.

Also presented in table (2.3) is a calculation of the overtone frequencies using a straight average of the calculated component frequencies rather than a weighted average. (Recall the intensity problem is still very much up in the air.) Because of the approximations inherent in the theory, the results should improve with increasing v where approximations like the neglect of Fermi resonance should begin to average out. Comparison of the straight average with the weighted average results suggests that some weighting of the components according to their anharmonic contribution and to their statistical degeneracy is indicated. This is also indicated by comparison of the intensity distributions in the observed spectra which show that the intensity contributions of the pure overtone components which appear at higher energy because of their lower anharmonicity are less than the contributions involving combinations of the two normal modes. (This observation will be developed and incorporated into the theory in subsequent sections.)

Previous workers have found considerable structure in the overtone bands (23), particularly for v=2 and v=3. In an attempt to find the width of a rotation-vibration band for a single normal mode component and thus to give a comparison with the overall width and shape of a complete overtone band, a rotational envelope was constructed for the normal mode components using a crude diatomic rigid rotor approximation.

Certainly this symmetric top (in the ground state) molecule is not linear; the presence of the C_3 axis of rotation requires that two of the three principal moments of inertia be equivalent so that the rotational energies are not accurately given by a simple diatomic rigid rotor expression. The crude calculation is inherently unphysical. However to get a rough idea of a bandwidth expected from a rovib band this model should suffice. The moment of inertia was found using the principal axis of rotation as the rotation axis (I is approximately $5 * 10^{-40}$ gm cm^2). The rotational spacing was calculated as

$$\Delta(\Delta E) \approx \hbar^2/I \qquad (2.56)$$

which gives a value of 11 cm^{-1}. The observed separation (23) for v=3 is 11 cm^{-1}. The intensity factors for the rotational lines were calculated in the usual way;

$$\text{Intensity } \alpha(2J+1)\exp(-J(J+1)h^2/2IkT) \qquad (2.57)$$

This model gave a rough estimate of what width of rotation-vibrational band to expect (specifically around 100 cm^{-1}) and using the computed energy levels ($X_{12} = 0$) as band centers and the weighting factors as intensities a rotation-vibration spectrum was constructed. The result for v=3 is shown in figure (2.3).

The observed spectrum although it has similar characteristics, shows low intensities for components farther away

Figure (2.3) Calculated (B) and observed (A) band structure for the v=3 NH stretching overtone of ammonia. The calculated curve was obtained with $X_{12} = 0$. The observed curve was schematically obtained from the data of H. J. Unger in his 1933 paper (Phys. Rev. 43, 123, 1933.)

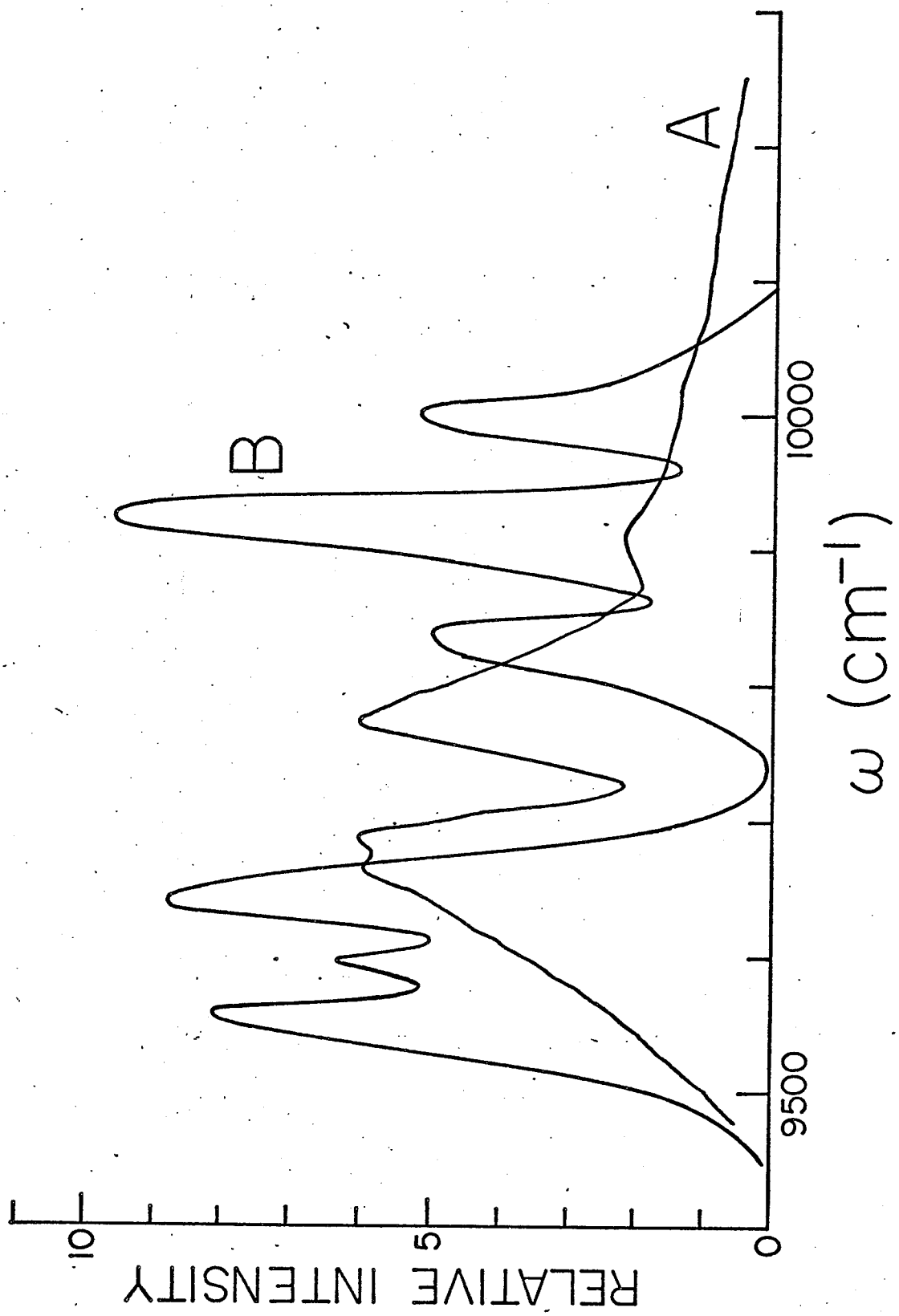
RELATIVE INTENSITY
0
5
10
9500
10000
ω (cm⁻¹)
A
B

from the quoted average band energy. This result is also observed for v=2, i.e. as was noted before, the overall bandwidth is narrower than is calculated. (Certainly the differences do not arise out of the choice of rovib model, namely the diatomic rotar model.) However, it should be noted that some areas of the overtone spectrum (especially around 10 000 - 10 500 cm^{-1}) where activity is predicted, have not been investigated experimentally. This prediction of activity is based on the model of activity developed to this point and as will be shown is subjected to some interesting changes which make further experiments in the above mentioned regions of great theoretical interest.

In attempting to interpret the observed band shape, (figure (2.3)), it is clear that it is not interpretable as the rotational envelope for a single rotation-vibrational band corresponding to a single normal mode component. In terms of normal mode components, the low energy portion of the band is made up of combination components and the extreme high energy end is made up of pure overtone components of the two individual normal modes. Even for v=3 it seems that the description of this band in terms of normal mode components is breaking down since the normal modes themselves are rather ill-defined at this stage of excitation. It would even appear to be physically more reasonable to think of the band as the rotation vibration envelope corresponding to a local-mode overtone. The influence of this

observation on the theory is significant.

Another molecule which presents a new test of the theory, especially in its averaging over degenerate vibrations qualities, is methane.

F. METHANE: A FIRST LOOK

The methane overtone spectrum is treated in two ways. Here the local-mode analysis, exactly similar to the one for ammonia is used to generate the expected overtone band maxima which can be compared to observed values, some of which were obtained by Adel and Slipher (45) using absorption cells hundreds of miles long, that is, the atmospheres of Jupiter, Saturn, Uranus and Neptune. Later the methane spectrum, recorded using apparatus described herein is used as an example which illustrates the concepts involved in the more general local-mode approach. The higher overtone bandshapes have not been previously recorded.

First, however, the focus of attention falls on the position of the overtone maxima. The CH stretching modes for methane are written as;

$$
\begin{aligned}
Q_{A_1} &= \tfrac{1}{2}(r_1+r_2+r_3+r_4) \\
Q_{T_2} &= \tfrac{1}{2}(r_1+r_2-r_3-r_4) \\
Q_{T_2'} &= \tfrac{1}{2}(r_1-r_2+r_3-r_4) \\
Q_{T_2''} &= \tfrac{1}{2}(r_1-r_2-r_3+r_4)
\end{aligned}
\qquad (2.58)
$$

where hereafter A is used to refer to the non-degenerate mode and T to the triply degenerate mode. Again it is assumed that bending and stretching modes are separable. Using the same

procedure as for ammonia and benzene, relations between local-mode and normal-mode anharmonicity constants are generated. With the qualification that only some average X_{TT} is defined, from the excitation of A one obtains,

$$X_{AA} = (2X_{11} + 3X_{12})/8 \tag{2.59}$$

and from the excitation of the three degenerate modes,

$$X_{TT} = (14X_{11} + 5X_{12})/16 \tag{2.60}$$

and finally from the excitation of A and the three components of T,

$$X_{AT} = (84X_{11} - 18X_{12})/24 \tag{2.61}$$

Note that the averaging procedure over triply degenerate components represents a more serious approximation here than for the case of double degeneracy. The value of X_{11} is again found using Herzberg's (17) value for X_{CH} of the CH molecule and the Morse relation, and iterating to find the best value of X_{11} for methane. Taking the values for the methane and CH stretching frequencies from Herzberg and the values of the corresponding dissociation energies from Knox and Palmer's 1961 paper (25), one obtains $X_{11} = -55$ cm^{-1}. Once more assuming that $X_{12} = 0$, the following values of the normal-mode anharmonicities are obtained,

$$X_{AA} = -14 \text{ cm}^{-1},\ X_{TT} = -48 \text{ cm}^{-1},\ X_{AT} = -194 \text{ cm}^{-1} \tag{2.62}$$

Once again large normal-mode coupling is predicted by this model. Using the same form of intensity factors as for ammonia, component energies and weighted averages are computed and the results given in table (2.4). The observed spectra show considerable structure so that the average energies don't have much meaning for the lower overtones. The presence of a large degree of degeneracy in the stretching vibrations of this molecule makes assignments based on the normal mode components generated by this model ambiguous.

On the basis of the results of table (2.4) the anharmonicity constants appear to be slightly too large; particularly perhaps X_{AT}. Since X_{AT} depends quite strongly on X_{12} (2.61), more so than the case of the off-diagonal constant for ammonia (2.52), a non zero value of X_{12} would give higher energies here (note the negative sign in front of the X_{12} gives a lower value to the anharmonicity and thus higher energies). Also the averaging procedure over the degenerate modes has introduced additional approximations for methane and may be responsible for some of the disagreement between theory and experiment.

As mentioned before, this is not the last look at the methane overtone spectrum. A more detailed look at the band shapes of the spectrum will help in understanding the results summarized in table (2.4). This work follows more naturally after a discussion of the general local-mode model and so the methane problem is left for the moment.

Table (2.4)

Calculated and Observed CH-Overtone Frequencies in Methane

Component		Symmetry	Calculated Frequency	Weighted Average	Observed Frequency (1)
A	T				
0	2	T_2+E+A_1	5 944	5 809	5 585
1	1	T_2	5 741		5 775
					5 861
					6 006
0	3	$A_1+T_1+2T_2$	8 771		8 421
2	1	T_2	8 433	8 578	8 604
1	2	T_2+E+A_1	8 471		8 807
					8 900
					9 047
0	4	$2E+2A_1+T_1+2T_2$	11 500		
3	1	T_2	11 099	11 179	11 270
2	2	T_2+E+A_1	10 970		11 885
1	3	$2T_2+T_1+A_1$	11 104		
0	5	$A_1+E+2T_1+4T_2$	14 134		
4	1	T_2	13 737	13 729	13 790
3	2	T_2+E+A_1	13 441		
2	3	$A_1+T_1+2T_2$	13 410		
1	4	$2A_1+2E+T_1+2T_2$	13 640		
0	6	$3A_1+A_2+3E+2T_1+4T_2$	16 670		
5	1	T_2	16 347		
4	2	T_2+E+A_1	15 886	16 093	16 155 (24)
3	3	$A_1+T_1+2T_2$	15 688		
2	4	$2A_1+2E+T_1+2T_2$	15 752		
1	5	$A_1+E+2T_1+4T_2$	16 080		

G. TRANSITION FROM NORMAL-MODE BASIS

The successful description of the overtone spectrum of ammonia and the partial description for methane demonstrates that a local-mode analysis of the XH stretching vibrations in small molecules is valid, and the method is not restricted to large molecules such as benzene and naptha-lene. The major observations drawn from the examples thus far studied might be summarized as follows;

1. Off-diagonal normal mode couplings far greater than force constant calculations have been able, thus far, to predict are necessary in order to even approximately describe observable spectra on any kind of normal-mode basis.

2. For liquid phase or gas phase overtone spectra at high pressure the resolution of bands is not sufficient to study off-diagonal local-mode couplings.

3. The observed width of overtone bands in general is much smaller than might be expected for a normal-mode overtone-combination envelope, despite the fact that in first order all these transitions are forbidden.

What general conclusions do these observations imply? The concept of excitation of specific normal modes in overtones

higher than v=4 seems to push the normal-mode model too far (not a surprising result considering the origin of the normal-mode concept). The description of the excited state in terms of a linear combination of normal modes, and the further presumption that all symmetry allowed normal-mode combinations will be excited, appears to be invalid for a highly vibrationally excited molecule. It seems the effects of mechanical as well as electrical anharmonicity couple the states of a given combination to such an extent that the normal-mode states become ill-defined and a broad band is observed instead of sharp individual peaks.

In this model, therefore, an average energy is all that can be hoped for at this level of approximation. This result is rationalized on a local mode basis in terms of the expectation that for high excitations one wouldn't expect the large number of 'allowed' states of the molecule which the normal-mode analysis predicts, but instead the relatively small number corresponding to multiple excitation of the local modes.

Before proceeding a few general comments are in order. The conclusions just drawn about the model and our understanding of the excited state of a molecule may seem obvious and hardly worth the labour. After all, that molecules vibrate anharmonically is well established. However the fact that the anharmonic modes are themselves coupled to

other modes is less well known and seldom included in model calculations of photophysical processes; for example, Franck Condon factors. Off-diagonal couplings introduce difficulties in calculations and correspondingly in conceptual pictures of these processes. The size of the off-diagonal couplings in relation to the diagonal couplings, has never been satisfactorily dealt with and shown to be necessary to understand experiment. What if the local modes themselves are much more closely related to the stationary states of the molecular Hamiltonian, (which are believed to be the states excited by the photons) than heretofore imagined? This question is investigated below in some detail.

H. A GENERAL LOCAL-MODE THEORY

The XH_n overtone problem is now tackled from a slightly different point of view. The absorption of infrared radiation will be described as corresponding to the excitation of localized modes of vibration rather than a set of symmetry allowed combinations of anharmonic normal modes. This type of approach also makes it possible to begin an investigation of more complicated combination regions of overtone spectra which involve combinations of high and lower frequency modes. More detailed examination of general patterns in overtone spectra and bandshapes makes it clear that the methods of the previous sections could be developed further but that they overlook an overall simplicity characteristic of all the observed overtone spectra. This section is an attempt to interpret this overall simplicity in the light of the ideas developed earlier.

The earlier part of this work has illustrated the importance of off-diagonal, normal-mode coupling (X_{KL} where $K \neq L$) and in fact predicted much larger off-diagonal coupling than recent force constant calculations had indicated (21). The coupling effects in all the cases studied appeared so large that it seems unreasonable to think of the overtone bands past $\Delta v = 4$ as superpositions of symmetry allowed normal-mode overtones and combinations. However, the relatively accurate numerical predictions of band maxima do

suggest that the local-mode approach is very useful and, in fact, physically meaningful. In order to try to understand the numerical success of the calculations in (3), and the previous work, and given this problem with the large off-diagonal couplings in the normal mode representation, let us examine in some detail the features of the experimental band shapes and band widths in the overtone regions.

The basis for the selection of the contributing normal mode components in (3), and the work on methane and ammonia, were the symmetry requirements of the vibrational state. The components were also assigned a weighting factor based on the anharmonic contribution to their energy. Although these "selection rules" gave rise to satisfactory predictions of band maxima, they are shown here to be deficient in that they are unable to account for some of these specific characteristics of the observed spectra. In particular the observed overtone bands are much less complex than expected on an anharmonic normal-mode basis as developed in these earlier descriptions. The observed spectra have a much smaller band width than might be expected if the selection rules mentioned above were operative. It would appear that the radiation field effectively only sees a specific group of the symmetry allowed components. In fact the relatively intense regions of these overtone spectra correspond, in normal mode language, to the most anharmonic combination modes. On

this basis, an attempt to describe the XH stretching contributions to these overtone spectra solely in terms of local mode concepts without any recourse to normal mode components is described.

Parts of the experimental overtone spectrum of ammonia obtained by Unger (23) are used to introduce the model. The Δv_{CH} = 4, 5 and 6 bands of liquid dichloromethane have been recorded and the model has been used to provide a detailed analysis of its overtone spectrum.

I. OCCUPATION NUMBER MAPS

In order to facilitate comparison of a theoretical model for the eigenstates responsible for the optical absorption of a polyatomic molecule in the overtone region with the observed transitions between the actual eigenstates of the molecule, a state counting algorithm was employed. To calculate where any overtone or combination state of any of the possible combinations of the 3N-6(5) vibrational modes would appear in an energy level diagram, the state level counting algorithm of Beyer and Swinehart as described and extended to include anharmonic effects by Stein and Rabinovitch in 1973 (26) was used. The results were used to construct an occupation number map (hereafter referred to as an ONM)*, that is, a map of the number of possible overtone and combination states that a set of n anharmonic, but essentially independent oscillators would generate at any particular energy E. (E here is defined with respect to the zero point energy of the molecule so that the energies in the map directly reflect the difference in energy between the ground and excited state.)

Some type of algorithm is a practical necessity for molecules of any size because of the large number of combination modes that a set of 3N-6(5) oscillators will generate at

*The term occupation number is used here. The concept is synonomous with the overall degeneracy of a state characterized by energy alone. The term is defined, specifically, to distinguish it clearly from the concept of a set of degenerate oscillators.

high energies. Changing the number and type of modes used to generate the ONM, and then comparing the maps with observed bands provides a useful means of assigning transitions within the framework of a particular model.

J. BACK TO AMMONIA

Now the ammonia overtone spectrum is reconsidered by taking a closer look at the general structure of the entire spectrum and also by considering in a more detailed manner the shape of a typical overtone band. Ammonia is chosen since it is one of the very few molecules for which the band shapes in the overtone region are recorded in the literature past $\Delta v=3$. Even still, there are parts of the overtone spectrum which are still to be recorded and would be of interest to this work.

Experimental spectroscopic data for detailed comparison with theory have been obtained from Unger's 1933 paper (23) and data for more general discussion from the papers of Robertson and Fox (27), Badger (28), Lueg and Hedfeld (29), and Jung and Gude (30). All the data represent relatively high pressure gas phase spectra (1-5 atm.), although Unger notes that the results are not too much different for liquid ammonia. This data is presented schematically, with model calculations, in this section in order to give a 'sense' of the general structure of a typical overtone spectrum rather than for details of any particular band.

Assignments of various bands differ widely among these authors and this is a problem on which this approach can shed some light. For example, the assignments of Robertson and

Fox are based on a greatest common denominator sequencing technique in which the physical basis behind selections rules are not considered. Badger's and Unger's assignments were physically more acceptable and, in fact, the model described here retains much of the physical character of the vibrational modes that their assignments imply.

Previous work on benzene, methane, and ammonia indicated that the most anharmonic 'normal-mode' combinations appeared with the most intensity in these XH overtone spectra. Physically this is reasonable and is consistant with theory, since the distortion from the Hermite polynominal nature of the corresponding excited state function would be the greatest for a very anharmonic motion, which would give rise to a source of intensity for these 'forbidden' transitions. The most intense bands, in local-mode language, correspond, in general, to excitation localized in single XH oscillators; conceptually, an excitation of a local mode of vibration.

In order to explore this observation further, an ONM was constructed using a model where NH stretching modes were treated as three degenerate local modes, and the bending modes treated as normal harmonic bending modes (specific details are given below). The pure local mode overtones (all the energy localized in one of the three NH stretching oscillators) were identified for $\Delta v_{NH} = 2$ to $\Delta v_{NH} = 6$ in the ONM. Also modes corresponding to combinations of these pure over-

tone excitations plus one quanta of a bending mode were identified in the ONM and these states were plotted in figure (2.4) along with the experimental data.

In figure (2.4) the experimental data is compared to the energy levels of this select group of overtone and combination bands taken from the ONM of NH_3 constructed from the modes given below. The experimental data are schematic representations of data from (27) - a, (23) - b, (29) - c, (28) - d, and (30) - e. (The doublet structure representation of the bands over 9000 cm^{-1} oversimplifies the observed structure and this is discussed more thoroughly below.) Since the data is taken from various sources, the intensities are not comparable, except to say that the usual behavior of generally, (although not monatonically), decreasing intensity with increasing wave number is observed. The calculated overtones and combinations in the ONM are based upon oscillators with frequencies and degeneracies 3363 (3), 1628 (2), and 950 (1) cm^{-1}, and anharmonicities (X_{11}) of -70, 0 and 0 cm^{-1} respectively. These data were selected as follows. The bending frequencies were obtained from Herzberg (1) and the NH stretching frequency was taken to be a value between the normal-mode fundamentals at 3337 and 3414 cm^{-1}, selected to give the best fit for the NH overtone progression in figure (2.4). The NH stretching anharmonicity constant X_{11} was obtained using the Morse relation and data for the NH molecule.

Figure (2.4) Calculated and observed band maxima for the overtone region of ammonia. The observed bands are schematic representations of data obtained from; ref. (27)-a, ref. (23)-b, ref. (29)-c, ref. (28)-d, and ref. (30)-e. The intensities of the observed bands decrease with increasing energy in general. The calculated transition levels represent (i) NH stretching overtones, (ii) and (iii) combination bands built upon adjacent NH stretching overtone. Calculated bands use oscillator frequencies and anharmonicities 3363(-70), 1628 (0) and 950 (0) cm^{-1}. For the (i), (ii) and (iii) structures no intensity relationships are implied.

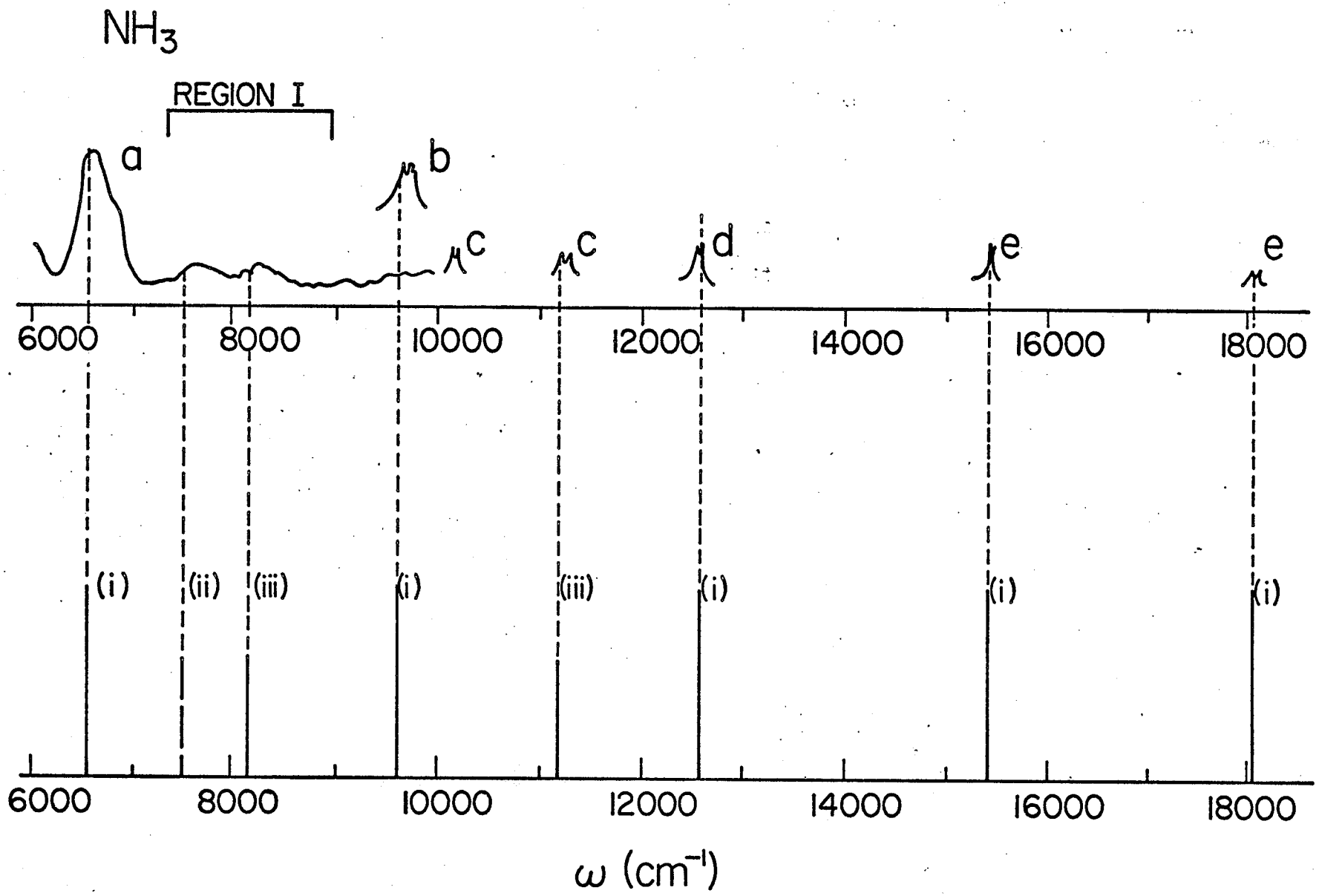
NH3
REGION I
a
b
c
c
d
e
e
6000
8000
10000
12000
14000
16000
18000
(i)
(ii)
(iii)
(i)
(iii)
(i)
(i)
(i)
6000
8000
10000
12000
14000
16000
18000
ω (cm⁻¹)

The similarity of the calculated structures and observed overtone and combination bands in figure (2.4) is striking especially in the higher frequency regions where the structure of the experimental spectra was expected to be much more complex. (This correspondence is described more fully in the section on dichloromethane.) The calculated bands labeled(i) represent multiple excitations of single NH stretching oscillators. The bands labeled (ii) and (iii) represent these same multiple excitations plus single excitation of one of the molecule's 'harmonic' bending modes.

Region I (shown in figure (2.4) is not a pure XH overtone region, and its features, (in the combination region of the spectra), are investigated in more detail in order to explore the possible sources of intensity in the observed spectrum.

Activity in region I does not reflect pure XH stretching-mode activity, be they anharmonic local modes or normal-mode combinations of a more complex structure. Structures in this region reflect the existence of mixture modes; modes representing combinations of high and lower frequency oscillators which are coupled. If the NH stretching modes are treated at this point as anharmonic normal modes, then meaningful analysis of region I cannot be carried out using the ONM technique, as programmed here, since off-diagonal couplings play such an important role in that model. However since the local-mode representation becomes increasingly more

diagonal relative to the normal-mode representation at high energies of excitation, the treatment of these modes as independent oscillators represents a more suitable first order approximation. Thus an ONM was constructed in this region using a model which treated the XH stretching modes as anharmonic local modes and the XH bending modes as harmonic normal modes of vibration using the same frequencies and anharmonicities as were described for the construction of figure (2.4). The two higher frequency modes were assigned degeneracies of three and two. The ONM generated in this region without any selection of contributing combinations consists of 24 components of different energies with many of these components themselves being multifold degenerate. This data is represented by the curve in figure (2.5) which was constructed in the following way.

Each level in the ONM was assigned a weight proportional to its degeneracy. As before each component was assumed as a centre of a Lorentzian band contour function (3) with a bandwidth of 80 cm^{-1}, enough to remove the fine structure, which has little meaning in this type of analysis. The product function was formed and plotted as curve (ii) in figure (2.5). Figure (2.5) (i), shows a graphical plot of the numerical intensity data obtained from Unger's paper (23). There seems to be considerable correspondence between the two curves.

It is important to notice that experimentally, these mixture-mode structures (ii and iii) disappear at higher energies whereas the pure XH stretching overtone bands disappear relatively more slowly. Within the framework of this ONM model this observation can be stated in the form of a selection rule which has physical meaning. Specifically, high frequency, single oscillator, multiple excitations are more active than lower frequency single oscillator excitations and combination band or mixture mode excitations. In the section on dichloromethane, where more experimental data are available, these rules will be refined and examined more critically.

Finally it is of interest to note that the pure overtone progression in figure (2.4), (6600, - 9800, 12600, 15440, 18150 cm^{-1}), as given in Herzberg (1), consists of bands of relatively narrow bandwidths (usually less than 300 cm^{-1}). By comparison, the spectrum expected on the basis of anharmonic normal-mode components would exhibit both greater complexity and greater spectral breadth. This point is discussed and illustrated in some detail for dichloromethane. Also these bands exhibit some rovib structure when gas phase spectra are examined.

Figure (2.5) The experimental overtone spectrum taken from the numerical data of Unger (23) (i), and an ONM representation of the position and degeneracy of overtone and combination states (ii) of the modes of frequency and anharmonicity 3363 (-70), 1628 (0) and 950 (0) cm^{-1} of degeneracies 3, 2 and 1 respectively. The calculated Lorenzian product funtion was constructed assigning each component a weight proportional to its degeneracy. The bandwidth of each bandfit component is 80 cm^{-1}.

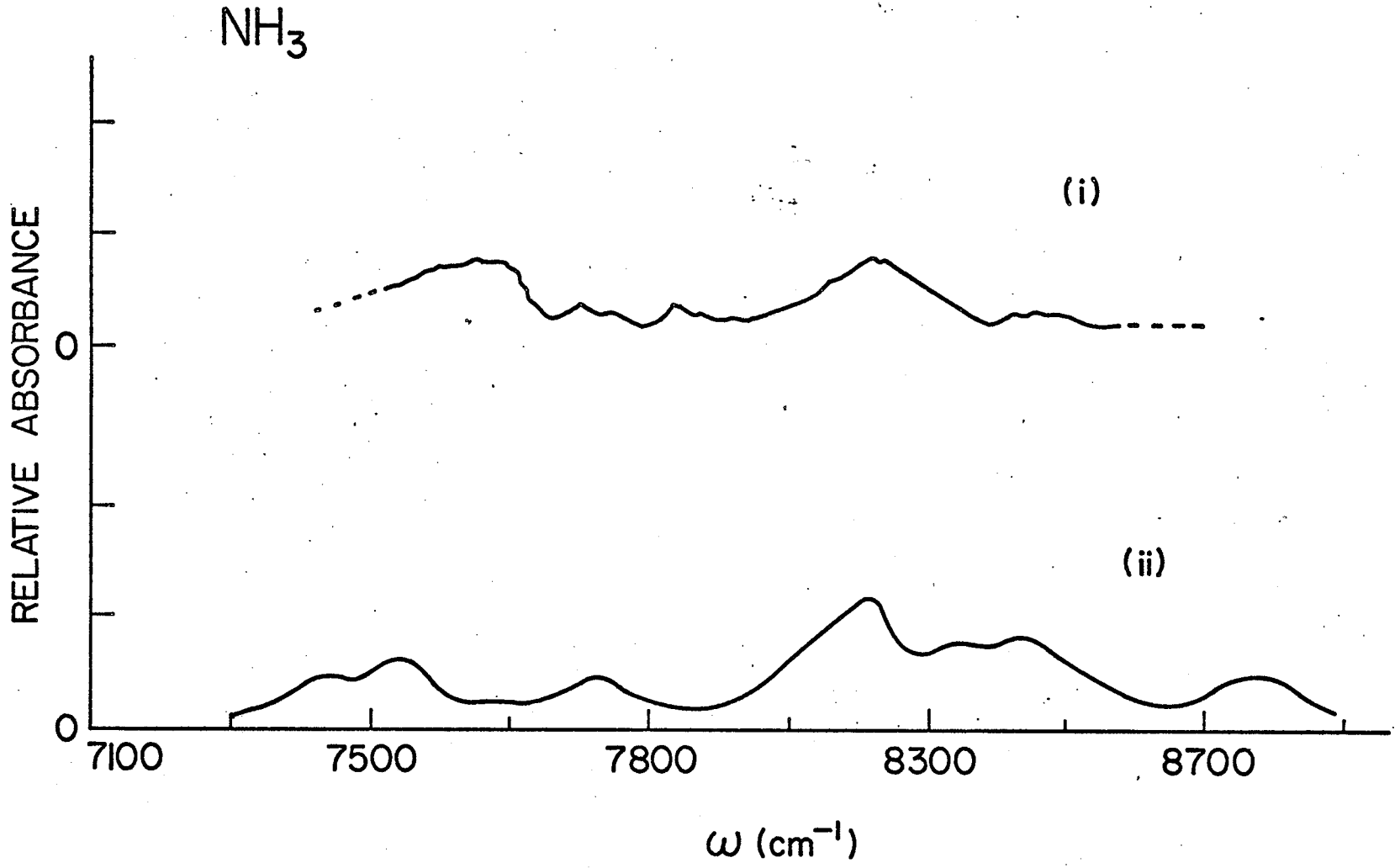
NH3
RELATIVE ABSORBANCE
0
0
(i)
(ii)
7100
7500
7800
8300
8700
ω (cm⁻¹)

K. DICHLOROMETHANE

Now the overtone spectrum of CH_2Cl_2 is considered. It is of interest for at least two reasons. Firstly the spectrum could be recorded by equipment available. Secondly, comparison with the methane spectrum provide a meaningful test of the generality of the general local mode theory. In particular one might expect the spectra to be quite similar for these two molecules and indeed similar to the spectrum of chloroform. That this does actually turn out to be the case will be expanded on later, but here, the general local mode theory is developed within the context of the overtone spectrum of this molecule.

The overtone spectrum lower in energy than 9260Å ($10800\ cm^{-1}$) was taken from the pure liquid room temperature spectrum of Ellis (31). The higher energy overtone spectrum to $19000\ cm^{-1}$ was obtained on the Cary 14 spectrophotometer using a 0.1 to 0.2 absorbance slidewire with the IR tungsten source as the analyzing light. Two 5 cm quartz cells were placed back to back to give an effective path length of 10 cm. Spectral quality dichloromethane from Matheson, Coleman and Bell was used as received. The spectra are shown in figures (2.6), (2.7), and (2.8) where the bands corresponding to the CH overtones Δv_{CH} = 4, 5, and 6 are identified. The band maxima corresponding to these overtones occur at 8850Å, 7223Å and 6165Å respectively (11309, 13845 and $16219\ cm^{-1}$). The

Figure (2.6) Overtone spectrum of liquid dichloromethane at 296°K in the range from 9400 to 6400Å.

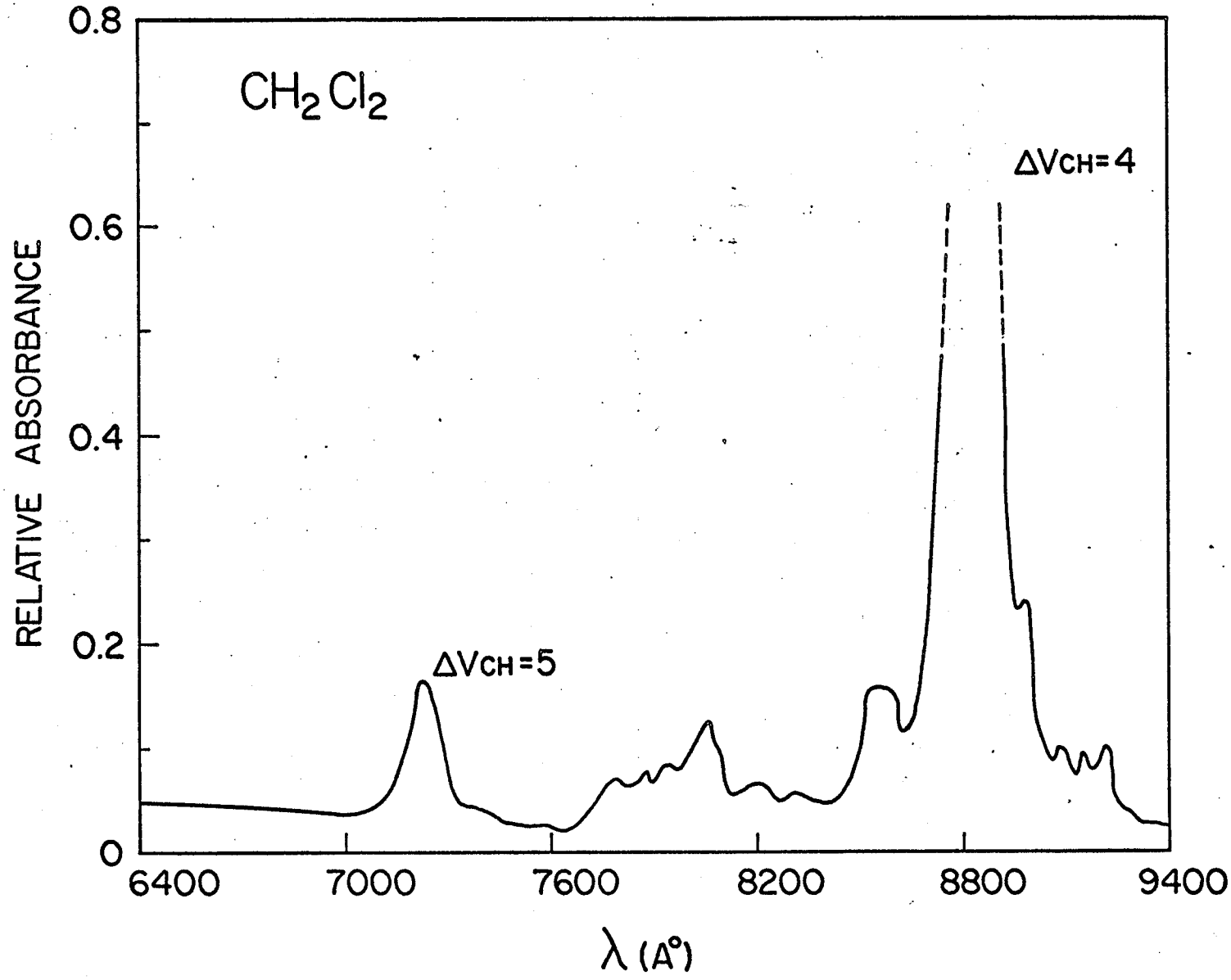
CH_2Cl_2
ΔVCH=4
ΔVCH=5
RELATIVE ABSORBANCE
0.8
0.6
0.4
0.2
0
6400
7000
7600
8200
8800
9400
λ (A°)

Figure (2.7) Overtone spectrum of liquid dichloromethane at 296°K in the range 7500 to 5200Å.

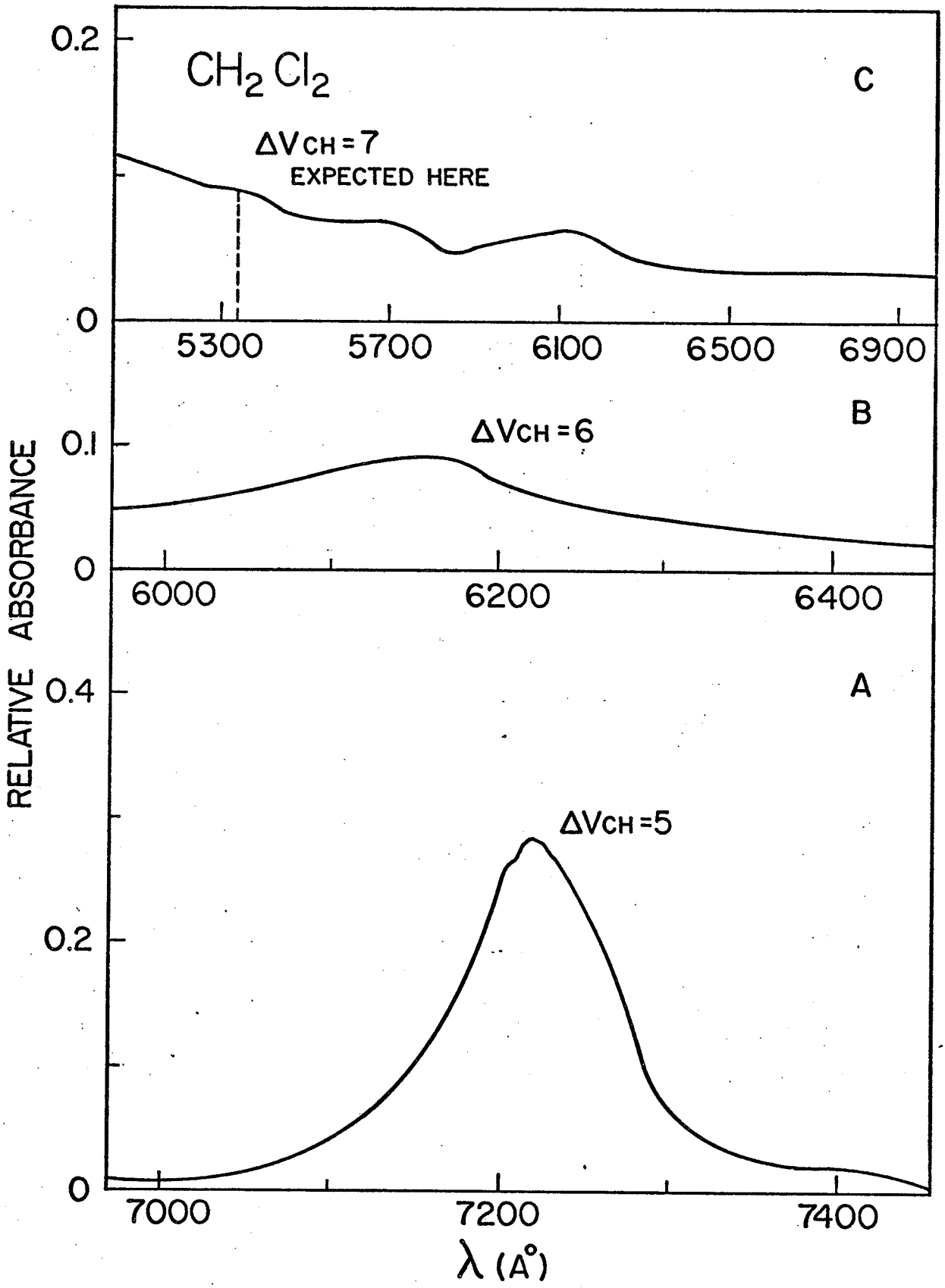
CH_2Cl_2
C
$\Delta V_{CH} = 7$
EXPECTED HERE
0.2
0
5300
5700
6100
6500
6900
B
$\Delta V_{CH} = 6$
0.1
0
6000
6200
6400
A
$\Delta V_{CH} = 5$
0.4
0.2
0
7000
7200
7400
λ (A°)
RELATIVE ABSORBANCE

Figure (2.8) Calculated and observed CH stretching overtone band of dichloromethane corresponding to $\Delta v_{CH} = 4$. A- (----), the calculated bandfit curves for the anharmonic normal-mode components taken from Table I, (————), the low resolution experimental spectrum. B- (-------), computed bandfit spectrum of overtones and combinations of the modes with frequency and anharmonicity 2991 (-55), 2991 (-55), and 1429 (0) cm^{-1} with a weighting of the fundamental local mode overtone 50 times that of a combination band of the same degeneracy. All computed components were assigned a bandwidth of 80 cm^{-1}.

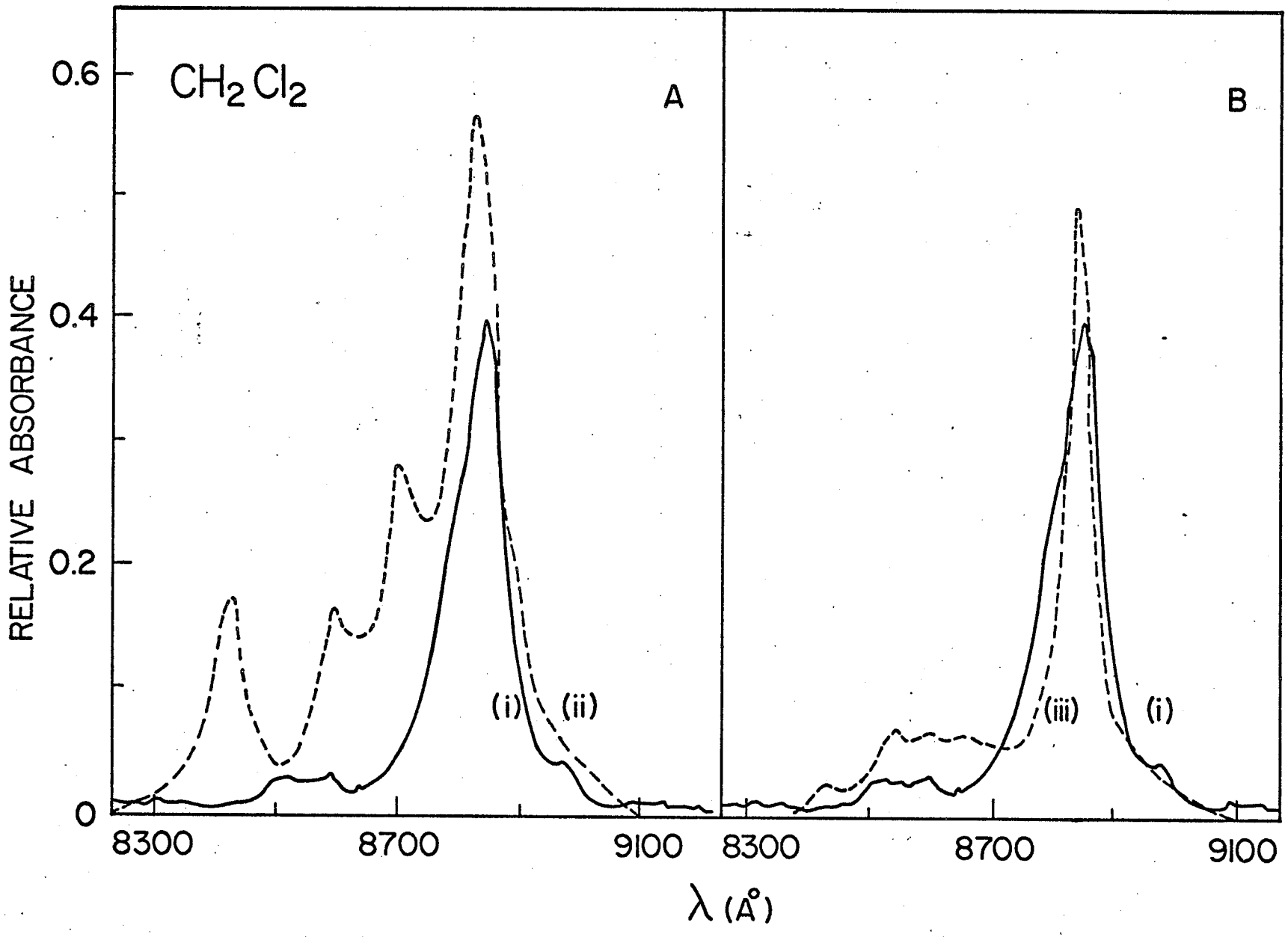
CH_2Cl_2
A
B
0.6
0.4
0.2
0
RELATIVE ABSORBANCE
(i)
(ii)
(iii)
(i)
8300
8700
9100
8300
8700
9100
λ (Å)

(90T)

band at 8850Å has been observed previously by Vierling and Mecke (32) at somewhat lower resolution.

In the ground state dichloromethane has a tetrahedral structure and belongs to the point group C_{2V} (1). It has two CH stretching modes of A_1 and B_1 symmetry respectively. In terms of local coordinates, s_i, the normal coordinates, in the approximation of high frequency mode separation, are

$$Q_{A_1} = (1/\sqrt{2})\ (s_1 + s_2)$$

and

$$Q_{B_1} = (1/\sqrt{2})\ (s_1 - s_2) \qquad (2.63)$$

Using the methods described earlier, one can write the normal mode anharmonicity constants in terms of local-mode anharmonicity constants as

$$\begin{aligned} X_{A_1A_1} &= (2X_{11} + X_{12})/4 \\ X_{B_1B_1} &= (2X_{11} + X_{12})/4 \\ X_{A_1B_1} &= 4X_{11} - X_{A_1A_1} - X_{B_1B_1} \\ &= (6X_{11} - X_{12})/2 \end{aligned} \qquad (2.64)$$

The local-mode generation of normal-mode anharmonicity constants depends on the evaluation of only two constants, X_{11} and X_{12}, the first of which can be estimated in principle

using the Morse relation as in II. On physical grounds one might expect the X_{12} to be small as for the cases of ammonia and methane discussed earlier. This anharmonic normal-mode model is discussed below in relation to a purely local-mode representation.

The CH stretching progression can be identified, from this data, as the series of bands 5970, 8696, 11309, 13845, and approximately 16240 cm^{-1}. This last band is very weak and broad and there is considerable uncertainty as to how to define its rovib origin. The other features of the overtone spectrum, such as the combination activity between 8300 and 7600 $\mathring{A}$ in figure (2.4), can also be interpreted in the local mode scheme. In the present report, these regions are discussed only briefly.

Two observations which are related to the general characteristics of the experimental spectra, are of considerable importance in trying to understand the origins of optical absorption.

1. Overtone spectra of hydrocarbons with different types and numbers of $R\text{-}CH_n$ functional groups give rise to very similar overtone band structures. (See for example figure 1 of reference (31).)

2. The observable bandwidths of the XH overtone bands are generally less than 300 cm^{-1} and are often closer to 150 to 200 cm^{-1}. For example, the $\Delta v_{CH} = 5$ overtone band (part A

of figure (2.7)) of dichloromethane has an approximate width at half height of 280 cm^{-1}.

If these bands were built up of all possible symmetry allowed normal-mode combinations, on the basis of an intensity scheme as described earlier (intensity greater the more anharmonic the mode), a much more complex, or at the very least a broader band, would be expected. Anharmonic normal-mode component energies as determined by the local-mode analysis (equations (2.64)) assuming $X_{11} = -55$ cm^{-1} and $X_{12} = 0$ have been given in table (2.5). The components for $\Delta v_{CH} = 5$ range in energy from 14600 to 13838 cm^{-1}. As can be seen from part A of figure (2.7), there does not seem to be corresponding structure in the observed spectrum even taking into account decreasing intensity with decreasing anharmonic contribution to the energy. This lack of structure for overtone bands is quite generally observed. Note also that the CH stretching overtone progression for dichloromethane, is more closely related to those modes in table (2.5) which are more anharmonic than even the anharmonically weighted averages, at least for the higher overtones where the local mode model is expected to have the most meaning. In fact the observed overtone progression appears very much like the series of the most anharmonic components. Physically, as can be seen from equation (2.63), this corresponds to the multiple excitation of a single local oscillator. The most intense structures in the observable overtone spectra

Table (2.5)

Calculated and Observed CH Overtone Frequencies in Dichloromethane (cm^{-1})

Component		Calculated[a] Frequency	Weighted[b] Average	Observed Band Maximum
A_1	B_1			
2	3	5 913		
0	2	5 867	5 871	5 970
1	1	5 848		
3	0	8 787		
0	3	8 979	8 786	8 696
2	1	8 631		
1	2	8 695		
4	0	11 606		
0	4	11 862		
3	1	11 340	11 502	11 309
2	2	11 294		
1	3	11 468		
5	0	14 370		
0	5	14 690		
4	1	13 994		
3	2	13 838	14 125	13 845
2	3	13 902		
1	4	14 186		
6	0	17 079		
0	6	17 463		
5	1	16 593		
4	2	16 327	16 656	16 240
3	3	16 281		
2	4	16 455		
1	5	16 849		
7	0	19 733		
0	7	20 181		
6	1	19 137		
5	2	18 761	19 093	
4	3	18 605		
3	4	18 669		
2	5	18 953		
1	6	19 457		

a - Obtained with $X_{12} = 0$.

b - Obtained with $X_{12} = 0$ using anharmonically weighted averages.

correspond, in local-mode language to an overtone progression of excitations of single oscillators rather than the more complicated motions where several (identical) oscillators are excited simultaneously. This information along with observation 2 above imply a very simple first order interpretation of an overtone spectrum for a molecule from this class of molecules. For higher overtones the molecule and radiation field interact in such a way that, effectively the molecule selects those photons which will lead to states of localized excitation, local oscillators. The possibility that the localized functions might be much more closely related to the eigenstates of the molecular Hamiltonian than is recognized in normal-mode calculations has been discussed earlier and thus the observed pattern of behavior is not altogether surprising.

If the observed spectral band maxima do correspond to multiple excitations of single oscillators with 'unusually' high intensity, and other combination bands appear with much less intensity, then there will be some differences in the bandshapes predicted on this basis from those obtained by using the weighting schemes described earlier, that is when the normal-mode intensity based selection rules are used.

For example, consider the $\Delta v_{CH} = 4$ band which has been presented in figure (2.8) along with two bands calculated on the basis of two models. The solid curve represents

the experimental liquid phase spectrum at a slightly lower resolution than is optimally possible under our experimental conditions. The dotted curve in part A represents a bandfit spectrum constructed on the basis of procedures in (3) and (33), and based on the overtones and combinations of the two normal modes with frequencies and anharmonicities 2984 (-27.5), 3048 (-27.5) (off-diagonal coupling = $3X_{11}$ = -165 cm^{-1} as given by equations (2.64) with X_{12} = 0). This is the anharmonic normal-mode representation of the CH overtone band. The components (listed in table (2.5) are weighed relative to each other by their anharmonicities only. All components were assigned a halfwidth of 80 cm^{-1}.

It is clear from the diagram why relative success was obtained in reproducing band maxima in (3) and subsequent work in the anharmonicity weighting scheme of averages, since the lower frequency components, by virtue of their anharmonicity, are given the most weight. What is not clear is why the other high frequency components which are symmetry allowed (although forbidden in any first order calculation as are any overtone or combination transitions due to the nature of the Hermite polynomials), are apparently relatively weak. Also note that within the framework of that work there is no accounting at all for activity at a lower frequency than the most anharmonic CH mode. Considering the great difficulty in trying to understand the oscillator strengths for overtone transitions, the reason for the apparent

lack of fit could be explained by assuming that the theoretical analysis using the anharmonicity weighting as a measure for the relative oscillator strengths is not adequate. For example the high frequency modes might be thought of as having their intensity 'stolen' by fundamentals or lower frequency overtones of the correct symmetry. Specifically, higher order perturbation calculations might be attempted given that some fairly accurate potentials could be established. However there is no guarantee that the series of corrections to the normal-mode functions would converge and the final wavefunctions still would be accurate only within the manifold of approximations that went into the establishment of the effective vibrational Hamiltonian (e.g. adiabatic vibrational manifold). The solution to the problem using this approach seems impossible given the present state of data on the excited states of polyatomic molecules. Here it is simply assumed that the local excitations do carry enhanced optical absorption relative to the combination states and the consequences of this assumption are illustrated in part B of figure (2.8). As for ammonia, this is a local-mode representation of the CH oscillators with the parameterized fundamental stretching frequency along with a normal-mode frequency for the bending mode. The dotted curve here represents a bandfit spectrum based on overtones and combinations of the three modes with frequencies and anharmonicities 2991 (-55 cm^{-1}), and 1429 (0). The local-mode

fundamental overtone (all the energy localized in a single oscillator) was assigned an arbitrary weighting relative to the other combination modes (**arbitrary in the sense of using this as a variable parameter**) which in turn were weighted relative to each other only according to their degeneracies in the ONM. All components were assigned a half-width of 80 cm^{-1}. The local-mode fundamental frequency is not exactly the same as either of the corresponding normal-mode component frequencies. The value 2991 cm^{-1} gave a better fit for all the overtone bands investigated than with either 2984 or 3048 cm^{-1}. The difference here is not large nor is it unexpected given the physical nature of the problem. The X_{11} used here, -55 cm^{-1}, is the CH stretching local-mode anharmonicity constant computed for methane in (33) The dissociation energy for the reaction $CH_2Cl_2 \rightarrow CHCl_2 + H$ was not available for use in the Morse relation. Since X_{11} for benzene was only -57.7 cm^{-1}, it is apparent that this constant does not change radically with structure, so that taking X_{11} for dichloromethane the same as that for methane should not introduce serious errors. The correspondence of curves (i) and (iii) in figure (2.8) suggest the following selection rules for the model;

1. Local-mode overtones involving high frequency oscillators are the most intense but decrease rapidly in intensity with increasing Δv.

2. Combination bands involving degenerate oscillators of

high frequency and combination bands involving modes of high and lower frequency appear with much less intensity than pure 'local-mode overtones'.

For example, the curve labeled (iii) in figure (2.8) was constructed assuming the local mode overtones were 50 times more intense (this number is corrected for degeneracy) than a combination band, and as stated earlier all the combination bands were weighted relative to each other according to their degeneracies. The bandwidth of 80 cm^{-1} used to construct (iii) was arbitrary. The nature of curve (iii) is quite different from the normal-mode component curve. However, in the construction of (iii), there are three parameters; fundamental local mode frequency, bandwidth and weighting of the fundamental overtone relative to the other components. The first parameter, the fundamental frequency was used for all the overtones in the dichloromethane series. The second of the parameters was adjusted to remove fine structure from the calculated spectrum (as in (3)). The final parameter, is the weighting ratio. It could be further refined to bring curves (iii) and (i) into finer agreement (actually a value of 80 gives the best fit) but the curves illustrated in the figure point out the nature of the result obtained in this kind of analysis.

A very similar pattern of behavior to that illustrated in figure (2.8) is expected for higher overtone bands.

The actual behavior is illustrated in figure (2.9) for the $\Delta v_{CH} = 5$ overtone. As before the dotted curve in part A is the bandfit curve of the six components listed in table (2.5) for the CH stretch overtone and combination bands weighted according to their anharmonic contribution to the energy. The solid curves correspond to the experimental spectrum (figure (2.7)). The dotted curve in figure (2.9) part B represents a bandfit analysis of the states taken from the ONM using the modes and anharmonicities 2991 (-55), 2991 (155), 1429 (0) cm^{-1} with levels weighted, as before, according to their degeneracies in the ONM except for the CH fundamental overtone which was assigned a weight 200 times that of a combination band of the same degeneracy. Lower ratios gave wings in the bandfit spectrum which are not observed experimentally. Experimentally, as shown in figure (2.7), an almost structureless band with a small amount of asymmetry on the high frequency side is observed. The band-width used in the bandfit analysis was 150 cm^{-1}. The two structures in part B of the figure compare quite favorably. The slight shift in peak maxima probably reflects the crudeness of the parameter choice. No attempt has been made to adjust X_{11} and, for example, if X_{11} were chosen as -56 cm^{-1} rather than -55 cm^{-1} the calculated peak would be shifted 30 cm^{-1}. This data reflects the existance of another important selection rule, namely that within the framework of this model, combination bands fall more quickly in intensity than the local-mode

Figure (2.9) Calculated and observed CH stretching overtone band corresponding to $\Delta v_{CH} = 5$. A- (------), the calculated bandfit curves for the anharmonic normal mode components taken from table (2.5); (————), schematic representation of the low resolution experimental spectrum. B- (-----), computed bandfit spectrum of the overtones and combinations of the modes with frequencies and anharmonicities 2991 (-55), 2991 (-55), and 1429 (0) cm^{-1} with a weighting of the fundamental local mode overtone 200 times that of a combination band of the same degeneracy. All computed components were assigned a bandwidth of 150 cm^{-1}.

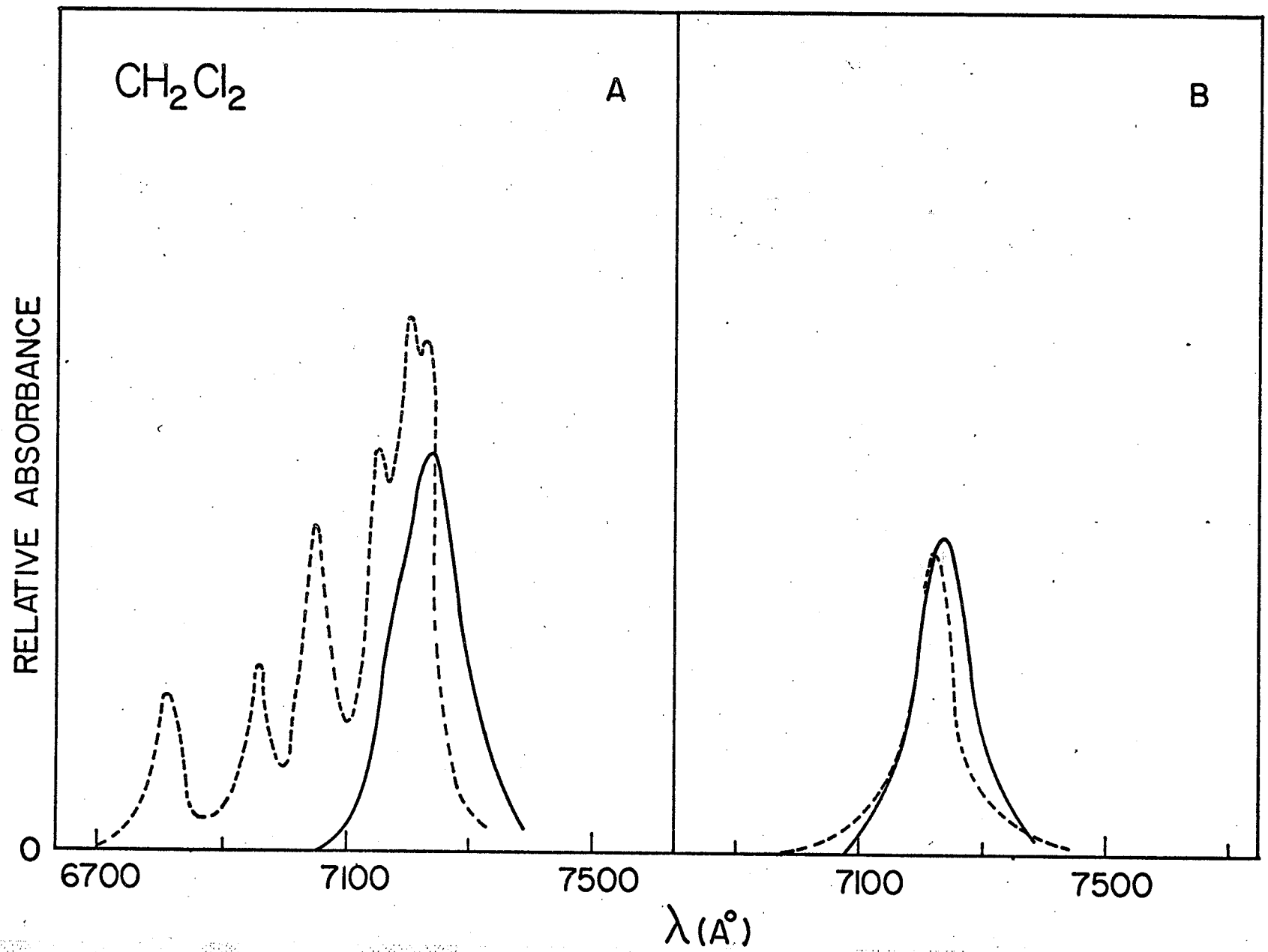
CH_2Cl_2
A
B
RELATIVE ABSORBANCE
0
6700
7100
7500
7100
7500
λ (A°)

fundamental overtone bands. This result is positive in the following sense. The intensity of the combination bands will increase relative to the overtone component towards the lower overtones. This is what is required for convergence at lower Δv to the more traditional normal-mode overtone combination pattern, which generally does fit the data in first and second overtone regions in many molecules (1, 34). At higher energies, the eigenstates of the molecular Hamiltonian, excited in the radiation field, correspond physically to more localized states than the eigenstates lower in energy.

It should also be noted that if this trend of overtone patterns is followed, one would expect that bandshapes for even higher overtones, should they be resolved, would be very simple and correspond almost entirely to the effective excitation of fundamental local-mode overtones. There are problems with clean spectra at higher overtones (figure (2.6) part C) but a similar analysis was performed for the $\Delta v_{CH} = 6$ band. Within the framework of this model, the structural aspects observed for the band in figure (2.7) part B correspond to the rovib structural aspects expected for single oscillator excitation along with noise from the optical region. Once again the anharmonic normal-mode pattern expected is not observed, in agreement with the conclusions reached above.

The overtone band corresponding to $\Delta v_{CH} = 7$ is lost

in the background so that no details of its structure may be investigated. The expected local-mode overtone comes at 18600 cm^{-1} (5380Å) and this position is indicated in part C of figure (2.7).

Finally, there is optical activity in the regions between the CH overtone bands even at the higher overtones. For example, in figure (2.6) in the 7600Å to 8200Å region there are a complex series of structural features. A very similar series of structural features is observed in the 9800 to 10600Å region. These structures vanish for higher overtones and are very prominant at lower energies near the 'harmonic' fundamentals. Both of the regions mentioned above fall out of the scope of the anharmonic normal-mode analysis given earlier but have interpretations within the framework of this ONM method. A brief discussion of the region between 7600 and 8200Å follows to introduce some general aspects of a more comprehensive study of these regions in overtone spectra.

The observed maximum in the central structure (figure (2.6)) falls at approximately 8050Å (12422 cm^{-1}) which is approximately 1100 cm^{-1} to the high energy side of the observed (1) band maximum for the $\Delta v_{CH} = 4$ overtone. (A similar maximum is observed at approximately 10300Å (9700 cm^{-1}) approximately 1000 cm^{-1} to the high energy side of the $\Delta v_{CH} = 3$ band). The ONM constructed using frequencies and

anharmonicities 2991 (-55), 2991 (-55), and 1266 (0) (the latter frequency being a normal harmonic CH bending mode frequency of the CH_2Cl_2molecule) yields states at 12195, 12305, 12435, 12565, 12650 and 12655 cm^{-1}. A similar map constructed for the modes 2991 (-55), 2991 (-55), and 1429 (0), where again the 1429 mode corresponds to a CH bending mode, gives rise to states ranging from 12725 to 13275 cm^{-1}. This suggests that the more intense combination activity involves a combination of CH stretch and CH bending vibrations (first order description) of a specific physical nature since here combinations involving the 1266 cm^{-1} appear to contribute more to the observed features than the corresponding combinations for the 1429 cm^{-1} vibration. That is, all possible combination bands of high and low frequency oscillators are not optically active, but instead, only select ones. More work is required here to say whether these observations in relation to this model have physical significance.

L. GENERAL CH OVERTONE ACTIVITY

To conclude this introduction of a new approach for the description of overtone bands for XH_n moieties, it is of interest to compare the overtone spectra for a series of halogenated hydrocarbons whose CH_n structure varies. For example in (32) the overtone bands corresponding to $\Delta v_{CH} = 4$ are illustrated for a large series of halomethanes and ethanes, some corresponding to gas phase spectra and others to liquid phase spectra. Two observations are of importance here. Firstly, in this large series of compounds where the anharmonic normal-mode overtone spectral structure would be expected to vary widely, there are surprisingly little band-shape differences. The largest halfwidths are of the order of 200 cm^{-1} and quite often are much less. The largest bandwidths occur for the structures $C_1H_nY_m$ where n is the largest, but this is expected in the local-mode model as the number of nearly degenerate oscillators is greatest. This simplicity of band structure is what is expected within the framework of the model developed here. Secondly, it is of interest to note that some rovib structure is generally observable in the gas phase overtone spectra. This structure offers the possibility of a comparison of this structure with more detailed model calculations where the effects of rotation are included.

To be more specific, it might be useful to look at

some overtone spectra taken for a series of related hydrocarbons in higher overtone regions. Also some hydrocarbons with nonequivalent CH groups are examined in relation to the theory. The spectra of methane and ethane were recorded using the apparatus and techniques described in the appendix and the spectra of the alkyl-substituted benzenes were recorded as described for the dichloromethane data.

The methane and ethane overtone spectra are shown, as recorded (see appendix) in figure (2.10) in the region from $\Delta v_{CH} = 3$ to $\Delta v_{CH} = 6$ ($\Delta v_{CH} = 7$ not resolved) and the calibrated spectra are shown in figure (2.11). The methane spectrum is a composite of two spectra taken at 1150 psi using two slidewires. The same is true for the ethane spectrum where the pressure was 580 psi. The research grade samples were obtained from Phillips Petroleum Company.

The band maxima for the $\Delta v_{CH} = 4$, 5, and 6 transitions were measured as an average over several spectra run at different speeds and the results are summarized in table (2.6). The line spectra of the CH stretching overtones of these compounds have been previously reported (35). The data here helps to define the rovib origins of the bands and records the less intense combination regions of the spectrum. The difficulties with these line spectral assignments were mentioned by Herzberg (1). The difficulties of assignment of bands is at least partially resolved here. Here the main

Figure (2.10) The overtone spectra of methane and ethane in the region from 14000Å to 5000Å. The gas phase spectra were taken at 1150 and 580 psi respectively in the 10 cm cell described in the appendix.

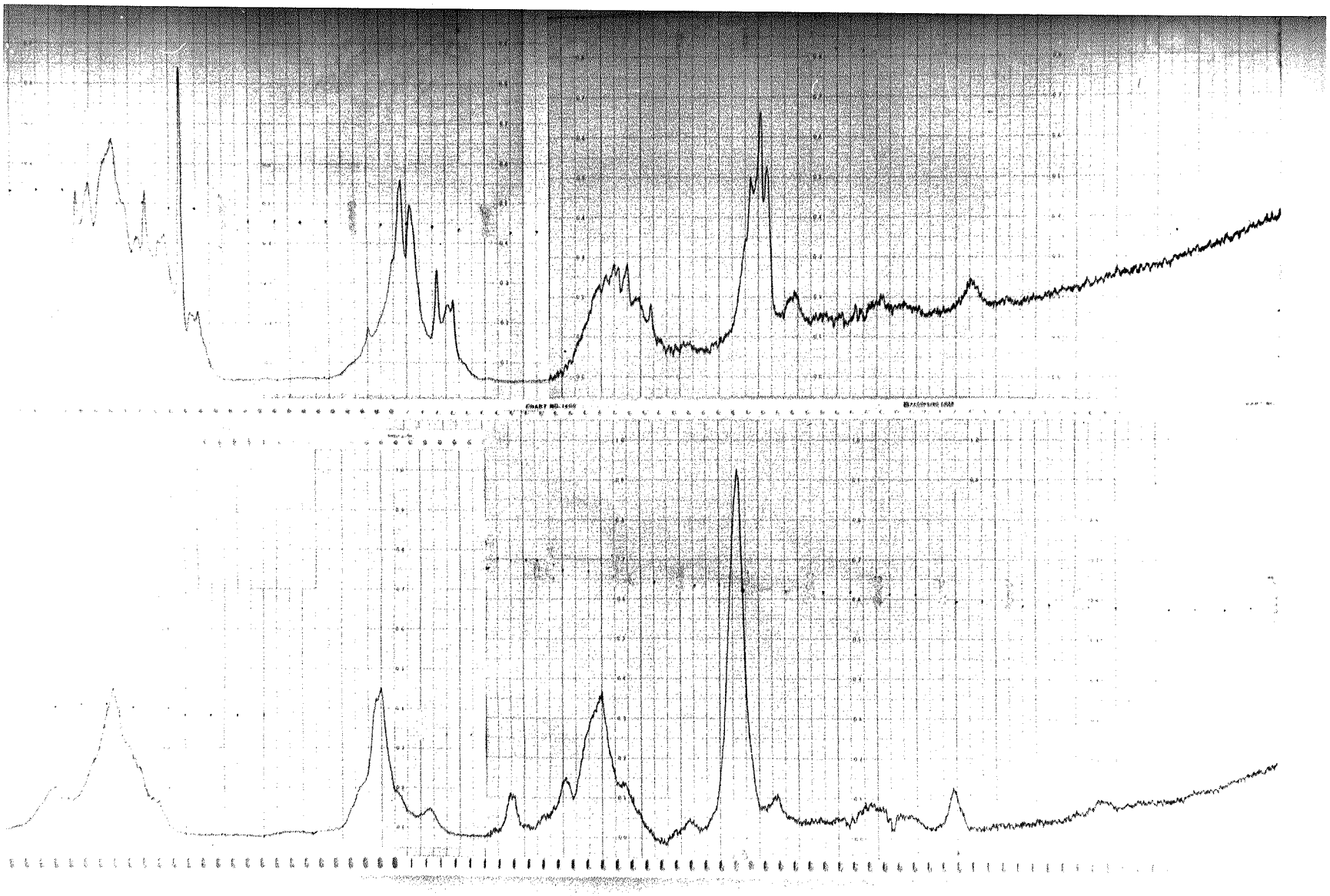

Figure (2.11) Calibrated overtone spectrum of methane and ethane in the region from 14000Å to 5000Å. The gas phase spectra were taken at 1150 and 580 psi respectively.

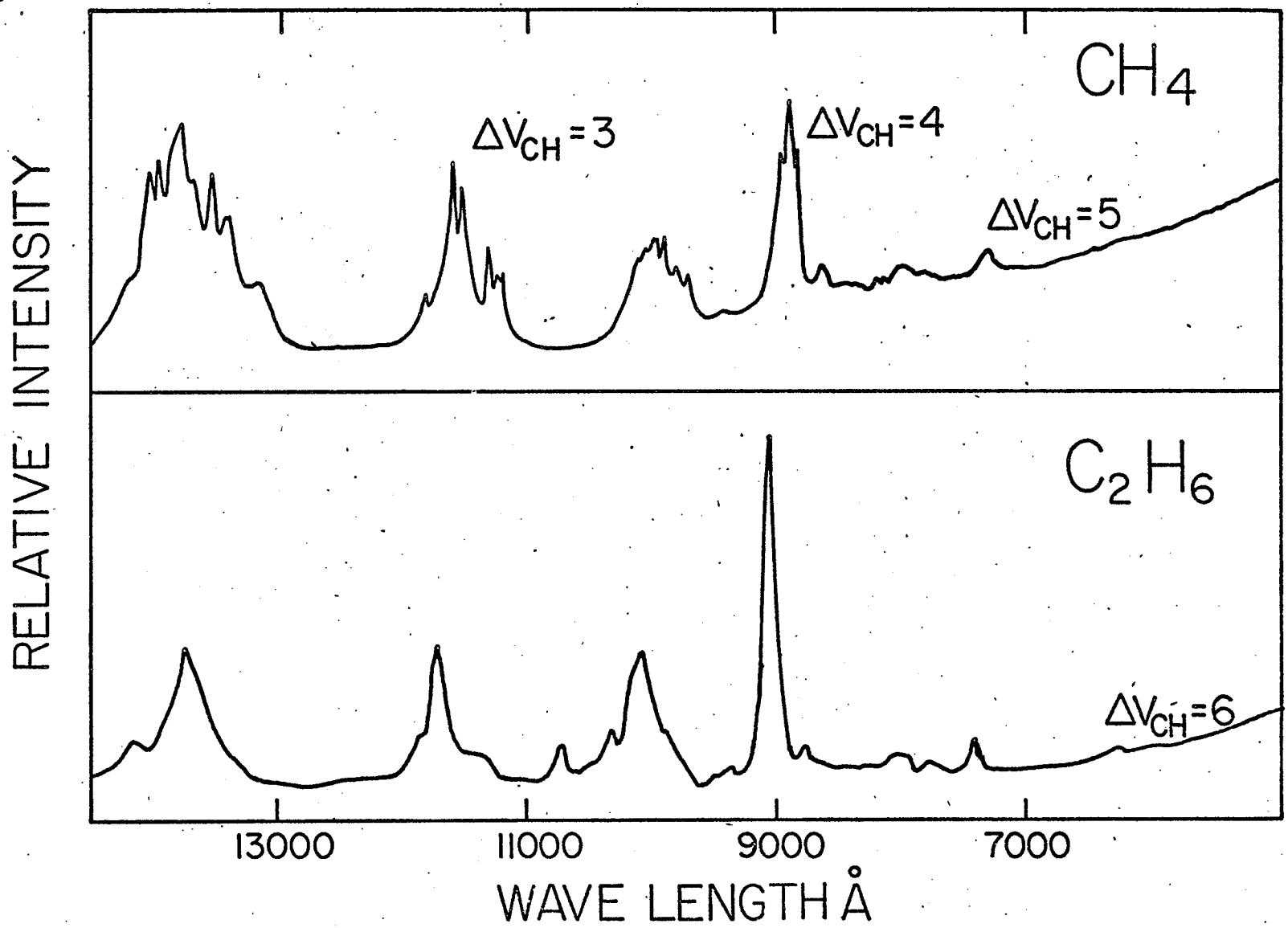
CH4
ΔVCH=3
ΔVCH=4
ΔVCH=5
C2H6
ΔVCH=6
RELATIVE INTENSITY
13000
11000
9000
7000
WAVE LENGTH Å

Table (2.6)

Molecule	Overtone			
	$\Delta v = 4$	$\Delta v = 5$	$\Delta v = 6$	$\Delta v = 7$
Methane	8 880Å	7 269Å		
	8 860Å[a]	7 250Å	6 190A	5 430A
Ethane	9 062Å	7 424Å	6 330Å	5 600Å
	9 020Å[a]	7 420Å	6 320Å	

a - approximate bandmaximum from line spectra (24)

interest lies in the comparison of the general features of these spectra to those of related molecules.

There is a striking similarity between the two overtone spectra especially in the higher overtone regions. The number and symmetries of the normal-mode fundamentals might have led one to expect rather more complicated bands for the ethane molecule (in a normal-mode approach). These spectra look very much like the dichloromethane spectrum described earlier. That is, a local-mode pattern seems to develop for both of these molecules. Superpositions of these spectra with the spectra of benzene, dichloromethane, and chloroform show that the spectra are almost identical (except for frequency shifts to be discussed) past $\Delta v = 3$ or 4. The common features among the spectra are not limited to the CH overtone regions entirely.

The very evident frequency shifts of the CH overtones among the molecules discussed in this report raise the question of what one might expect in the overtone spectrum of a molecule which contains non equivalent CH_n groups. If the local-mode model is applied one might expect to see, for a molecule with two types of nonequivalent CH groups, two components for each overtone band, providing the CH bonds are enough dissimilar that the local-mode fundamental frequencies of the CH groups are significantly different (see below). In order to predict whether or not the components would be resolved one requires a measurable characterizer of the CH bond to be

correlated to overtone frequencies . This is discussed in more detail below.Perhaps one might even expect some correlation between the integrated areas under such peaks, if resolved, and the relative numbers of equivalent CH bonds within each group. This would imply that the transition moment was more sensitive to the electronic structure at a CH bond than the internal symmetries of its environment. Such an observation would correspond to the local-mode model but not really to a normal-mode model of the excited states, as can be seen by the lack of such peak area correlations for the fundamental vibrations. To look at this question experimentally, the overtone spectra of benzene, toluene and the three xylenes were obtained. The results are given below.

The room temperature overtone spectra of liquid benzene, toluene, o-xylene, m-xylene, and p-xylene were obtained using the procedures described for dichloromethane. The samples obtained from Matheson, Coleman and Bell were used as received. The spectra are compared in figure (2.12) and the calibrated spectra are shown in figure (2.13) for the Δv_{CH} = 5, 6, and 7 regions. The benzene spectrum has also been obtained by other workers and is included here for the purposes of comparison.

The doublet nature of the Δv_{CH} = 5 bands is immediately apparent with the peaks around 7400-7200Å at about the same wavelength as the alkyl CH groups of methane and

Figure (2.12) The overtone spectra of benzene, toluene, o-xylene, m-xylene, and p-xylene in the region from 8000A to 5000A at 25^{o} C.

٤٥ سم
٥٥ سم
٦٥ سم
٧٥ سم
١٠٠ سم

Figure (2.13) The calibrated overtone spectra of benzene, toluene, o-xylene, m-xylene, and p-xylene in the region 8000A to 5000A at 25°C. The assignments are based on the generalized local-mode model described in the text.

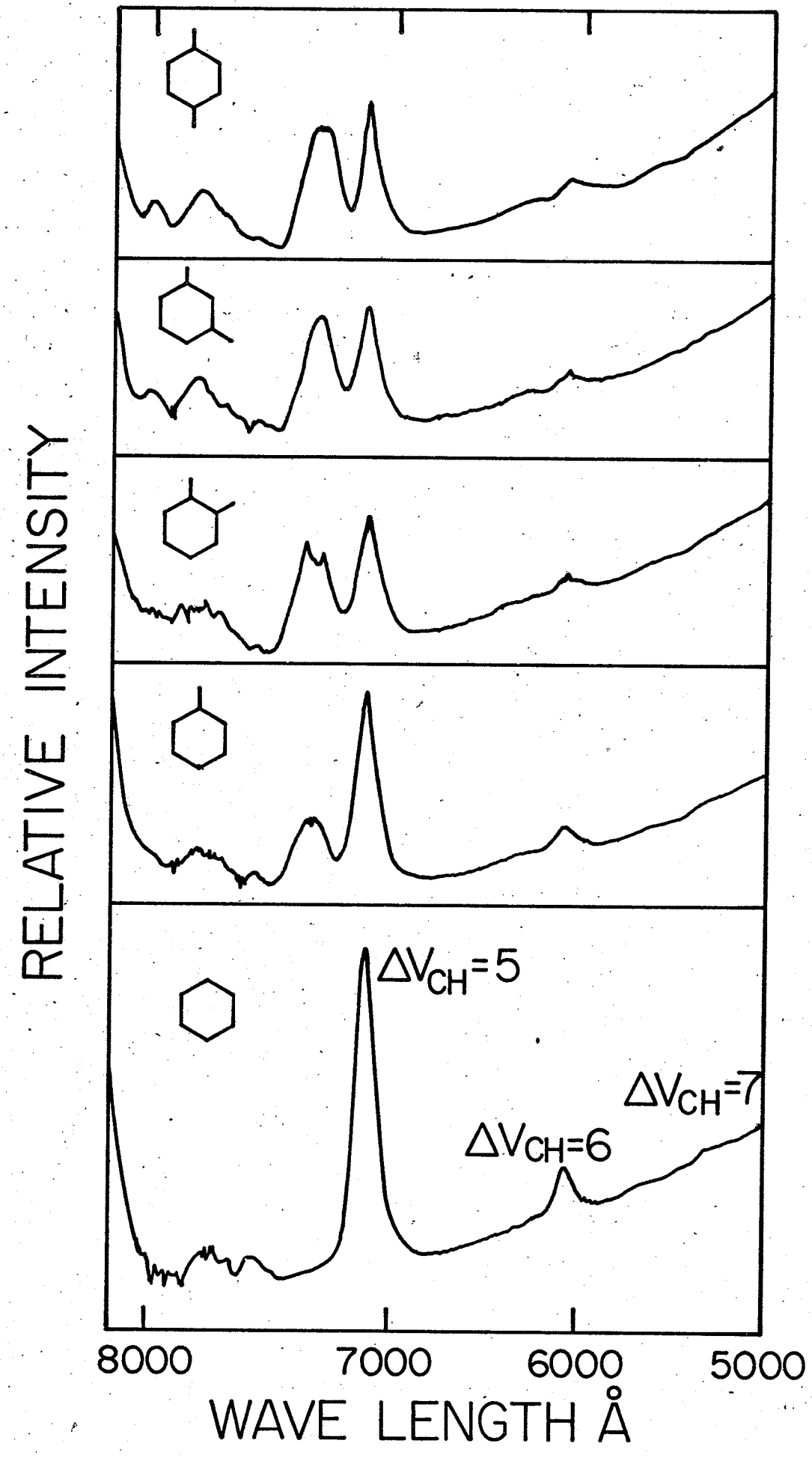
RELATIVE INTENSITY
ΔVCH=5
ΔVCH=6
ΔVCH=7
8000
7000
6000
5000
WAVE LENGTH Å

ethane described earlier, and the peaks around 7100-7200Å in the aryl CH region as the spectrum of benzene itself demonstrates. The doublet structures appear for the Δv_{CH}=6 region as well, although there, the band intensity is rather weak. It is evident that there is some correlation between peak area and the number of equivalent protons when one compares the spectrum of toluene to that of the xylenes. As one proceeds towards the lower CH overtone regions, these doublets appear to become more complex (approaching the normal mode overtone pattern). This behavior is observed starting at the Δv_{CH} = 3 overtone as figures (2.14) and (2.15) demonstrate. All these figures appear almost like a superposition of the benzene and ethane (as opposed to methane) overtone spectra from these regions. The reason for this is discussed below.

The resolution of the doublets is forecast on the basis of the following empirical plot (figure (2.16)) of frequency of the observed Δv_{CH} = 5 overtone band maximum versus the deuterium decoupled frequency of the normal CH stretching vibration (the frequency of the Δv_{CH} = 1 vibration when all but one H has been replaced by a deuterium). For example, in toluene the alkyl and aryl fundamentals are separated by about 100 cm^{-1}. For Δv_{CH} = 5 this difference is magnified approximately 5 times in the local-mode model. Since the bandwidths are much less than 500 cm^{-1} these

Figure (2.14) The calibrated overtone spectra of benzene, toluene, o-xylene, m-xylene, and p-xylene in the $\Delta v_{CH} = 4$ stretching region at 25°C. The assignment is based on the general local-mode theory.

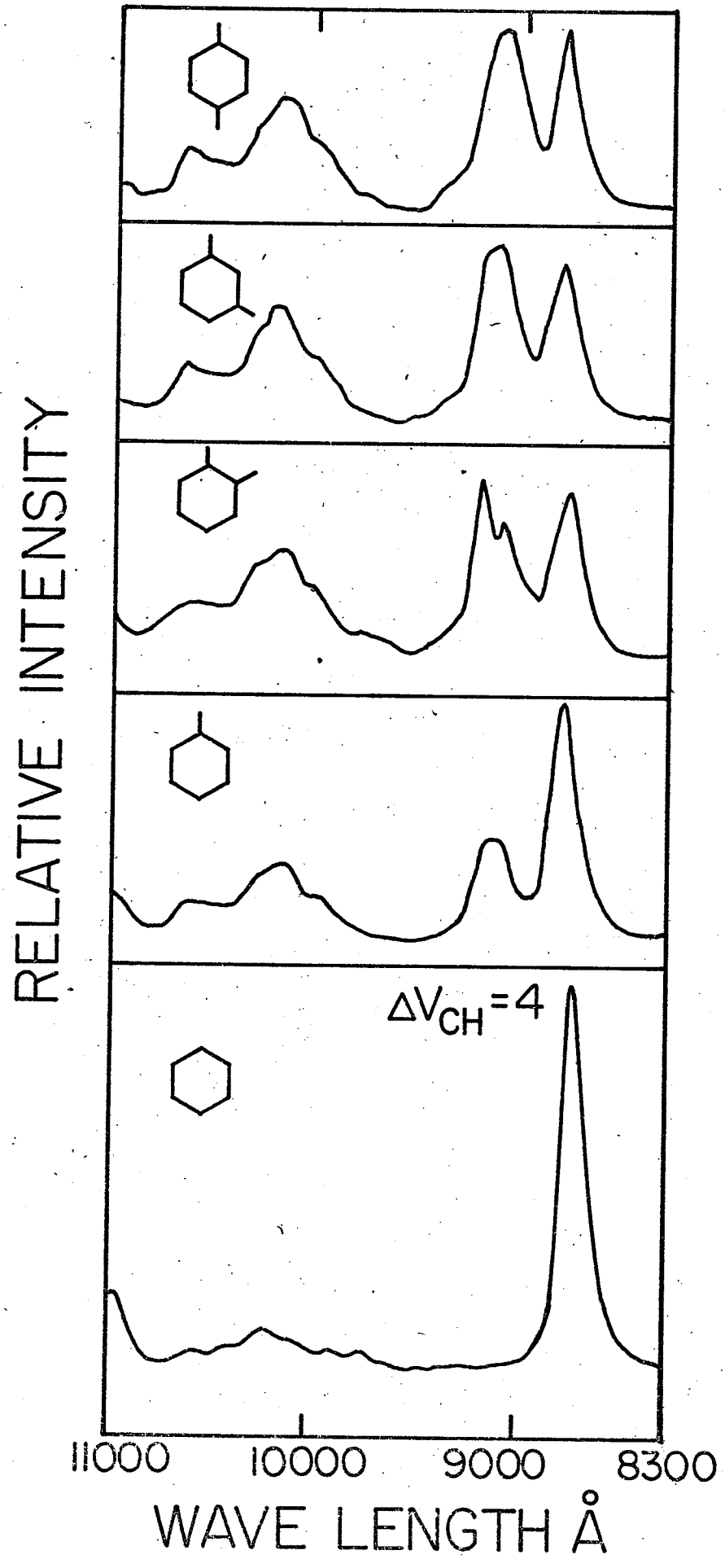
RELATIVE INTENSITY
$\Delta V_{CH}=4$
11000
10000
9000
8300
WAVE LENGTH Å

Figure (2.15) The calibrated overtone spectra of benzene, toluene, o-xylene, m-xylene, and p-xylene in the $\Delta v_{CH} = 3$ stretching region at 25°C. The assignment is based on the general local-mode theory.

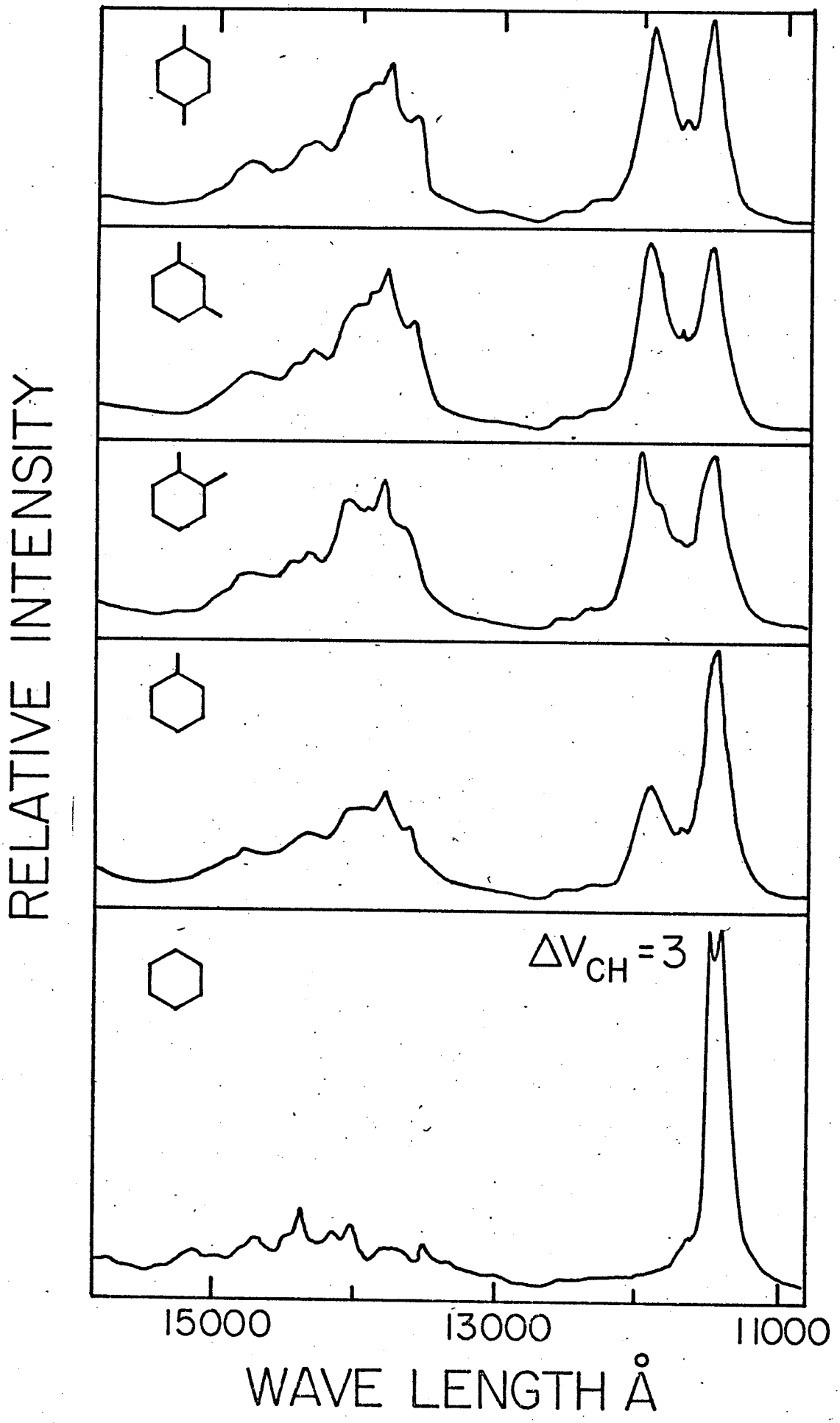
RELATIVE INTENSITY
$\Delta V_{CH} = 3$
15000
13000
11000
WAVE LENGTH Å

Figure (2.16) Correlation of observed $\Delta v_{CH} = 5$ overtone band maxima with the frequency of the CH stretching mode arising from molecules where all but one H atom has been replaced by a deuterium.

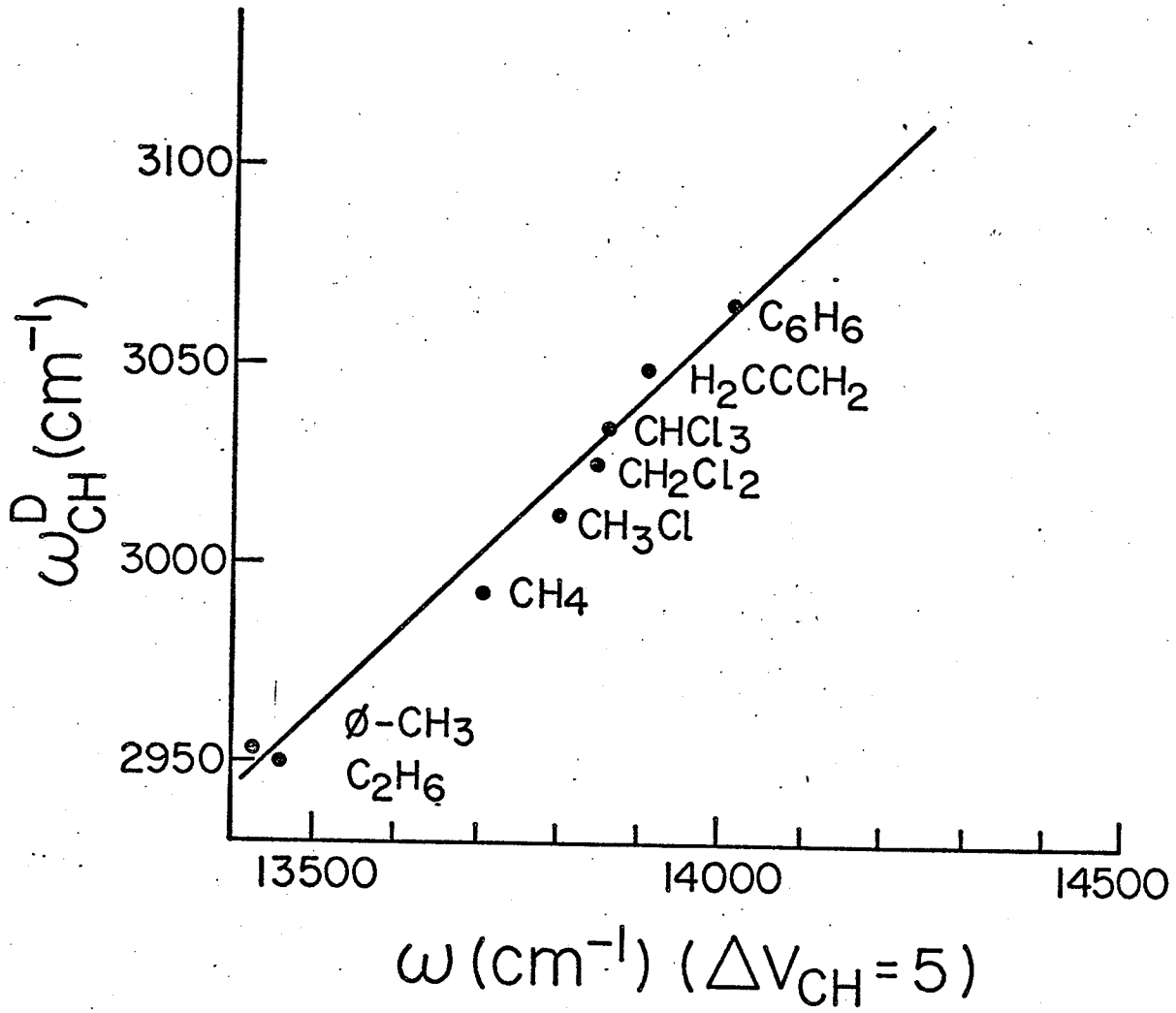
3100
3050
3000
2950
ω^D_{CH} (cm^{-1})
C_6H_6
H_2CCCH_2
$CHCl_3$
CH_2Cl_2
CH_3Cl
CH_4
Ø-CH_3
C_2H_6
13500
14000
14500
ω (cm^{-1}) ($\Delta V_{CH}=5$)

groups give rise to distinguishable bands in the overtone spectrum. The linearity of figure (2.16) suggests that knowing the fundamental frequencies of a CH oscillator in a molecule is enough to predict the CH overtone pattern even if there are more than one nonequivalent type of CH group in the molecule.

For example, $H^{12}CCl_3$ and $H^{13}CCl_3$ differ in fundamental CH stretching frequency by about 10 cm^{-1} (36). According to figure (2.16) the $\Delta v_{CH} = 5$ bandmaxima should therefore fall approximately 50 cm^{-1} apart. Since the bandwidths for the $\Delta v_{CH} = 5$ overtones are normally around 150 - 200 cm^{-1} for a degenerate group of CH oscillators in this region, the components for these molecules should express themselves in a significant broadening of the observed CH overtone band in an equimolar mixture of these two compounds.

This same type of analysis applies to the other Δv_{CH} transitions as well. These regularities represent a significant simplification from the predictions from a normal-mode approach to the complicated C_mH_n polyatomic overtone bands. This last section has illustrated the type of experiments that might be attempted to study the predictive capacity of the generalized local-mode theory of polyatomic anharmonicity.

M. CONCLUSIONS

Experimental bandshapes and bandwidths for XH_n overtone spectra are quite simple and do not seem to support theories which think of them in terms of complex structures built out of a large series of anharmonic normal-mode overtones and combinations. The energies and anharmonicities of such bands are very close to what would be expected for simple diatomic like XH stretching motions where the excitation energy is localized in a single oscillator rather than delocalized in a set of degenerate oscillators. This observation is in agreement with the earlier sections of this work which showed that for higher energies, a local-mode representation of the system led to a more diagonal form for the potential energy matrix than the corresponding anharmonic normal mode representation. Physically this implies that in a first order description the eigenstates of the molecular Hamiltonian which contribute to absorption can be thought of as localized states. Evidence suggests that this representation becomes increasingly appropriate at higher and higher energies. This first order representation of the vibrational states would simplify both a conceptual picture of photophysical decays in molecules containing these XH_n moieties and also the corresponding calculations in the theory of radiationless decay (e.g. Franck Condon factors), providing that the same type of selection rules are shown to be operative in these processes. The immediate priorities, in my opinion,

insofar as extension of this work is concerned, would lie in a fairly comprehensive study of infrared overtone spectra of a wide variety of molecules, and then perhaps looking to resonance Raman for data on the same or similar molecules. The selection rules for small molecule resonance Raman data appear to be quite restrictive and this data in conjunction with the infrared data might yield more insight into the nature of vibrationally excited states in polyatomic molecules.

CHAPTER 3

THERMAL REACTIONS: THE ROLE OF VIBRATIONS

Molecular beam and chemiluminescence studies are giving gas kineticists their first detailed look at the role of vibrational degrees of freedom in thermal chemical reactions. Single vibronic level excitation (SVL) and chemiluminescence studies are providing somewhat similar information about the role of vibrations in photochemical decay leading to chemical reaction. For many years, it was not as clear that for photochemical reactions, the vibrational degrees of freedom might play as important a role in the reaction as they were assumed to in the case of thermal reactions. The energies involved in thermal activation imply direct excitation of vibrational modes. However, the theories of vibronic interactions, developed in the context of general theories of radiative and nonradiative transfer (4) made the conceptual picture of the role of vibrations in such decay more clear than was understood in the case of thermal decay. Recent theories of reaction involving the concept of scattering states has unified the conceptual understanding of thermal and photochemical decay but does not yet allow much communication between theory and experiment. Statistical theories of the role of vibrations in chemical reactions can be

compared with experiment and although there is a corresponding sacrifice of details of the reaction mechanism in this type of theory, it does seem an excellent place to try to understand what the chemical consequences of anharmonic effects might be.

Here, the basic theory of thermal reaction, the Rice, Ramsberger, Kassel and Marcus (hereafter referred to as the RRKM theory (37)) is discussed with respect to its treatment of the vibrational problem. The purpose of the chapter is to put the study of anharmonicity into perspective, that is to see how it relates to theory.

The fundamental difference between RRKM theory and the theories of photochemical decay is that RRKM theory assumes that the energy distribution in the vibrational modes of the molecule, after activation (whatever form these modes may take) is a statistical one. The mechanism of distribution is not explicit in the theory. Entropy is quickly maximized. Without anharmonicity no distribution after excitation is possible. (Actually experimental evidence of energy flow is only beginning to appear in the literature (37). RRKM theory only requires a statistical distribution of energies and this could be achieved, in the thermal case, by direct thermal excitation of such a distribution.)

Some problems with the setup of the theory itself

are examined and related to predictions made by the theory which are the characterizers* commonly used in comparisons with experiment. A brief examination of the origin of the RRKM equations will help put the numerical work in perspective. The advantages of the general local-mode approach in state counting procedures from a theoretical and practical point of view will become more clear here. In no sense is this chapter a review of RRKM theory.

* The term characterizer is used here in reference to any measurable property of a physical system which helps to define that system and distinguish it from other similar systems.

A. GENERAL ASPECTS OF THE THEORY

The RRKM theory is concerned with the following sequence of events;

$$
\begin{aligned}
&A + M \xrightarrow{\delta k_1} A^* + M && \text{(activation)} \\
&A^* + M \xrightarrow{k_2} A + M && \text{(deactivation)} \\
&A^* \xrightarrow{k_a(E^*)} A^+ && \text{(decay)} \\
&A^+ \xrightarrow{k^+} \text{Products} && \text{(reaction)}
\end{aligned}
\qquad (3.1)
$$

where A is the reactant molecule, M is an energy bath and the k_1, k_2, k_a, k^+ are rate constants for the processes which depend on a variety of structural factors and are thus energy dependent in general. The most crucial aspect of the theory is the understanding of the processes of decay and reaction. These two processes taken together describe the decay of A^* in time and thus the relation of this theory to the dynamical theories of coupled systems becomes well defined. The RRKM theory does neglect tunneling effects and resonance effects (38, 39), so that the semiclassical formulation of the rate equations is not completely satisfactory from a theoretical point of view. The events symbolized by (3.1) suggest that a steady state in A^+ would be feasible and the assumption of such a steady state would give,

$$
[A^*] = \frac{k_1 [A] [M]}{k_2 [M] + k_a(E^*)} \qquad (3.2)
$$

where all the rate constants are complicated functions of energy. Here k_1 and k_2 are essentially collision frequencies modified by a cross section. In general these activations and deactivations are extremely complicated processes so that a priori theoretical determination of these functions is not a small problem. If one assumes that the transmission coefficient (probability) through A^+ is equal to 1 then,

$$\frac{d(\text{Products})}{dt} = k_a(E^*)[A^*]$$

thus

(3.3)

$$\frac{d(\text{Products})}{dt} = \frac{k_a k_1 [A][M]}{k_2[M] + k_a}$$

where it is assumed here that this expression describes the rate of appearance of those products appearing as a result of the decay of a molecule with energy E^*. The k_1 and $k_a(E^*)$ will be thermally averaged in the calculation to generate a rate constant which may be compared to experiment. A unimolecular rate constant is defined,

$$k_{uni} = \frac{1}{A} \frac{d(\text{Products})}{dt} = \frac{k_a(E^*)k_1[M]}{k_2[M] + k_a(E^*)} \qquad (3.4)$$

and, defining k_{inf} as the rate constant as M goes to infinity, (3.4) can be written,

$$k_{uni} = \frac{1}{\frac{1}{k_{inf}} + \frac{1}{k_1[M]}} \qquad (3.5)$$

To put experiment and theory into perspective it is useful to look at the shape of the curve which shows how k_{uni} changes with increasing pressure in the reaction mixture. For reasonable scales usually log k_{uni} is plotted against log M or in general log P. Two schematic representations of such curves are shown in figure (3.1). The curves illustrate what portion of the curves the literature on the subject (40) (dotted enclosure) generally encompasses. The difference in the curves further shows, schematically, the rather drastic effect a parameter such as the cross section for activation might have on the fall off. For interesting molecules, even how to go about figuring out a cross section, theoretically, is difficult. Also, unfortunately, the low pressure region of figure (3.1) is experimentally inaccessible insofar as a rate measurement is concerned. It is important to bear in mind how this parameter, the cross section, might affect the curve in the region that is studied because the RRKM theory tries to fit theory to experiment while neglecting for the most part the effects of complicating factors which might have an effect on activation and deactivation rates (k_1 and k_2). In the example shown, k_1 was changed by a factor of 2. The low pressure plateau in the rate is essentially the activation rate (collision rate times a cross section). Notice how the effect tends to be masked at higher pressures (the curves converge to a common log k).

Figure (3.1) A schematic representation of a rate constant fall off curve with pressure illustrating the experimentally accessible regions (dotted enclosure) and the type of change which occurs in the fall off curve when one of the parameters, such as cross section, is changed in the theoretical models of the phenomenon. The activation rate in curve B has been halved in comparison to curve A.

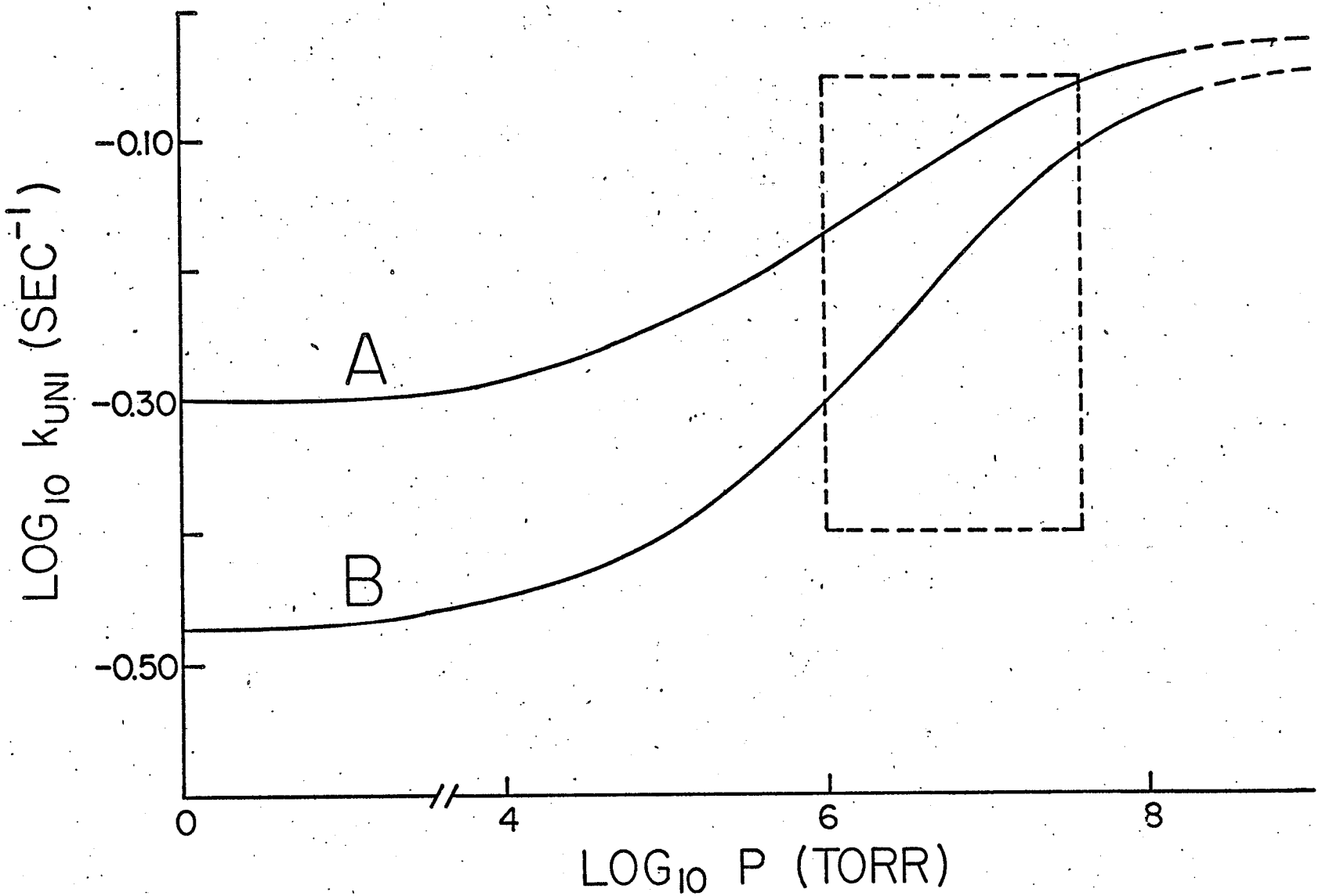
-0.10
-0.30
-0.50
A
B
0
4
6
8
LOG10 kUNI (SEC-1)
LOG10 P (TORR)

Bunker in 1973 (41) proposed that a third plateau would appear in fall off curves if the vibrational energy distribution is not thermal, that is if the RRKM random flow of vibrational energy is not valid. Unfortunately because of the effects of competing reactions this region, too, is experimentally inaccessible but this does offer exciting possibilities for the future. His argument is a simple one and is reviewed briefly here. At very high pressures any molecule of the ensemble with enough energy to react will have an extremely short lifetime because of the high rate of collisional deactivations. Only those molecules which are excited into vibrational modes closely coupled with the reaction coordinate will decay into the continuum before they have a chance to react. Normally reducing the pressure reduces the number of such excited molecules correspondingly but also increases the lifetime in the excited state so the number of reacting molecules per second stays about the same. As the pressure is lowered still more the lifetime between collisions is long enough that the only effect of a reduction in pressure is to reduce the number of excited molecules as in this region all the molecules with enough energy to react will react. Thus the rate falls with pressure in this region. Now suppose the set of oscillators are weakly coupled with the rest of the molecule. The pressure where the fall off begins to occur (lifetime so long that all molecules with energy to react do react) will occur at a much lower pressure

because of the weak coupling. Above this pressure the only reacting molecules are those in this small group closely coupled to the continuum. But now this small group behaves in exactly the same way as a normal RRKM molecule since they are strongly coupled amongst themselves. Thus as pressure is increased still further a second plateau will be reached corresponding to the pressure where the lifetime of the excited molecule is just long enough that any molecule with enough energy to react will react (with the important restriction that these molecules are only those excited into the closely coupled modes as opposed to the first fall off region where no such restriction applies). Thus non-RRKM behavior will lead to interesting so called 'false' plateaus. This gives one a clue on what to look for when a full dynamical treatment of excited state decay becomes possible. This type of future for this area of chemistry makes a non-ambiguous formation of RRKM rate equations a real necessity so that the statistical energy distribution assumption can be completely tested.

The central and most important assumption in RRKM theory is that there is a 'pseudo' equilibrium between A^* molecules and activated complex molecules A^+ and therefore the relative concentrations of these species at any time (after 'equilibrium' populations established) are determined by the laws of probability alone; i.e., by entropy or statistical effects. By pseudo the theory requires only that the

system's populations behave 'as if' there were such an equilibrium being established. At 'equilibrium' the number of molecules per second passing from A^* to A^+ equals the number per second traveling in the reverse direction (the flux of molecules in either direction is the same). The theory assumes that no molecules actually go from A^+ to A^* but that the molecules in A^*, passing to A^+, have no way of 'knowing' this and their rate is unaffected by the absence of a reverse flux. This lack of interference is a classical approximation and would be expected to hold for quantum systems only where a very large number of vibrational modes are strongly coupled and for short observation times.

Given this assumption the problem becomes one of essentially determining the partition functions, a feature which is common to equilibrium problems. That is, the molecules will be partitioned between A^+ and A^* exactly as they would be at equilibrium. At high pressures therefore, where,

$$k_a(E^*)[A^*] = k^+[A^+] \tag{3.6}$$

$$k_a(E^*) = k^+ \frac{[A^+]}{[A^*]}\Bigg|_{E^* \to E^* + dE^*} \tag{3.7}$$

i.e., steady state in A^+. The ratio $[A^+]/[A^*]$ can in principle be found by partition function considerations and all that remains is to identify k^+. Notice that the energy dependence of $k_a(E)$ is then understood by the changing ratio $[A^+]/[A^*]$ with

energy and the change of k^+ with energy. However, the 'crux' of the argument, the 'pinch' which controls the flow of molecules from A^* to A^+ is not easy to deal with. What is k^+? How fast do the molecules pass through the activated complex? How long does the energy linger or what is the time delay in the region of the activated complex?

The establishment of this time scale of reaction has been considered from many points of view; all leading to essentually the same result but few of them are satisfying from a theoretical or a conceptual point of view. Laidler (37) has discussed the general approaches. Here a few of the problems in their application are pointed out. The problems are included here since they are often not just approximations but are simply at variance with the nature of the process they are to describe. Thus they are of considerable theoretical interest, and since the question is unsettled, the problems should, perhaps, be raised once again.

Treating the partition function for the 'separable' reaction coordinate as a harmonic oscillator partition function with the oscillator frequency approaching zero,

$$\lim_{\nu \to 0} \frac{1}{1 - \exp(-h\nu/kT)} = \frac{kT}{h\nu} \qquad (3.8)$$

does not relate to any model or potential surface for a diatomic or a polyatomic. It ignores the origin of the expression $1/\left[(1 - \exp(-h\nu/kT)\right]$. The important factor which

emerges from the treatment kT/h (which has units of moles^{-1} sec^{-1}), sets the time scale for unimolecular reactions. Since the ν in equation (3.8) cancels when substituted in the expression for the rate (3.7) ($k^+ = \nu$), it was not necessary to examine any of the details of the model. (This criticism comes to mind rather quickly when one is preoccupied with a study of anharmonicity.)

Treating the passage over the activation barrier as a particle of mass m in a potential box of width a yields the same factor, kT/h. The 'particle's' mass drops out of the calculation since the heavier it is the slower it travels at any energy E but the heavier it is the greater the density of states in the box (at the activated complex). The width of the box drops out of the calculation since the narrower the box the faster it is traversed but also the narrower the box the less dense the stationary states for the particle at the activated complex. All these compensating factors yield once again a simple factor kT/h controlling the time scale of the reaction. The conceptual difficulties here are clear. There are no infinite or finite potentials in the region of the activated complex to define any type of box. If the box's walls were also considered in the limit where the potentials fall to zero, the method would be acceptable but in this case there would be no box at all and the element of the theory which supposedly gave rise to the time scaling of

the reaction would no longer be present.

Macomber and Colvin in 1969 (42) suggested that the potential 'walls', the restricting potentials, were those arising from collisions with other molecules. That is, motion in the reaction coordinate was restricted by the occurrence of collisions with other molecules in the vessel. A particle of mass 'm' was envisioned to be traveling in a box of width equal to the mean free path of flight of the molecules. In a unimolecular dissociation either one of the fragments can be thought of as the particle. Any two particles moving under the action of mutual central forces can be analysed from the point of view that one of them is fixed in space if at the same time a reduced mass is used for the moving particle (43). Thus the conceptual picture of one of these fragments moving over the potential surface with collisions placing quantum restrictions on its motion is not unreasonable and involves an approximation rather than a completely artificial physical model. Thus the translational 'continuum' of dissociated fragments is not a continuum but instead is quantized. The time scale of reaction is controlled by possible energy states of any such particles in 'boxes' of this size. This model forms a more satisfying basis for the derivation of k^+ even though the end result is approximately the same as the other two models. (Perhaps it should be kept in mind that the results are only identical for these models at rather high temperatures where the kinetic energies are

greater than the barrier heights by a considerable amount.) Notice that in this theory, albeit semiclassical, there is no pinch holding molecules in the form A^+. The reaction does not explode into the product continuum because only a fraction of the total number of activated molecules have the form A^+ for strictly statistical reasons and at all times. This corresponds to the so called strong coupling quantum mechanical models.

In summary, therefore, the time scale of a unimolecular dissociation, in the RRKM approximation is fixed by the thermal velocities of the fragments at energy $E^* - E_o$ along with the restriction that only a statistical fraction of such molecules exist out of the total number of activated molecules. The fraction is energy dependant, as are the thermal velocities of fragments, so that in general the kinetic parameters are energy dependant.

The rest of the basic framework of the theory has to do with taking averages over a Boltzman distribution of excited molecules A^*. The establishment of Boltzman populations of A^* and A^+ is assumed in pseudo-equilibrium arguments involving these states. Whether or not these arguments are good approximations largely depends on vibrational mode coupling strengths in relation to the time scale of the decay process. Experiment must answer many questions here and information on excited states is too scarce to discuss the assumption in detail.

B. THERMAL AVERAGES - DENSITIES OF STATES

To develop a rate expression which corresponds to kinetic observables, equation (3.4) must be summed over all possible E^*;

$$k_{uni} = \frac{1}{[A]} \frac{d}{dt} [A] = \int_{E^*=E_o}^{\infty} \frac{k_a(E^*)\, dk_1/k_2}{1 + \frac{k_a(E^*)}{k_2[M]}} \qquad (3.9)$$

where the Boltzman restrictions are contained implicitly in k_a, and dk_1/k_2. Look at the constant energy components of this summation. Recall from equation (3.7) that to evaluate $k_a(E^*)$ the ratio $[A^+]/[A^*]$ is needed and the equilibrium assumptions reduce this to a partition function problem, namely;

$$\left.\frac{[A^+]}{[A^*]}\right|_{\text{steady state}} = (1/2) Q_A^+ / Q_A^* \qquad (3.10)$$

where $Q = \sum_i P_i \exp(-E_i/kT)$ and P_i is the degeneracy of states or the occupation number of the states with energy E_i so that;

$$\left.\frac{[A^+]}{[A^*]}\right|_{E=E^*} = P_i^+ \exp(-E_i/kT) / P_J^* \exp(-E_J/kT). \qquad (3.11)$$

For small energy regions around E^*, all the terms in the exponential are approximately $\exp(-E^*/kT)$ and these will factor out of (3.11) and cancel.

$$\left.\frac{[A^+]}{[A^*]}\right|_{E=E^*} = \left. P_i^+ / P_J^* \right|_{E=E^*} . \qquad (3.12)$$

In order to perform the summation in (3.9), (3.12) is considered in small energy increments $E^* \rightarrow E^* + \Delta E^*$;

$$\left.\frac{[A^+]}{[A^*]}\right|_{E=E^* - E^* + dE^*} = \Sigma P_i^+ \; / \; \Sigma P_j^* \quad . \tag{3.13}$$

If P were a continuous distribution with respect to energy then;

$$\sum_{E^*}^{E^* + dE^*} P_i(E^*) = \left.\frac{d\Sigma P}{dE}\right|_{E^*} dE \tag{3.14}$$

for sufficiently small dE. Thus by defining;

$$N(E^*) = \left.\frac{d\Sigma P}{dE}\right|_{E^*} \tag{3.15}$$

then

$$\sum_{E^*}^{E^*+dE^*} P_i(E^*) = N(E^*)\, dE \tag{3.16}$$

where $N(E^*)$ is the gradient or state density. Using this substitution the decay rate constant (3.7) takes the form.

$$k_a(E^*) = \frac{L\, Q_1\, P(E^+)}{Q_1 h N(E^*)} \tag{3.17}$$

where L is a symmetry factor (35); Q_1^+/Q_1 are the rotational partition functions of A^+ and A^* respectively and h is Planck's constant.

This expression (3.17) leads to difficulties in the RRKM calculation and the origin of these difficulties is outlined below.

C. NATURE OF PROBLEM

Quite generally in chemical physics, theories of transitions between states of some zeroth order molecular Hamiltonian are formulated in terms of a quantity N(E), the density of states at energy E. Quantities such as rate constants for transitions which relate directly or implicitly to observables are developed in terms of N(E)'s rather than in terms of the more fundamental concept occupation numbers. This approach is used since at some time an averaging procedure over a specific energy range is usually carried out. If some analytic form of N(E) can be constructed, then the averaging will involve an integral $\int_{E_1}^{E_2} f(E)\ N(E)dE$ rather than a summation; and algorithms for integration are readily available.

In any problem, N(E) must eventually be evaluated numerically. The definition for quantized systems is extrapolated from the definition of the sum of states curve. However, the problem is that the sum of states W(E) is a step function which satisfies none of the criteria for the existence of a derivative at the points of interest so a new definition for N(E) is necessary. But, as will be shown below, the usual definition used for most practical algorithms is not entirely satisfactory unless in the calculation the defined N(E) is eventually carefully 'integrated' out of the problem. Only then will it be assured that the function

corresponding to a given observable will not depend on how this N(E) is defined. It is also shown below that the numerical calculation of N(E) neither approaches the value that a polynomial approximation to W(E) would yield nor is N(E) independent of the step size used for state counting, even for almost continuous data.

D. DENSITY OF STATES AND OCCUPATION NUMBERS

$N(E_i)$ is step size dependent. This can be demonstrated as follows. Consider a manifold of levels L_1, L_2, L_3 .....L_n with occupation numbers P_1, P_2, P_3 .....P_n. Associate with each level L_i an energy E_i; L_{i+1} an energy E_{i+1} etc.; where $E_{i+1} - E_i = \Delta E_i = \Delta E$ for all i = 1, 2, 3 ... ... n-1. If W_i is the sum of all occupation numbers from E = 0 to $E = E_i$, then the definition of density of states usually applied in practical algorithms is (42).

$$N_i = \frac{dW}{dE}\bigg|_{E = E_i} \simeq \frac{\Delta W}{\Delta E} = \frac{W_{i+1} - W_i}{E_{i+1} - E_i} = \frac{P_{i+1}}{\Delta E} \qquad (3.18)$$

A simple numerical example illustrates how the step size affects the numerical value of the density of states. The choice of ΔE becomes critical to the absolute value of $N(E_i)$ and the intuitive feeling for what $N(E_i)$ means becomes unclear in these quantized systems. For example, if we use the occupation numbers, $P_3 = 3$, $P_5 = 5$, $P_7 = 2$, and $P_i = 0$ for i = 3, 5, 7, then if we choose $\Delta E_i = 2$, we obtain

$N(E_1) = 3/2 = 1.5$ and $N(E_1)\ \Delta E = 3$

$N(E_3) = 5/2 = 2.5$ $N(E_3)\ \Delta E = 5$

$N(E_5) = 2/2 = 1$ $N(E_5)\ \Delta E = 2;$

but if we choose $\Delta E = 1$ (unnecessarily small for accurate state counting), then we obtain

$N(E_1)$	=	0	and	$N(E_1)\ \Delta E$	= 0
$N(E_2)$	=	3		$N(E_2)\ \Delta E$	= 3
$N(E_3)$	=	0		$N(E_3)\ \Delta E$	= 0
$N(E_4)$	=	5		$N(E_4)\ \Delta E$	= 5
$N(E_5)$	=	0		$N(E_5)\ \Delta E$	= 0
$N(E_6)$	=	2		$N(E_6)\ \Delta E$	= 2

Note that when $N(E) \neq 0$, although $N(E)$ itself is dependent on ΔE, the product $N(E)\ \Delta E$ is not dependent on ΔE for corresponding $N(E)$. Notice also that, in reality, the density of states is mostly zero in the energy space and undefined elsewhere since the first derivative $\left.\frac{dW}{dE}\right|_{E = E_i}$ is not continuous over E. This ambiguity in the density of states can't be avoided in chunky space; i.e., in quantized systems. The density of states must be eventually integrated out of the problem. Alternatively, theories can be formulated in terms of occupation numbers alone which are well defined and exact. The effect of this problem in calculations of practical interest will be demonstrated but first let us consider the same calculation, only now we will assume that the function W is continuously differentiable over E.

It is shown here that even if W were continuous, in molecular systems W increases so rapidly that the approximation

$$N(E_i) \simeq P_{i+1}/\Delta E \tag{3.19}$$

is extremely poor. For any numerical work, differential

quantities would be replaced by finite differences so that

$$W_i = \Sigma_{n=0}^{i} P_n \tag{3.20}$$

and

$$N(E_i) = (W_{E_i+\Delta E} - W_{E_i})/\Delta E \tag{3.21}$$

which for continuous W would converge to some limit as $\Delta E \to 0$. (As was already pointed out, this convergence does not take place in quantized systems. If P_{E_i} is not continuous, then letting ΔE get as small as possible will lead to a nonconverging set of values for $N(E_i)$.)

Suppose however, that $W(P_i)$ is continuous and in fact can be approximated by a polynomial. We will use an advancing difference polynomial as an example

$$W_E = (1 + \Delta)^E W_0$$

where $\Delta W_0 = W_1 - W_0$ and E is defined with respect to some standard energy. Therefore we have $W_E = 1 + E\Delta + \frac{E(E-1)\Delta^2}{2!} + \frac{E(E-1)(E-2)\Delta^3}{3!} + \ldots. W_0$ where if E is replaced by $E - E_\theta$, then W_0 is replaced by W_θ. Now

$$W_{E+\delta E} = \left[1 + (E+\delta E) + \frac{(E+\delta E)(E+\delta E-1)\Delta^2}{2!} + \ldots\right] W_0$$

and

$$W_{E+\delta E} - W_E = \left[\delta E\Delta + \frac{(2E\delta E - \delta E)\Delta^2}{2!} + \ldots..\right] W_0.$$

Thus if

$$N(E) = \lim_{\delta \to 0} (W_{E+\delta E} - W_E)/\delta E \tag{3.22}$$

then

$$N(E) = \lim_{\delta \to 0} \left[\Delta + \frac{(2E-1)\Delta^2}{2!} + \ldots\ldots \right] W_0 \tag{3.23}$$

Now, for molecular systems, the W_E are extremely rapidly rising functions of E (we will show below that they are in fact exponentially increasing).

Now

$$\Delta W_0 = W_1 - W_0 = P_1 \tag{3.24}$$

and

$$\Delta^2 W_0 = P_2 - P_1 \tag{3.25}$$

For such rapidly rising functions, certainly the Δ^2 and higher terms are not small. Successive differences don't converge quickly to zero, so that even if W_E were continuously differentiable, the computation of N(E) from numerical data would be difficult. (The best way around this problem is to go to a graphical solution where $(W_{E+\delta E} - W_E)\,\delta E$ may be found directly. This type of solution would be necessary even for small grain or step sizes.)

For the purposes of state counting, rotational and vibrational degrees of freedom are considered separable. This separability leads to a sum of rovib states and a

density of rovib states expression which can be partitioned into a sum of products of purely rotational factors and purely vibrational factors. Thus in examining any grain size dependence, rotations and vibrations can be treated separately. Here we will show that the grain size dependence of rotational densities is small and predictable so that the problems encountered with rovib state counts can be traced back mainly to the vibrational state count.

The sum of rotational states up to energy E_r is to a good approximation (40, 45)

$$W(E_r) = \sum_{E_r = 0}^{E_r} P(E_r) = \frac{Q_r}{\Gamma(1 + \frac{r}{2})} \left(\frac{E_r}{kT} \right)^{\frac{r}{2}} \qquad (3.26)$$

where r represents the number of rotational degrees of freedom in the model; Q_r the rotational partition function and Γ is the gamma function. Forst (45) has studied the relationship of $W(E_r)$ to an exact count of rotational states for different rotational models (r = 1, 2) and concludes it would be satisfactory for the RRKM type of integration where contributions due to very small E_r, although in error, would not affect the final result significantly. This formula is used in practice and so is treated here as the basic rotational state count approximation.

Now using finite differences, simulating the numerical approach used in practice, $N(E_r)$ is

$$N(E_r) = W(E_r + \Delta) - W(E_r) \,/\Delta$$

$$= \frac{Q_r}{\Gamma\left(1+\frac{r}{2}\right)}\left(\frac{1}{kT}\right)^{\frac{r}{2}} \left[(E_r + \Delta)^{\frac{r}{2}} - E_r^{\frac{r}{2}}\right]\Big/_{\Delta}$$

$$= \frac{Q_r}{\Gamma\left(1+\frac{r}{2}\right)}\left(\frac{1}{kT}\right)^{\frac{r}{2}} E_r^{\frac{r}{2}} \left[\left(1 + \frac{\Delta}{E_r}\right)^{\frac{r}{2}} - 1\right]\Big/_{\Delta},$$

(3.27)

and expanding the polynomial

$$N(E_r) = \frac{Q_r}{\Gamma\left(1+\frac{r}{2}\right)}\left(\frac{1}{kT}\right)^{\frac{r}{2}} \frac{E_r^{\frac{r}{2}}}{\Delta}\left[\frac{r}{2}\frac{\Delta}{E_r} + \frac{r}{2}\,\frac{r}{2} - 1\left(\frac{\Delta}{E_r}\right)^2 \frac{1}{2} + \ldots.\right].$$

(3.28)

In the three common models where r = 1, 2, 3, the expression in brackets is an alternating infinite series for r = 1, 3 and a very simple expression for r = 2. In fact for r = 2 the Δ dependence drops out completely.

The error in neglecting higher order terms in the expression for $r \neq 2$ depends only on the ratio (Δ/E_r) which is usually very small because of the nature of the counting which gives rise to $E_r >> \Delta$ in general. At worst $E_r = \Delta$, and in this case the series, in brackets, becomes

$$S = \frac{r}{2} + \frac{r(r-2)}{2\cdot 2\cdot 2!} + \frac{r(r-2)\ (r-4)}{2\cdot 2\cdot 2\cdot 3!} + \ldots\ldots \quad . \qquad (3.29)$$

This is a sum of products of terms which are all less than 1

so that this is an alternating decreasing series and therefore the truncation error in the series is less than the first term neglected. This is also true for the case when E_r is greater than Δ in which case the truncation error is much smaller and decreases as the ratio Δ/E_r. Most of the contributions to $W(E_r)$ are from states where $E_r >> \Delta$ so that one expects a trunkation error of very small magnitude and in fact the error δ, when only the first term in Δ is retained, is given by

$$\delta = \frac{r}{2}\,\frac{(r-2)}{2}\,\frac{1}{2}\left(\frac{\Delta}{E_r}\right)^2 + \cdots < \frac{r(r-2)}{8}\left(\frac{\Delta}{E_r}\right)^2 , \quad (3.30)$$

or expressed as a fraction of the approximation

$$\frac{\delta}{N(E_r)} = \frac{(r-2)}{4}\,\frac{\Delta}{E_r} . \quad (3.31)$$

Again for $r = 2$ the error δ is zero and only the approximating function introduces error.

Therefore, in the numeric evaluation of the density of rovib states the dependence of $N(E_r)$ on Δ will be slight and the analytic derivative of $W(E_r)$ with respect to E_r can be used for $N(E_r)$. Because of this insensitivity, attention can be focused solely on the vibrational part of the summation where the Δ dependence is quite different.

Now that at least the problems have been identified, a few examples in practical situations will illustrate their effect on calculations.

E. DENSITY OF STATES IN RRKM THEORY

With respect to the previous discussion there are two quantities of central importance in the RRKM theory.

$$W_E = \sum_{E^+_{vr}=0}^{E^+} P(E_{vr}) \text{ and } N^*(E^*) \tag{3.32}$$

where the + refers to 0 the energy that is free to flow statistically in the molecule, * represents energy above the ground state reactant molecule energy, and E^+_{vr} is the energy of a given rovib state.

The first, a sum of occupation numbers is no problem but there is a problem with the second quantity, the density of states, as was described in equations (3.10) to (3.17). The equation for density of states was

$$N^*(E^*)\, dE^* = \sum_{E^*}^{E^*+dE^*} P_i \tag{3.16}$$

The context of the use of $N^*(E^*)$ in equation (3.9) makes it clear that only the integration of dk_1/k_2 over all posible E^* would be physically meaningful. However, more serious than this limitation are the difficulties associated with any attempt to try to establish a numerical value for the density of states, $N(E^*)$, and thus for dk_1 (k_2 is usually assumed to be related to the classical collision frequency modulated by a cross section factor).

In practical work (44) the evaluation of $N(E^*)$ is

attained by changing the dE to ΔE, a finite difference, so that

$$N^*(E^*) = \sum_{E^*}^{E^* + \Delta E^*} P_i/\Delta E^* \quad . \tag{3.33}$$

However it has just been shown that this substitution leads to difficulties for non-continuous data since W_E is increasing so quickly.

Conceptually dk_1 has meaning but is defined in terms of a quantity, N(E), that is ill-defined. $N(E_i)$ must always enter a calculation as a product, $N(E_i)\Delta E_i$. How does N(E) actually enter the RRKM rate expression? The basic framework of the rate expression (3.9) is reproduced below

$$k_{uni} = \frac{L^+ Q^+}{h\, Q_1 Q_2} \int_{E^*=E_o}^{\infty} \frac{\Sigma P(E^+_{vr} \exp(-\Delta E^*/kT)}{1 + \dfrac{k_2^{-1} M^{-1} L^+ Q_1^+ \Sigma P(E^+_{vr})}{h\, Q_1 N^*(E^*)}} dE^* \quad . \tag{3.34}$$

This expression was originally defined in terms of $k_a(E^*)$, the rate constant for the transfer from the energized state to the activated state. Thus

$$k_a(E^*) = L^+ \frac{Q_1^+}{Q_1} \underline{\Sigma P}(E^+_{vr}) / N^*(E^*) \quad . \tag{3.17}$$

Again this quantity has intuitive physical meaning but both $k_a(E^*)$ and k_{uni} are not well defined, except for the latter when either high or low pressure limits are considered

since $N^*(E^*)$ drops out or enters as $\int N(E^*)dE^*$ respectively. Note that it is k_a which is calculated in the previously cited RRKM program (44). Even with $\int N^*(E^*)dE^*$, if ΔE is choosen too large, some states will be missed in counting and then $\int N^*(E^*)dE^*$ will again depend on the choice of ΔE. Thus the smaller one's choice of ΔE , the larger $N^*(E^*)$ becomes (approaches ∞). However, the smaller ΔE becomes the more accurate the integral $\int N^*(E^*)\ dE^*$.

Since most RRKM work has concentrated on the fall off region between high and low pressure limits (41) the above considerations are most important. Some of the conclusions that are reached concerning the numbers of active modes etc.,which shift the fall off curves into the experimentally observed curves may be overemphasized, since the problems mentioned above give rise to the same type of effects on the fall off curves as do changes in physical parameters (46). In order to see that the density of states problem actually affects the RRKM integration in magnitudes which are comparable to other factors in model calculations (40), one can look at equation(3.34) in greater depth in a typical situation where the grain size used in the integration is small enough that the graining problem is encountered. The equation has the form

$$k_{uni} = a \int_0^\infty \frac{W(E)\ \exp(-E/kT)}{1 + \dfrac{b\ W(E)}{N(E+E_o)\ P}} \qquad (3.35)$$

where P in the pressure, and when this expression is integrated numerically, it will be represented as a sum of integrands times the grain size

$$k_{uni} = a\ \Delta E \sum_{E=0}^{\infty} \frac{W(E)\ \exp(-E/kT)}{1 + \frac{b\ W(E)}{N(E+E_o)\ P}} \quad . \qquad (3.36)$$

(The sum is performed in steps of ΔE). It is useful to consider how an arbitrary term in the sum varies with grain size and then to consider the importance of that term in relation to others at any particular pressure. By looking at those pressures of interest in the fall off curves, the effect of the problem on the integration itself can be estimated.

In the region where fall off occurs, the only terms in equation (3.36) that can be of major importance in the integration are those where $b\ W(E)/N(E+E_o)\ P$ is comparable to the number 1. Recall that k_{uni} changes over several orders of magnitude on typical fall-off curves , and this would not occur if the major contributions to the integral were from terms where P was either very large or very small (in the latter case a linear dependence in predicted and this is not observed). Thus if k_{uni} is to be pressure dependent, the changes in k_{uni} with changing pressure must come from the terms in the summation where $b\ W(E)/N(E+E_o)$ are affected significantly by the addition of the constant 1. (note that although for very small P,(large denominator),k_{uni} is affected, but the whole term is itself too small to contribute to the

overall summation, so that again a pressure independence is predicted). Therefore, as an example, consider those terms where b $W(E)/N(E+E_o)$ P ranges from 0.01 to 100 i.e.,the denominator ranges from 1.01 to 101.Now if the grain size were halved, doubling $N(E+E_o)$, then the denominator would consist of terms like (1.005,1.25,2.0,10.0,50.0) instead of(1.01,1.50,3.0,19.0,99.0) terms originating from the original grain size. The ratios of corresponding denominators would then be (1.01:1,1.20:1,1.50:1,1.90:1,1.98:1) . Since the grain size has been halved, and thus $\Delta E \rightarrow \Delta E/2$, half the terms in the new summation will go to zero. However, the non-zero terms in the numerator of equation (3.36) will all be changed by this factor of 2. Thus in the example above the ratio of numerator to denominator for the single terms changes by factors of (1.98, 1.67, 1.33, 1.05, 1.01) in a doubling of the grain size. That is, when the grain size is doubled, all the terms which change significantly with pressure are changed, and this change is , on the average, about by a factor of 1.5:1. As mentioned previously the observed pressure dependence is large, and therefore the terms above must form a significant part of the overall summation. Thus, one would expect that halving the grain size would decrease the overall sum, k_{uni} ., by roughly 1.5:1, which corresponds to a change in log k_{uni} (at a given pressure) of about 0.2 units. Similarly, if the grain size were reduced by a factor of 10, one would expect a decrease in k_{uni} by a factor of approximately 2 to 6 times or log k_{uni} by from .3 to .8 units.These

shifts in the fall-off curves are comparable to many of the effects of model changes on fall-off curves described by Robinson and Holbrook (40), who illustrate the effects of frequency changes, deactivation rates, activation energies etc., on the rate curves*.

* Recently Christianson,Price and Whitehead (J.Phys. Chem.78,2326(1974)) reached the same conclusions using a different theoretical analysis. That there was a problem affecting rate constant calculations was noticed by Frey,Hopkins and Vinall (J.Chem.Soc.Faraday Trans.I 68, 1874(1972)) in a paper on the thermal isomerization of cyclobutenes.

F. ILLUSTRATIVE EXAMPLES

Examples of density of states calculations,using a harmonic oscillator model and both exact and approximate level counts, are illustrated in figures (3.2) and (3.3). The levels chosen for the model calculations have the following harmonic frequencies and degeneracies: 3000 (2), 1500 (3), 1000 (2), 900 (2), 500 (2), and 400 (1) cm^{-1}. The most efficient counting scheme for exact counts of energy levels is the Beyer Swinehart (BS) algorithm (26) which has been programed for the ONM work earlier. Both a harmonic and an anharmonic algorithm exist and the two have been combined for the state counts in the harmonic cases in figures (3.2) and (3.3) and in the anharmonic cases in figure (3.4). The results are exact for a step size of 1 cm^{-1} for integral frequencies. The computing time is almost directly proportional to the grain size and number of degrees of freedom involved so that if only estimates of occupation numbers are required, larger grain sizes can be used in relatively short computational times.

Curves 1 and 2 in figure(3.2)have been obtained on the basis of the BS algorithm and are exact for the grain sizes used (10 cm^{-1} for curve (1) and 50 cm^{-1} for curve (2)). The third count in figure (3.2) is an approximate count, the Whitten Rabinovitch semi-classical count (44), and is included here for the purposes of comparison. Both exact counts lead to the same sum of all levels (ΣP_i). Up to 24400 cm^{-1} the sum is 9.01×10^8. The point to note from figure (3.2) is that

Figure (3.2) Harmonic oscillator count for model system with frequencies (cm^{-1}) and degeneracies: 3000 (2), 1500 (3), 1000 (2), 900 (2), 500 (2), 400 (1).

1- An exact count with grain size 10 cm^{-1}.

2- An exact count with grain size 50 cm^{-1}.

3- Whitten Rabinovitch semi-classical count.

Counts (1) and (2) are exact and lead to a sum of levels up to 24400 cm^{-1} of 9.01×10^{8}.

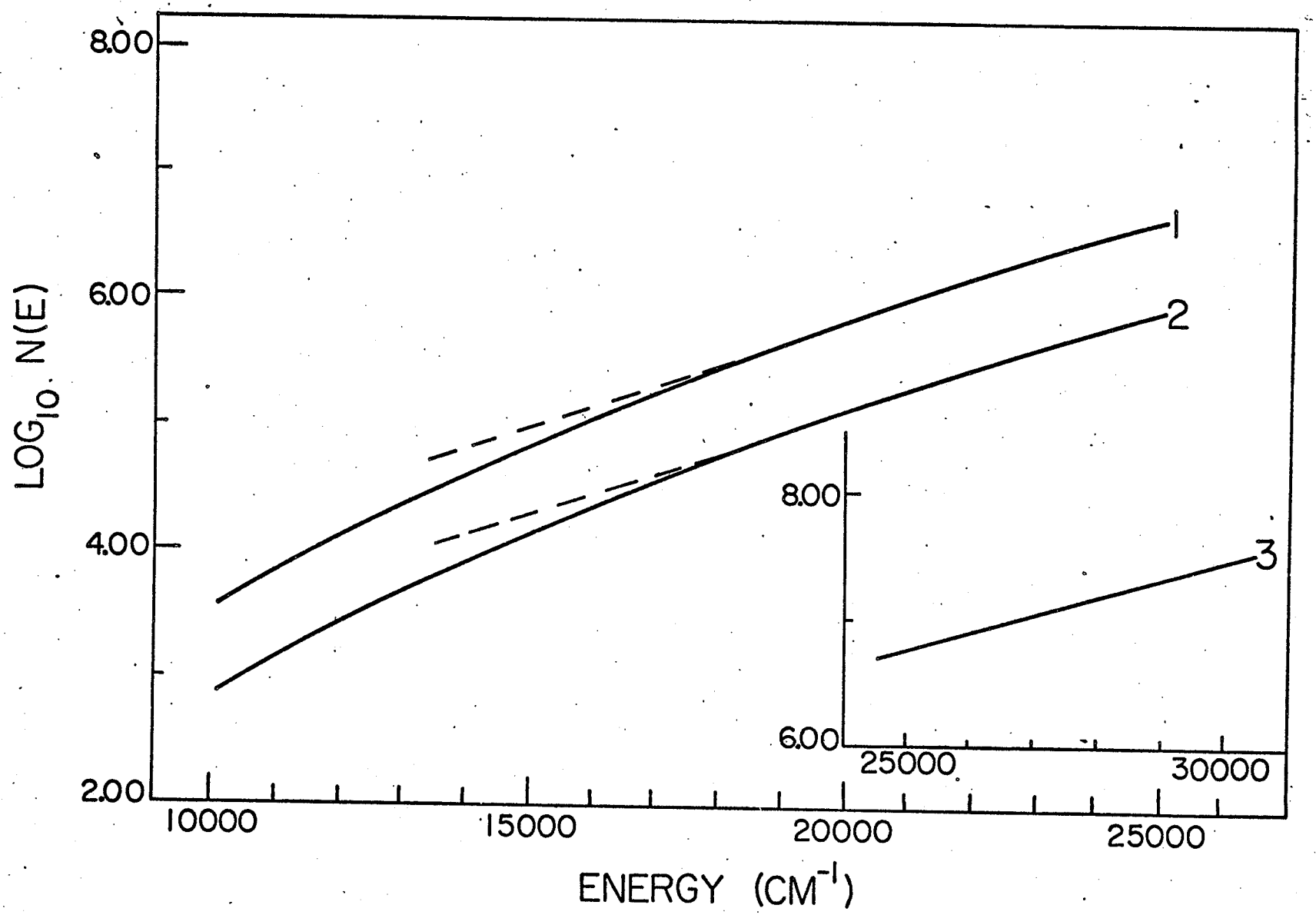
8.00
6.00
4.00
2.00
LOG10. N(E)
10000
15000
20000
25000
ENERGY (CM-1)
1
2
3
8.00
6.00
25000
30000

Figure (3.3) Harmonic oscillator counts for model system described in figure (3.2). The grain sizes and sum of states up to 24400 cm^{-1} are; (4)-300 cm^{-1}, 3.34 x 10^9. (5)- 200 cm^{-1}, 1.89 x 10^9. (6)- 100 cm^{-1}, 9.01 x 10^8.

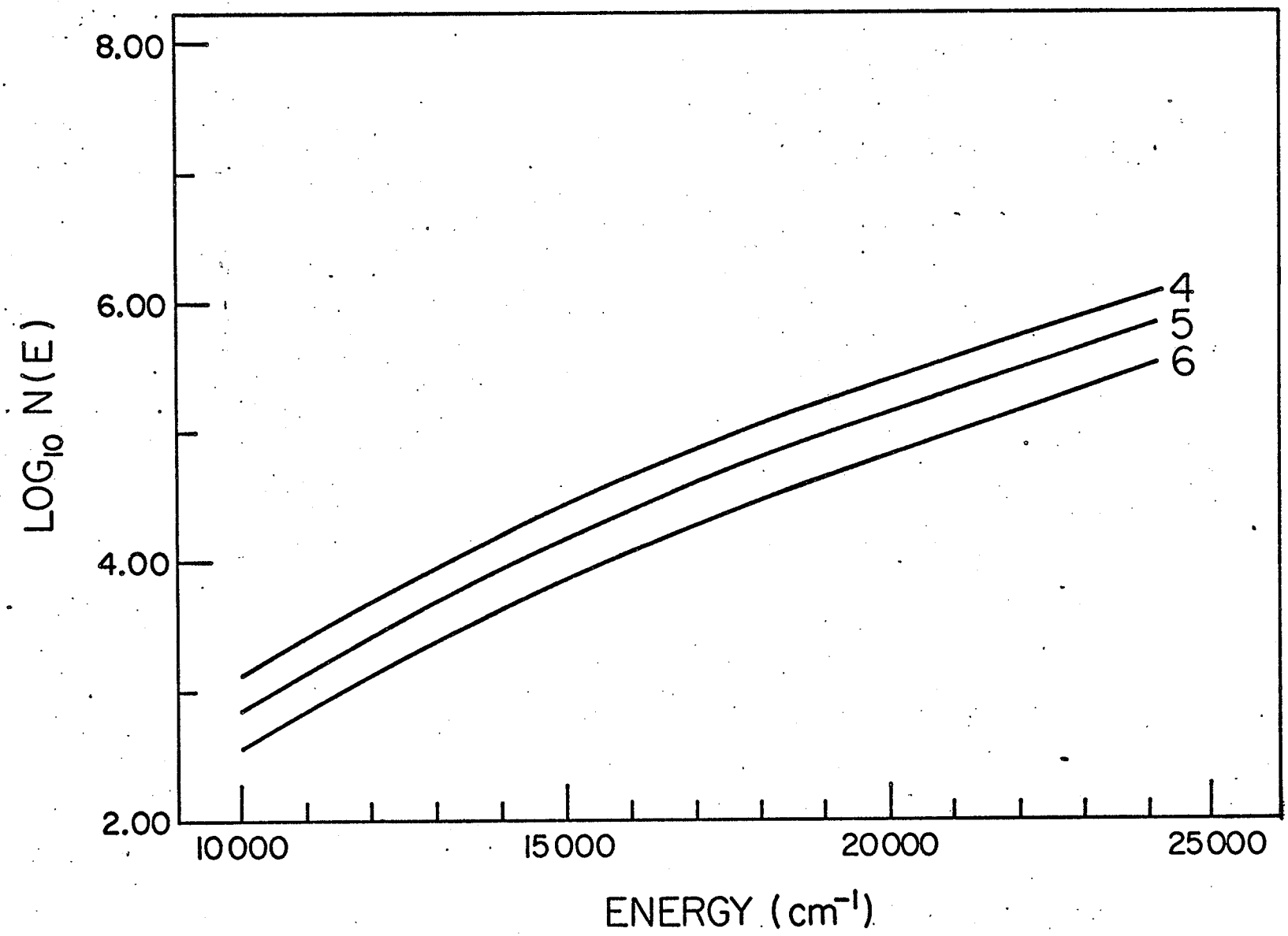
8.00
6.00
4.00
2.00
LOG_{10} N(E)
4
5
6
10000
15000
20000
25000
ENERGY (cm^{-1})

as predicted by the arguments given in the earlier sections, the density of states,as defined by equation (3.19),depends on the grain size even for these exact counts. The scale for density is logarithmic so that the spread between them represents a factor of 5, exactly the grain size ratio,with N(E) decreasing as the grain size increases.

In figure (3.3) all counts were obtained on the basis of the BS algorithm, but only curve (6) with a grain size of 100 cm^{-1} is exact. Curves (4) and (5) (grain sizes of 300 cm^{-1} and 200 cm^{-1} respectively) are approximate, and in fact the points here do not fall on as smooth a curve as the exact counts. Figure (3.3) illustrates two points. Curve (6) corresponds to the largest grain size that can be used while still maintaning an exact count. Yet it seems clear that in no way does N(E) approach a limit as this grain size is approached from above or below. Furthermore, the result observed for exact counts, namely that N(E) decreases with increasing grain size , no longer holds for the approximate counts, (4) and (5), which both show increased N(E) relative to (6). In fact, for approximate counts,it is impossible to predict apriori whether there will be overcounting of levels as in the case of curves (4) and (5) where the sums of states up to 24400 cm^{-1} are 3.34×10^9 and 1.89×10^9 respectively, or undercounting. These points are important since they demonstrate the dependence of N(E) on definition.

Finally,to illustrate the effect of anharmonicity on state counts, a series of BS anharmonic oscillator counts are illustrated in figure (3.4). The fundamental frequencies and degeneracies are the same as for figure (3.2) and (3.3) but the following (diagonal) anharmonicities (cm^{-1}) have been assigned to the six vibrational modes: curve (7)-(-80, -12, -8, -7, 0, 0), curve (8)-(0, 0, 0, 0, 0, 0), curve (9)-(-50, -5, 0, 0, 0, 0), and curve (10)- (-80, -5, 0, 0, 0, 0). The grain size used was 10 cm^{-1} and the sum of levels up to 24400 cm^{-1} is 1.10 x 10^{10}(7), 0.09 x 10^{10}(8), 0.17 x 10^{10}(9), and 0.17 x 10^{10}(10) respectively. Curve (8), the harmonic curve, included for the purposes of comparison, is the same as curve 1 of figure (3.2). It is interesting to note that over the energy range of the curves, which corresponds to moderate chemical energies (30-70 Kcal/mole), that the introduction of anharmonicity changes the state count sums significantly, and also changes N(E) quite substantially. An important point in this regard is that the harmonic curve (8) generally indicates a higher density of states than the anharmonic curves in this region, despite the fact that the sum of states is substantially lower for the harmonic case. This result is clearly a manifestation of the numerical procedure used to calculate N(E),and illustrates the misleading character of the N(E) function in this type of quantized system.

The anharmonic and harmonic level counts become exponential fairly quickly and therefore extrapolation of level

Figure (3.4) Direct counts using anharmonic oscillator models with fundamental frequencies (cm^{-1}) and degeneracies as in figure (3.2) and (diagonal) anharmonicities and sums of all levels up to 24400 cm^{-1} as follows;

(10)- (-80, -5, 0, 0, 0, 0) 0.17×10^{10} states.

(9)- (-50, -5, 0, 0, 0, 0) 0.17×10^{10}.

(8)- (0, 0, 0, 0, 0, 0) 0.09×10^{10}.

(7)- (-80,-12,-8,-7, 0, 0) 1.10×10^{10}.

The grain size used in all cases was 10 cm^{-1}.

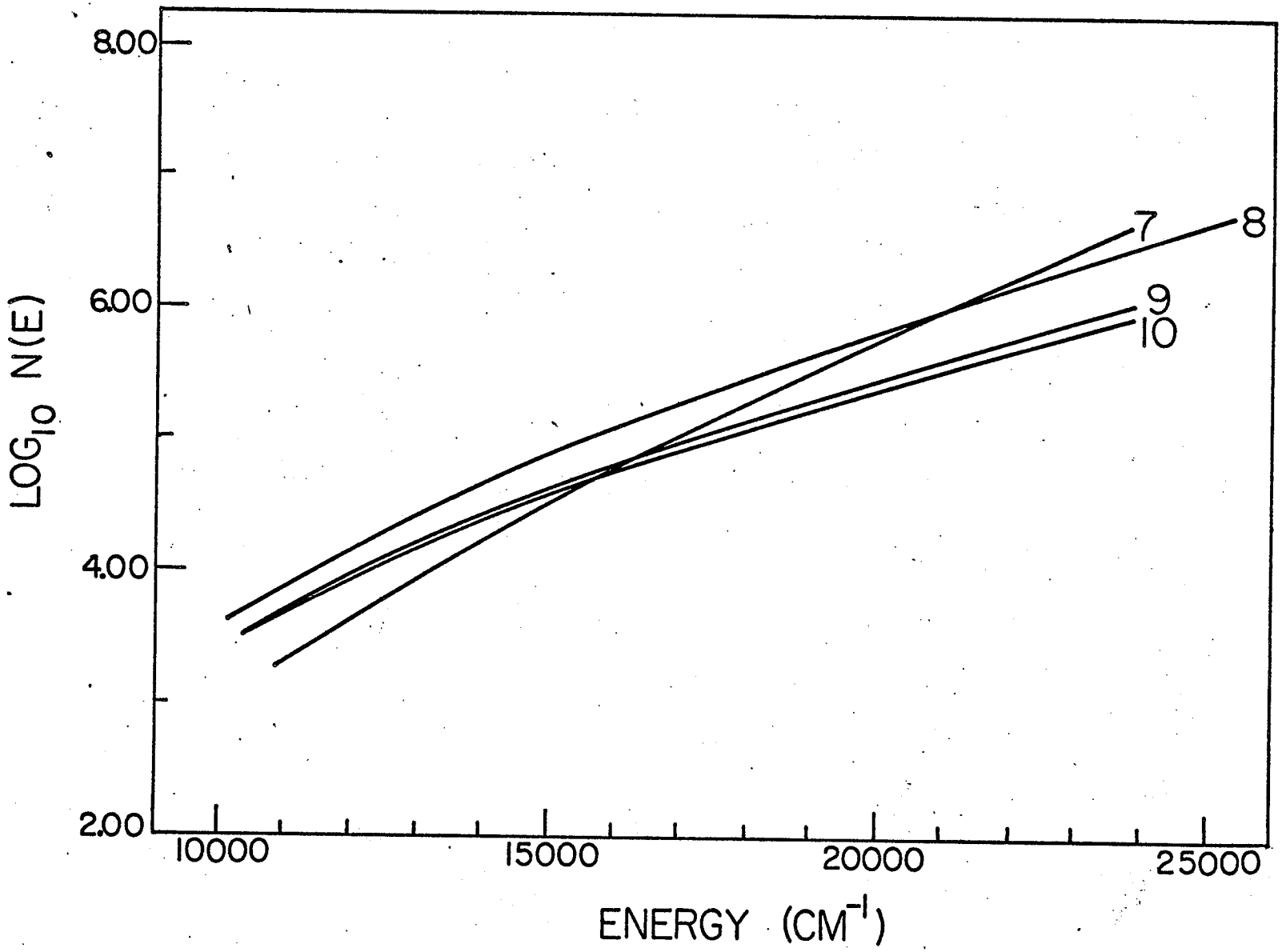
8.00
6.00
4.00
2.00
LOG10 N(E)
10000
15000
20000
25000
ENERGY (CM-1)
7
8
9
10

sums to higher energies from limiting slope calculations would be possible. However, the limitations of an anharmonic potential model should be kept in mind when considering energy limits for such extrapolations (26).

In summary, therefore, a few conclusions can be drawn. At thermal energies where the vibrational levels still form a discontinuous energy spectrum there is a great deal of difficulty in using the concept of density of states in calculations. For the purposes of dealing with fall-off curves in RRKM theory, a reformulation of the theory without the substitution described in equation (3.15) will be necessary to deal with real,quantized systems. Also, in dealing with photochemical reactions and with other radiative or radiationless vibronic transitions, where the energies involved imply a much smoother W(E) curve, care must be taken in calculating N(E) since $\Delta W/\Delta E_{E=E_i} = N(E_i)$ is only approximate for such rapidly increasing functions.

G ANHARMONICITY

To conclude this terse introduction to the RRKM theory of unimolecular reactions, a brief look at the concept of anharmonicity within the context of this rate theory follows. In Herzberg's classic work on the infrared and Raman spectra of polyatomic molecules (1) he says," .....These considerations emphasize the need for more detailed investigations of overtone and combination vibrations of all thermodynamically important molecules. .....". He was referring to the calculation of vibrational partition functions in that paragraph. The partition function of the harmonic oscillator

$$Q_i = (1+\exp(-h\nu/kT))^{-1} \qquad (3.37)$$

is not entirely adequate since it always will underestimate the actual partition function. In large molecules, where there are a large number of degrees of freedom,the anharmonic correction can be quite important as the N(E) curves of figure (3.4) indicate. Because the partition functions often appear as ratios, as for example in equation (3.10), there will be a tendency to have at least a partial cancellation of errors. However, because of the higher vibrational energies involved in an A^* state in comparison to the A^+state, complete cancellation would not be expected. For some thermodynamic calculations, where the absolute values of the partition functions are of importance, anharmonic vibrational partition functions are significantly different from the harmonic partition functions only for low frequency vibrators at high

temperatures. Consider the following set of partition functions. (In these caculations care must be taken to avoid models in which the 'anharmonic limit' is at a low enough energy that $E_{limit} \simeq kT$. Physically this is often the case, and this illustrates an important limitation to our conceptual understanding of rate processes, in so far as the models for these processes reflect that understanding.) In table (3.1) the effect of temperature and frequency is illustrated.

Table (3.1)

Oscillator Frequency and Anharmonicity	Temperature	Q(harm) equation (3.39)	Q(anharm) direct count	Q(anharm) / Q(harm)
100 (- 2) cm^{-1}	$300^{o}K$	1.6277	1.8850	1.1581
3400 (-70)	$300^{o}K$	1.0000	1.0000	1.0000
3400 (-70)	$1000^{o}K$	1.0076	1.0084	1.0008
800 (- 5)	$500^{o}K$	1.1116	1.1138	1.0020

Thus, for partitioning between states of the same total energy (eg., the A^{+} and A^{*} states), the anharmonic effect is quite important as well.

Anharmonic effects are the means by which the proposed random distribution of vibrational energy is achieved. This is implicit in the RRKM theory, even though the vibrational manifold is treated rather more like a set of uncoupled anharmon-

ic oscillators. Assuming that there is some degree of state selection (not a necessary assumption in the theory) in thermal activation of molecules, then the RRKM theory implicitly requires that the vibrational modes be coupled, to allow for complete randomization of the energy in times short in comparison with the time scale of the reaction. This is implicit in the calculation of the steady state ratio A^+/A^*. The theory at the same time presupposes the coupling to be small enough to allow the modes to be treated independently in so far as is needed for the calculation of the partition function (molecular energy levels). The idea of independent anharmonic modes suggests the local-mode model described earlier, where the potential energy matrix is relatively more diagonal than in the normal mode basis. This conclusion is independent of the lack of knowledge of selection rules for overtone spectra. Even though off-diagonal , local-mode couplings may be difficult to extract from spectroscopic data, the fact that combination bands do appear in the overtone spectra is enough to establish that the zeroth order modes are coupled and thus a mechanism for energy randomization established.

Inasmuch as the RRKM theory is a vibrational theory of unimolecular reactions, the very occurrence of dissociation presupposes the paramount importance of mechanical anharmonicity. If the concept of local modes finds application here, a new simplicity in both calculation and concept of fundamental unimolecular reaction mechanism may emerge.

APPENDIX

HIGH PRESSURE GAS CELL APPARATUS

In order to obtain gas phase infrared spectra at pressures in the range from 1 tol50 atm. a stainless steel gas line was constructed to take the gas from standard cylinders to a high pressure cell which was obtained from Beckman Instruments. The system is illustrated and a convenient mode of operation, which allows the gas to be manipulated in a relatively controlled fashion, is described.

A list of components of the system,which appears in figure (A.1) is given below.

Components

A	F-076	Beckman high pressure gas cell with quartz windows.
B	SS-1RS4	Whitey Forged Body Valve (regulating valve).
C	SS-4P-4N	Nupro perge valve.
D	SS-400-3TTF	Swagelok female branch T joint.
E	J-4878	Marsh pressure guage,2½"-¼" bottom connect (0-3000 psi.).
F	SS-402-1	Standard ¼" stainless steel Swagloc nut and ferrule.
G	SS-400-7-4	Female connector.
H	#15-3S	Nitrogen Nipple (¼" male pipe).

Figure (A.1) High pressure gas line assembly for use in the measurement of the infrared spectra of gases. The mode of operation is discussed in the text.

HIGH PRESSURE GAS LINE

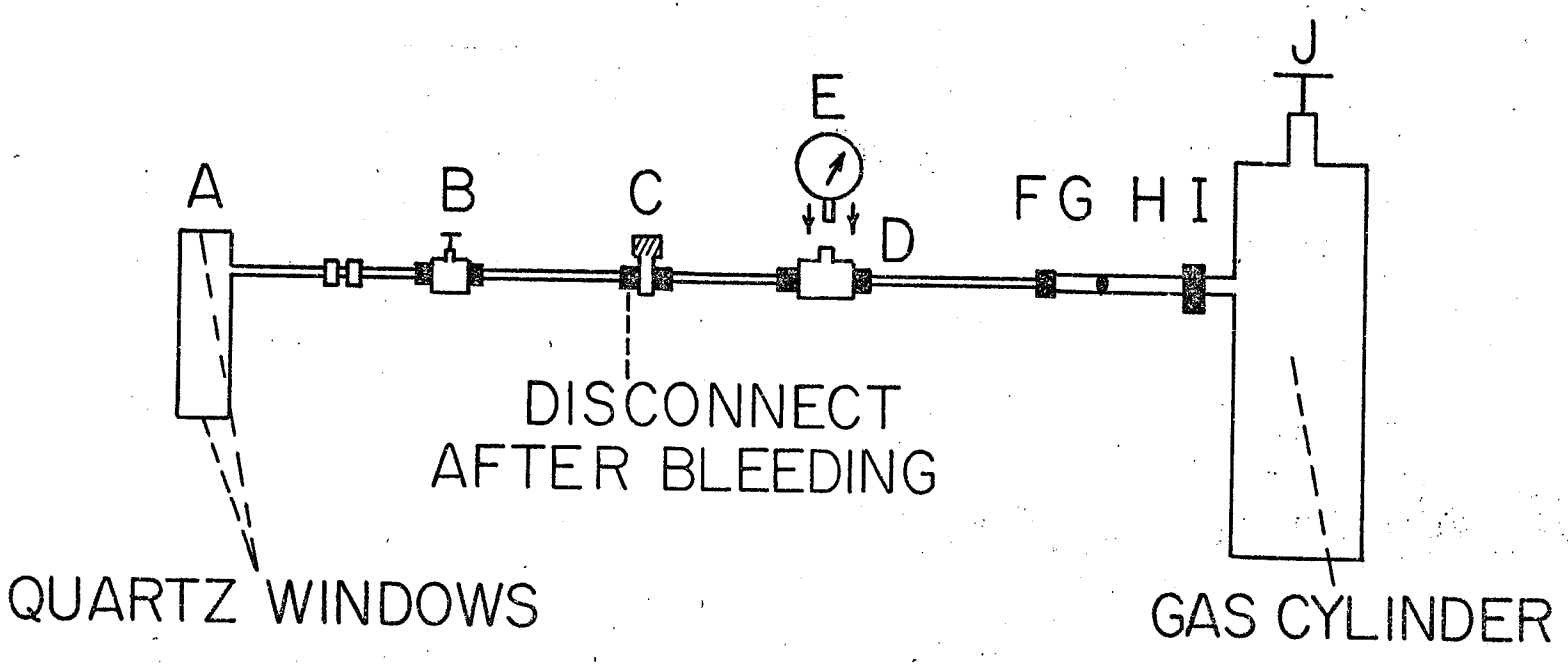

I	#92	Nitrogen nut.
J		Any standard high pressure cylinder.
Tubing		¼" stainless steel tubing.

Parts H,I and J are changed for the different gas cylinders. The numbers in the table above are for the nitrogen cylinder. Teflon tape is required to make seals between D and E, G and H, and I and J (mostly stainless steel to brass connections).

By manipulation of the regulating valve at B and the cylinder valve J, the system may be pressurized slowly for maximum protection of the quartz windows. This also allows the system to be pressurized to any pressure (±≃20 psi) between the maximum cylinder pressure and 1 atm., without the use of further regulating valves.

To pressurize the gas cell the following sequence of manipulations has been found safe and convenient:

1. Seal up entire system with valve B closed.
2. Pressurize to valve B which remains closed.
3. Shut off cylinder valve.
4. Open valve B.
5. Open cylinder valve J.
6. Close valves J and B.
7. Bleed system from C.
8. Disconnect at C (leaving gas cell free for measurement.

Making Swagloc seals with stainless steel is more difficult than with copper tubing but once the seal has been made the

system may be dismantled and reassembled with ease, and there seems to be no difficulty in obtaining the seal again.

REFERENCES

1. G.Herzberg, Infrared and Raman Spectra, Van Nostrand, Princeton,N.J.(1945).
2. E.B.Wilson, J.C.Decius and P.C.Cross,Molecular Vibrations, M^{C}Graw-Hill, New York (1955).
3. B.R.Henry and W.Siebrand,J.Chem.Phys.49,5369(1968).
4. B.R.Henry and M.Kasha, Ann.Rev.Phys.Chem.19,161(1968).
5. A.Vogel,Elementary Practical Organic Chemistry, Longmans (2nd edition)(1966).
6. F.Cotton, Chemical Applications of Group Theory,Wiley, New York (2nd edition) (1971).
7. W.H.J.Childs,Proc.Roy.Soc.Lond.153,555(1936).
8. W.V.Norris and H.J.Unger,Phys.Rev.43,467(1933).
9. I.R.Levine,Quantum Chemistry Vol.I,Allyn and Bacon(1970).
10. W.Siebrand,J.Chem.Phys.46,440(1967).
11. R.M.Hochstrasser,Molecular Aspects of Symmetry,W.A. Benjamin (1966).
12. K.Scholz,Z.f.Physik.78,751(1932).
13. J.Pitha and R.N.Jones,Can.J.Chem.45, 2347(1967).
14. W.Siebrand and D.F.Williams,J.Chem.Phys.49, 1860(1968).
15. R.J.Hayward,B.R.Henry and W.Siebrand,J.Mol.Spectrosc. 46,207(1973).
16. J.Morgan, Geometric and Physical Optics, M^{C}Graw-Hill, New York (1953).
17. G.Herzberg, Spectra of Diatomic Molecules, Van Nostrand, Princeton,N.J.(1939).
18. J.A.Kerr,Chem.Rev.66, 465(1966).

19. J.W.Ellis, Trans.Far.Soc.25,888(1928).

20. J.Barnes and W.H.Fulweiler, Phys.Rev.32, 618(1928).

21. J.Bron and M.Wolfsberg,J.Chem.Phys.57, 2862(1972).

22. Y.Morino,KKuchitsu and S.Yamamoto, Spectrochim.Acta 24A, 335(1968).

23. H.J.Unger, Phys.Rev.43, 123(1933).

24. A.Adel and V.M.Slipher, Phys.Rev.46, 902(1934).

25. B.E.Knox and H.Palmer, Chem.Rev.61,247(1961).

26. S.E.Stein and B.S.Rabinovitch,J.Chem.Phys.58,2438(1973).

27. R.Robertson and J.J.Fox,Proc.Roy.Soc.Lond.120A,161 (1928).

28. R.M.Badger, Phys.Rev.35,1038(1930).

29. V.P.Leug and K.Hedfeld,Z.f.Physik 75,599(1932).

30. G.Jung and H.Gude,Z.Physik.Chem.B18, 308(1932).

31. J.W.Ellis,Phys.Rev.28, 25(1926).

32. O.Vierling and R.Mecke,Z.f.Physik 99,204(1935).

33. R.J.Hayward and B.R.Henry, J.Mol.Spectrosc.50,58(1974).

34. Y.Tanaka and K.Machida,J.Mol.Spectrosc.51,508(1974).

35. A.Adel and V.M.Slipher,Phys.rev.46,902(1934).

36. K.H.Schmidt and A.Muller, J.Mol.Spectrosc.50,115(1974).

37. K.J.Laidler,Theories of Chemical Reaction Rates, M^{c}Graw-Hill,New York(1969).

38. A.Messiah,Quantum Mechanics,North Holland (1958).

39. E.Merzbacher, Quantum Mechanics,John Wiley (1961).

40. P.J.Robinson and K.A.Holbrook, Unimolecular Reactions, Wiley Interscience (1972).

41. D.L.Bunker and W.L.Hase,J.Chem.Phys.59, 4621(1973).

42. J.D.Macomber and C.Colvin,J.Chem. Kinetics 1, 483(1969).

43. E.H.Kennard, Kinetic Theory of Gases,M^{C}Graw-Hill, New York,(1938).

44. Q.C.P.E. Program #234, Indiana university Chemistry Department.

45. W.Forst,Chem.Rev.71,339(1971).

46. A.E.Trotman-Dickenson, Gas Kinetics, Butterworths, New York (1955).